CATECHOLAMINE-REGULATED PROTEIN 40 IN PARKINSON'S DISEASE

ROLES OF CATECHOLAMINE-REGULATED PROTEIN 40 (CRP40) AS A THERAPEUTIC AGENT AND BIOMARKER IN PARKINSON'S DISEASE

By JOVANA LUBARDA, HONS. B.SC.

A Thesis Submitted to the School of Graduate Studies in Partial Fulfilment of the Requirements

for the Degree Doctor of Philosophy

DOCTOR OF PHILOSOPHY (2013)
(Neuroscience)
McMaster University
Hamilton, Ontario

TITLE: Roles of Catecholamine-Regulated Protein 40 (CRP40) as a Therapeutic Agent and Biomarker in Parkinson's Disease

AUTHOR: Jovana Lubarda, B.SC. (McMaster University)

SUPERVISOR: Professor Joseph Gabriele

NUMBER OF PAGES: xi, 196

Abstract

Parkinson's disease (PD) is a complex neurodegenerative movement disorder involving protein misfolding, mitochondrial dysfunction, and oxidative stress. The current dissertation, motivated by a lack of valid biomarkers and sustainable therapies, examined the potential application of a novel target for therapeutics and diagnostics of PD – the multifunctional, heat-shock like protein Catecholamine-Regulated Protein 40 (CRP40). The goal of this program of research was to elucidate further the implications of CRP40 in PD using a variety of molecular biology, bioinformatics, and clinical approaches through integrative collaborations with academia, government, and industry partners to translate scientific findings into real world solutions. Chapters 2 and 3 explored the potential therapeutic use and structure-function relationships of CRP40 through elucidating the smallest functional piece of this protein that was six times smaller, and validating a negative control for these experiments (Heat-Shock Protein 47). These initiatives could eventually lead to a small drug that could cross the blood-brain barrier and be targeted to the specific brain regions affected in PD. Chapter 4 examined the potential mechanisms of CRP40, and suggested that this protein may protect neurons from oxidative stress, maintain energy levels, and mitochondrial homeostasis, with important future implications for a variety of disorders. Finally, Chapter 5 presented compelling evidence for the potential use of CRP40 as a valid biomarker for early detection of PD and monitoring of disease progression. Overall, findings suggest that CRP40 may be a critical target for future breakthroughs in the diagnosis and treatment of PD.

Acknowledgements

This thesis is dedicated to my parents and brother for their love, unwavering support, and for working so hard to give me all of the opportunities in this world to follow my dreams and reach the pinnacle of happiness.

I would like to express my sincere and deepest gratitude to my graduate supervisor and mentor Dr. Joseph Gabriele, whom I also consider a great friend. I thank him for his ingenuity and for always inspiring scientific excitement and creativity, and for believing in me and giving me all of the opportunities to succeed. Dr. Gabriele's brilliant scientific talents and business capabilities have allowed me to have an incredible, rich and fulfilling experience that I will never forget. I would also like to extend my gratitude to an exceptional and outstanding woman, Dr. Eva Werstiuk, who has been my scientific and life mentor for many years and has supported me throughout my graduate studies. I would also like to thank Dr. Kathryn Murphy, the director of the McMaster Integrative Neuroscience Discovery and Study Program for valuable lessons, Dr. Ram Mishra for his guidance and support, Dr. Shucui Jiang for her help and great conversations, and my laboratory colleagues for their collaboration. I am also thankful for the financial support provided to me during my graduate training from Ontario Graduate Scholarship and Natural Sciences and Engineering Research Council of Canada.

Finally, I would like to thank everybody who I met in my life. In different ways, you have all helped me get to where I am today – the road to the top.

Table of Contents

List of Figures and Tables

List of Abbreviations and Symbols

2', 7'-Dichlorodihydrofluorescin (DCFH); 2', 7'-Dichlorodihydrofluorescin diacetate (DCFH-DA); 6-hydroxydopamine (6-OHDA); Acetate citrate dextrose (ACD); Adenosine diphosphate (ADP); Adenosine triphosphate (ATP); Adenylyl cyclase (AC); Analysis of variance (ANOVA); Apoptosis-inducing factor (AIF); Base pairs (bp); Bovine standard albumin (BSA); Catecholamine-Regulated Protein 40 (CRP40); Catechol-*O*-methyltransferase (COMT); Central nervous system (CNS); Cyclic adenosine monophosphate (cAMP); Cyclic guanosine monophosphate (cGMP); Deionized (DDI); Deoxyribonucleic acid (DNA); Diethylpyrocarbonate (DEPC); Dimethyl sulfoxide (DMSO); DOPA decarboxylase (DDC); Dopamine (DA); Ethylenediaminetetraacetic acid (EDTA); Fetal bovine serum (FBS); G protein-coupled receptors (GPCRs); Glutathione S-transferase (GST); Heat-shock protein 47 (Hsp47); Heat-shock protein 70 (Hsp70); Heat-shock proteins (Hsp); Highly fluorescent 2', 7'-Dichlorodihydrofluorescin (DCF); Hydrogen peroxide (H_2O_2); L-3,4-dihydroxyphenylalanine ($_L$-dopa); Luria-Bertani (LB); Magnetic resonance imaging (MRI); Magnetic resonance spectroscopy (MRS); Medial prefrontal cortex (mPFC); Monoamine oxidase (MAO); National Center for Biotechnology Information (NCBI); Nuclease free H_20 (NF H_20); Parkinson's disease (PD); Phenylethanolamine *N*-methyltransferase (PNMT); Phenylmethylsulfonyl fluoride (PMSF); Phosphate Buffer Saline-EDTA-Bovine Serum Albumin (PEB); Phosphate-buffered saline (PBS); Polymerase-chain reaction (PCR); Pre-pulse inhibition (PPI); Protein kinase A (PKA); Protein kinase C (PKC); Quebec Consortium for Drug Discovery (CQDM); Reactive oxygen species (ROS); Reverse-transcriptase polymerase

chain reaction (RT-PCR); Ribonucleic acid (RNA); Roswell Park Memorial Institute (RPMI); Single-photon emission computed tomography (SPECT, DaTscan); Sodium dodecyl sulfate polyacrylamide gel electrophoresis (SDS-PAGE); Substantia nigra pars compacta (SNc); Tritiated dopamine ([^{3}H]-DA); Tumour suppressor protein (p53); tyrosine hydroxylase (TH); Ventral tegmental area (VTA); β-D-1-thiogalactopyranoside (IPTG); γ-aminobutyric acid (GABA)

Declaration of Academic Achievement

This thesis is composed of a total of six chapters. Chapter 1 provides a general introduction and background for research. Chapters 2 through 5 are written in the style of empirical journal articles. Chapter 6 examines the importance of the research and the theoretical implications/future directions of this work. Parts of Chapter 5 have been published in the Journal of Movement Disorders; I was specifically involved in data collection, data analysis with our laboratory technician Nancy Thomas, statistical analysis with Dr. Mark Ferro, and preparation of the final manuscript, with editing assistance from colleague Sarah Groleau. For Chapters 2 through 4, I oversaw all aspects of research and for Chapters 2 and 3, I was also assisted by our laboratory technician, Nancy Thomas, in carrying out the experimental procedures. I designed and executed all of the studies in Chapter 4. I also performed statistical analyses and wrote summaries for each study, which were presented in my graduate committee meetings.

Figure 1.1 was an image available in the public domain, and is therefore not under copyright. All of the other figures were produced from our laboratory.

This research was supported by grants awarded to Dr. Gabriele from the Natural Sciences and Engineering Research Council of Canada (NSERC), and the Quebec Consortium for Drug Discovery (CQDM) along with pharmaceutical partners Merck, Pfizer, and Astra-Zeneca. I received support from the Ontario Graduate Scholarship for year 1 of this research and the NSERC Alexander Graham Bell Canada Graduate Scholarship for years 2 and 3 of this research.

Chapter 1: General Introduction to Neurodegenerative Diseases and Catecholamine-Regulated Protein 40 (CRP40)

1.1 Catecholamines

Catecholamines are neurotransmitters and/or hormones found in the peripheral systems of the body as well as the central nervous system (CNS) (Verheij and Cools, 2008). They consist of dopamine (DA), norepinephrine and epinephrine, which are synthesized from the amino acid tyrosine (Vallone et al., 2000). Norepinephrine functions as a neurotransmitter in the brain as well as in postganglionic sympathetic neurons. DA has crucial neurotransmitter functions in the CNS and the periphery through regulating the biological activity of the kidneys. Epinephrine is released from the adrenal gland and formed through *N*-methylation of norepinephrine. Epinephrine acts on various catecholamine receptors in a variety of target organs.

The biosynthesis pathways of catecholamines have been well characterized (Figure 1.1).

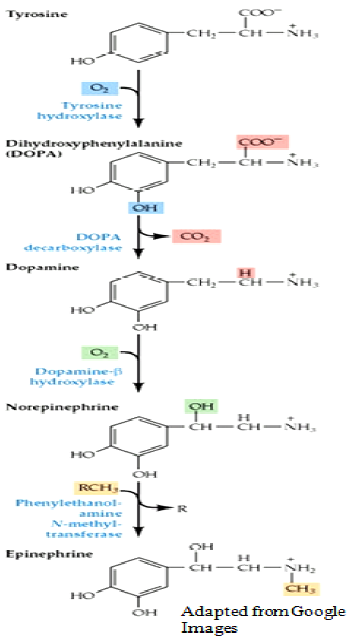

Figure 1.1 Biosynthesis pathway of catecholamines.

Tyrosine hydroxylase (TH) is the rate-limiting enzyme for biosynthesis of catecholamines and is found in all catecholamine-synthesizing cells (Verheij and Cools, 2008). TH, a homotetrameric enzyme, catalyzes the addition of a hydroxyl group to the *meta* position of tyrosine, utilizing molecular oxygen and biopterin as cofactors (Verheij and Cools, 2008). This reaction results in the formation of L-3,4-dihydroxyphenylalanine ($_{L}$-DOPA). The next important enzyme in the biosynthesis pathway is DOPA decarboxylase (DDC), a pyridoxine-dependent enzyme. DDC is found throughout the body in neurons containing catecholamines and serotonin as well as in the kidneys and blood vessels. DDC has a low K_m and high V_{max} with respect to $_{L}$-DOPA. Also, DDC efficiently catalyzes the removal of a carboxyl group from DOPA and participates as the final enzyme required for the synthesis of dopamine by converting $_{L}$-DOPA to DA (Verheij and Cools, 2008). Unlike DA, the catecholamines epinephrine and norepinephrine require β-hydroxylase for synthesis. β-hydroxylase uses molecular oxygen to catalyze the addition of a hydroxyl group to the carbon on the side chain of DA, forming norepinephrine. Epinephrine synthesis requires an additional step catalyzed by the enzyme phenylethanolamine *N*-methyltransferase (PNMT), which transfers a methyl group from *S*-adenosylmethionine to the nitrogen of norepinephrine. PNMT is found in brainstem neurons as well as in cells of the adrenal medulla.

Small concentrations of catecholamines are present in the cytosol where they are metabolized by enzymes including monoamine oxidase (MAO) (Verheij and Cools, 2008). Catecholamines are mostly concentrated in storage vesicles of pre-synaptic nerve terminals. The vesicles mediate the release of catecholamines following action potentials

through voltage-gated exocytosis mediated by calcium. Briefly, action potentials cause the opening of voltage-gated Ca^{2+} channels in the pre-synaptic nerve terminals. An influx of calcium into the terminal promotes vesicular fusion to the neuronal membrane and causes release of its contents into the extraneuronal space. Despite the changes in activity of catecholamine neurons, the concentration of catecholamines within nerve terminals remains relatively constant. This is achieved through upregulation of expression of TH and β-hydroxylase enzymes (Verheij and Cools, 2008).

Free catecholamines within the nerve terminal, which are not protected by vesicular storage, are either recycled back into pre-synaptic terminals by transmembrane transporter molecules (e.g., the DA 12-transmembrane transporter molecule) or inactivated by MAO or catechol-*O*-methyltransferase (COMT) enzymes. MAO is a flavin-containing enzyme found on the outer membrane of mitochondria and functions by oxidatively deaminating catecholamines to aldehydes, which can then be converted to acids by aldehyde dehydrogenase or reduced to glycols by aldehyde reductase. The enzyme COMT, which is found in all cells including erythrocytes, inactivates catecholamines by introducing a methyl group donated by *S*-adenosyl methionine. For example, COMT metabolizes DA to homovanillic acid, which can be excreted through urine.

A variety of signalling pathways are activated by catecholamines (Vallone et al., 2000). Catecholamine receptors, which are present on pre-synaptic and post-synaptic neurons, bind ligands and transmit signals via G proteins. Rapid intracellular processes mediated by catecholamines include regulation of ion channels or modulation of neuronal

firing rate, which affect neuronal function and response to neurotransmitters. Long-term effects of catecholamines on neuronal function are exerted by changes in gene expression which may affect the rate of synthesis of receptors, ion channels, and other proteins in the cell.

1.2 Dopamine overview

DA is the most abundant neurotransmitter in the CNS and constitutes 80% of the catecholamine content in the brain (Vallone et al., 2000). DA neurons project to various structures in the forebrain and are essential for vital motor, cognitive and motivational CNS functions, including voluntary movement, sleep, feeding, reward, attention, working memory and learning (Beaulieu and Gainetdinov, 2011). Dysregulation of the dopaminergic systems in the brain has been linked to multiple neurological and neuropsychiatric disorders. One such disorder related to DA-dysfunction is Parkinson's disease (PD), which is a progressive degenerative movement disorder resulting from the loss of striatal DA innervations in the brain (Ehringer and Hornykiewicz, 1960). DA has also been implicated in disorders such as schizophrenia, depression, attention-deficit hyperactivity disorder, Huntington's disease, and Tourette's syndrome (Beaulieu and Gainetdinov, 2011). In peripheral tissues, aberrations in DA activity have been linked to several somatic disorders, including hypertension and kidney dysfunction (Beaulieu and Gainetdinov, 2011). It is evident that DA is involved in many critical functions and significant research has been conducted in order to elucidate the neuroanatomy of DA systems as well as the structure and function of DA receptors.

1.2.1 Dopamine Neuron Systems

Dopaminergic innervations are the most prominent in the brain and are localized in nine distinct cell groups from the mesencephalon to the olfactory bulb (Cave and Baker, 2009). These neurons give rise to four dopaminergic projection pathways: 1. nigrostriatal; 2. mesolimbic; 3. mesocortical; and 4. tuberoinfundibular. The dopaminergic neurons in the substantia nigra pars compacta (SNc), which are the A9 neurons, project mainly to the striatum and terminate at the caudate and the putamen regions (Vallone et al., 2000). The DA neurons of the SNc also innervate extrastriatal basal ganglia nuclei (e.g., subthalamic nucleus) and play important roles in basal ganglia motor control (Hassani et al., 1997). The A10 neurons of the ventral tegmental area (VTA) project along the mesolimbic and mesocortical pathways to limbic and cortical areas which play roles in emotional control and learning (Chinta and Andersen, 2005). The mesolimbic dopaminergic system is characterized by VTA projections to the nucleus accumbens, olfactory tubercle, septum, amygdala, and hippocampus, whereas the mesocortical dopaminergic system is described by medial VTA projections to prefrontal, cingulate, and perirhinal cortices (Chinta and Andersen, 2005). Since there is considerable overlap between the mesocortical and mesolimbic neuronal projections, the two systems are often referred to collectively as the mesocorticolimbic system. The fourth dopaminergic pathway, the tuberoinfundibular pathway, involves transmission of DA from the hypothalamus to the pituitary gland and plays a role in the secretion of certain hormones, including prolactin (Vallone et al., 2000).

1.2.2 Dopamine receptors

Dopamine exerts its physiological actions by acting on a family of related G protein-coupled receptors (GPCRs) (Vallone et al., 2000). The receptors are divided into two major groups and include the D1 and D2 dopamine receptor classes. This classification was based on early findings that D1, but not the D2 receptor class, has the ability to couple to adenylyl cyclase (AC) and modulate cyclic adenosine monophosphate (cAMP) production (Spano et al., 1978). Further molecular biology approaches, including cloning of DA receptor families, have identified multiple DA receptor subtypes based on their structural and pharmacological properties. These include the D1-class DA receptors which are the D1 and D5 receptors and the D2-class DA receptors which are the D2, D3, and D4 receptors (Beaulieu and Gainetdinov, 2011). Although the D1 and D2 DA receptor classes have distinct pharmacological properties, they share a high level of homology in their transmembrane domains, including phosphorylation and palmitoylation sites on C-terminal regions which may be responsible for receptor desensitization and formation of a putative fourth intracellular loop (Beaulieu and Gainetdinov, 2011).

All DA receptors are characterized by a seven transmembrane-spanning domain structure owing to a high-degree of similarity in their primary amino acid sequences. Intracellular signalling is mediated via heterotrimeric G proteins and receptor function has typically been associated with regulation of cAMP and protein kinase A (PKA). The D1-class DA receptors couple to the $G\alpha_{s/olf}$ family of G proteins and stimulate cAMP production through activation of AC (Beaulieu and Gainetdinov, 2011). This class of receptors is localized to post-synaptic sites on DA-receptive cells, such as on striatal γ-

aminobutyric acid (GABA) medium spiny neurons. In contrast, the D2-class DA receptors couple to the $G\alpha_{i/o}$family of G proteins, which leads to an inhibition of AC and a decrease in cAMP production. Interestingly, members of this DA receptor class such as the D4 receptors are expressed both pre-synaptically and post-synaptically on DA neurons and DA target cells, respectively (Rondou et al., 2010). The D2-class receptors also differ in their genetic structure from the D1-class receptors due to the presence of several introns in their coding regions (six for D2, five for D3, and three for D4 dopamine receptors); this structure allows for generation of alternative splice variants of the D2-class receptors (Gingrich and Caron, 1993). Indeed, the D2 DA receptor has at least two splice variants, the D2-short and the D2-long receptors, which have shown differences in localization (e.g., D2-short is present pre-synaptically; D2-long is expressed post-synaptically) and pharmacological properties (De Mei et al., 2009).

DA receptors display a wide range of expression patterns in the brain and the periphery. Of the D1-class of DA receptors, the D1 receptors are expressed mainly in the nigrostriatal, mesolimbic and mesocortical areas such as the caudate-putamen (striatum), nucleus accumbens, substantia nigra, olfactory bulb, amygdala and frontal cortex, while the D5 receptors show low levels of expression in multiple regions including the premotor cortex, substantia nigra, hypothalamus, hippocampus and the dentate gyrus (Rankin et al., 2010). Of the D2-class of DA receptors, the D2 receptors show high levels of expression in the striatum, nucleus accumbens, and olfactory tubercle and have also been found in the substantia nigra, VTA, hypothalamus, amygdala and hippocampus (Vallone et al., 2000). The D3 receptors have also shown sparse expression in the

striatum, SNc, and the VTA; however, the highest level of D3 receptor expression has been observed in limbic areas such as the nucleus accumbens (Beaulieu and Gainetdinov, 2011). The D4 receptor is sparsely expressed in the brain in areas such as the frontal cortex, amygdala, substantia nigra pars reticulata, and globus pallidus (Rondou et al., 2010). In terms of the peripheral expression of the D1 and the D2 classes of DA receptors, they have been found in varying proportions in the heart, blood vessels, gastrointestinal tract, kidneys, adrenal glands and sympathetic ganglia (Beaulieu and Gainetdinov, 2011). The expressional patterns of DA receptors throughout the body support the concept that DA receptors play a role in a wide variety of physiological processes.

The functions of the different classes of DA receptors have been extensively studied. The various DA receptor subtypes in the brain participate in locomotion, attention, decision making, impulse control, motor learning, reproductive behaviour and regulation of food intake (Rondou et al., 2010). Examples of other functions mediated by DA receptors outside the CNS include participation in vision, olfaction, hormonal regulation (e.g., secretion of renin from kidneys, which is mediated by D1 DA receptors), blood pressure regulation and gastrointestinal motility (Beaulieu and Gainetdinov, 2011).

The control of locomotor activity by DA, which has been widely studied, is mediated by the D1, D2, and D3 DA receptors (Missale et al., 1998). In contrast, the D4 and D5 receptors do not seem to be critical for movement control. Locomotor activity is stimulated by the activation of D1 DA receptors on post-synaptic neurons. The roles of the D2 DA receptors in locomotion are variable and depend on their expression patterns.

Thus, activation of pre-synaptic D2 DA receptors leads to a decrease in DA release and inhibits locomotor activity, while stimulation of the post-synaptic receptors potentiates locomotor activity (Missale et al., 1998). As well, the D2 DA receptors play a role in regulating pre-synaptic firing rate and synthesis and release of DA in response to extracellular neurotransmitter levels (Beaulieu and Gainetdinov, 2011). The role of D3 DA receptors in locomotion is somewhat less clear, but it has been suggested that these receptors may inhibit locomotion through autoreceptor functions or post-synaptic receptor-mediated mechanisms (Joseph et al., 2002). The D3 DA receptors also participate in reward and reinforcement mechanisms and are a major topic of interest in drug addiction research. Other notable roles of the DA receptors, such as the D1 and D2 DA receptors, include involvement in learning and working memory mechanisms mediated by the prefrontal cortex (Goldman-Rakic et al., 2004). Evidence has also pointed to the possible role of D2 DA receptors in psychotic reactions in schizophrenia and bipolar disorder due to the fact that most clinically effective anti-psychotic medications block D2 DA receptors (Roth et al., 2004). Indeed, much of the attention has been focused on the D1 and D2 DA receptors due to their important roles in the CNS. Further study of the physiological roles of the D3, D4 and D5 receptors may provide greater understanding of the integrated roles of DA in the brain and lead to more refined pharmacological interventions for dopaminergically-driven disorders.

1.2.3 Dopamine in human diseases

Numerous studies have focused on the impact of DA cytotoxicity in neurodegenerative diseases such as PD, as well as other impairments including mitochondrial dysfunction, oxidative stress and aberrations to the ubiquitin-proteasome systems (Miyazaki and Asanuma, 2009). DA is usually stable within synaptic vesicles, however, it may become cytotoxic following damage to DA neurons. This process may lead to the spontaneous oxidation of excess cytosolic DA or $_{L}$-DOPA to superoxide anions, DA quinones, or DOPA quinones (Tse et al., 1976). DA quinones can also arise from enzymatic oxidation of DA by several enzymes including prostaglandin H synthase, lipoxygenase, tyrosinase and xanthine oxidase, which may result in neurotoxicity (Miyazaki and Asanuma, 2009). Further, DA quinones can be oxidized to form cyclized aminochromes (e.g., DA-chrome), which can then be polymerized to form melanin. DA quinones exert their cytotoxic action by targeting various bioactive molecules. It is well known that DA or DOPA quinones catalyze irreversible covalent modifications of proteins with cysteine residues, forming 5-cysteinyl-DA or 5-cysteinyl-DOPA reaction products, which inhibit protein function (Miyazaki and Asanuma, 2009). The cytotoxicity caused by quinones is related to representative hypotheses of PD. DA quinones cause inflammation and may be linked to degeneration of dopaminergic neurons through the following mechanisms: quinones attack mitochondria in the brain, reduce its function, and open mitochondrial permeability transition pores (Berman and Hastings, 1999). Quinones also lead to formation of ubiquitin and α-synuclein-positive inclusions leading to death of DA neurons (Fornai et al., 2003). More recently, DA has been directly linked

to PD through its ability to covalently modify and functionally inactivate the Parkin protein, which is involved in familial PD (LaVoie et al., 2005). Further, DA or $_{L}$-DOPA quinones can react with tyrosine residues of α-synuclein or lysine residues to firm a Schiff base and inhibit conversion of toxic protofibrils to fibrils, which may cause destruction of synaptic vesicular membranes (Volles et al., 2001). As well, the damage to proteins by DA quinones may be potentiated by dysfunctional protective mechanisms, which may involve molecular chaperone proteins. Indeed, DA-induced neurotoxicity may be an important factor in the pathogenesis and progression of PD.

1.3 Parkinson's Disease

1.3.1 Clinical characteristics and challenges in Parkinson's disease research

PD is a progressive neurodegenerative disorder characterized by various motor and non-motor clinical symptoms. 1-2% of the population is affected by PD and it is estimated that the number of cases will double by 2050 (Schapira, 2009). PD is characterized by selective degeneration of the nigrostriatal pathway, loss of dopaminergic neurons, and the appearance of Lewy bodies in surviving neurons (Yao and Wood, 2009). Despite the apparent simplicity of this disease model, scientists have encountered significant challenges in developing disease-modifying treatments for this disorder. Perhaps one of the stumbling blocks may have been the realization that many of the non-motor features of PD are not necessarily due to the degeneration of the dopaminergic transmitter system (Lang and Obeso, 2004). Interestingly, it has been found that 30-50% of non-DA neurons are also lost by end-stage of PD. These include cholinergic cells in

the nucleus basalis of Meynert (e.g., related to cognitive deficits), monoaminergic cells in locus coeruleus, cells of the pedunculopontine tegmental nucleus (e.g., associated with gait problems), and hypothalamic hypocretin cells (e.g., related to sleep disorders in PD) (Obeso et al., 2010). As well, there have been difficulties in developing a sustainable therapeutic for PD. The predominant therapy for PD (e.g., $_{L}$-DOPA), which has been used for the past 30 years, has been shown to lose efficacy and lead to dyskinesias and behavioural problems. Another consideration in the PD puzzle is the lack of definitive biomarkers and reliable, standardized tests for diagnosis of PD in its early stages. Furthermore, current diagnostic methods for PD, which are based on clinical interviews, are often unreliable and flawed. A 1999 study in Wales found that 25% of 402 patients on medication for PD had no Parkinsonism (Maera et al., 1999). In addition, recent research has given support to the heterogeneous view of the disease, which includes various subtypes of PD based on the age of onset, clinical features as well as the rate of progression (Selikhova et al., 2009). Distinguishing between the tremor-predominant form of PD, which is observed in the younger population and leads to a slow decline of motor function, versus the "postural imbalance and gait disorder" form, which worsens more rapidly and is observed in people over seventy years of age, may be useful for future development of individualized therapies.

Several studies have suggested that PD may be preceded by premotor abnormalities. These include olfactory dysfunction, cardiac sympathetic denervation, sleep abnormalities, constipation, depression and pain (O'Sullivan et al., 2008). Longitudinal studies may be useful in examining individuals with such premotor

symptoms and determining their risk of developing the disease. As well, such studies may uncover biomarkers for early diagnosis and provide opportunities for certain lifestyle modifications, which may delay the onset of motor problems in PD.

The primary factors that cause disability in PD are gait dysfunction, balance problems, swallowing and speech difficulties, autonomic disturbances and cognitive decline (Schrag et al., 2007). Other motor features including tremors, rigidity and akinesia, which seem to be related to the loss of striatal DA, can be largely reduced with dopaminergic drug treatment and functional neurosurgeries (Obeso et al., 2010). It is estimated that 30-80% of individuals with PD suffer from related dementia, which significantly affects their quality of life (Aarsland et al., 2008). The mechanisms of cognitive decline in PD could be further studied by incorporating current knowledge about the roles of striatofrontal and hippocampal pathways in PD and utilizing neuroimaging tools in conjunction with neuropsychological and anatomical analyses (Beauchamp et al., 2008).

1.3.2 Mechanisms and pathways of Parkinson's disease

Significant research has been conducted in order to discover a unifying mechanism that accounts for neurodegeneration that occurs in PD (Obeso et al., 2010). Thus far, researchers have not been able to determine a single cause for PD. Most cases of PD seem to be idiopathic and specific environmental factors responsible for the disease have yet to be discovered. One example of neuronal degeneration of the dopaminergic system in the SNc caused by environmental factors is intoxication with 1-methyl-4-phenyl-1, 2, 3, 6-tetrahydropyridine (Obeso et al., 2010). Still, the clinical and

pathological consequences of this toxin do not fully mimic those that occur in PD (Obeso et al., 2010). Other environmental factors may also contribute to the vulnerability of the substantia nigra to cell death and degeneration by causing mitochondrial dysfunction and oxidative stress. As well, abnormalities in protein function seen in PD may be caused by defective molecular chaperone proteins (Obeso et al., 2010).

Considerable efforts have been made to uncover genes that are responsible for PD. It is estimated that 2-3% of late-onset cases and about 50% of the early-onset cases of PD are due to genetic mutations (Farrer, 2006). Mutations in three genes have been linked to late-onset PD with Lewy body pathology: *SNCA*, which encodes α-synuclein; *LRRK2*, which encodes leucine-rich repeat kinase 2; and *EIF4G1,* which encodes elongation factor 4G1 (Obeso et al., 2010). It is suggested that mutations which cause an overexpression in α-synuclein may be especially harmful since this protein has been linked to toxicity in dopaminergic neurons as well as the development of non-motor symptoms (Farrer et al., 2004). Mutations in the *LRRK2* gene, which encodes a large protein that has been suggested to play crucial roles in adult neurogenesis and dopaminergic signalling, represent the highest risk for the development of familial PD (Zimprich et al., 2004). Other mutations that have been specifically linked to early-onset PD, which affects individuals under 45 years of age, have been characterized as recessive loss-of-function mutations in genes encoding the proteins Parkin, PINK1, and DJ-1. Parkin plays a role in autophagic degradation of dysfunctional mitochondria while PINK1 is a mitochondrial protein kinase (Obeso et al., 2010). Expression of both Parkin and PINK1 in animal models appears to induce mitochondrial fission and promotes the

survival of nigrostriatal neurons (Lutz et al., 2009). DJ-1 mutations are not very common; however, they affect a protein involved in redox sensing and may leave cells vulnerable to oxidative damage (Obeso et al., 2010). Continuing to study genetic components such as those described above may increase the understanding of molecular pathways as well as provide clues for mechanisms of SNc death and roles of Lewy bodies in the pathology of PD, which are still largely unknown.

1.3.3 Therapeutic approaches in Parkinson's disease

$_{L}$-DOPA has been the mainstay of PD therapy for the past four decades. While initially being able to compensate for the loss of dopaminergic neurons, $_{L}$-DOPA fails to halt disease progression and eventually leads to motor complications as well as psychiatric problems such as hallucinations and delirium (Obeso et al., 2010). The development of DA agonists, which are used in early stages of the disease, along with atypical neuroleptics (e.g., clozapine) has somewhat alleviated these problems and improved the therapeutic outcomes of PD patients.

Furthermore, the development of valid animal models has opened up new avenues for investigation of potential therapies for PD. One of the traditionally used models for studying the disease has been the 6-hydroxydopamine (6-OHDA) animal model (Ungerstedt and Arbuthnott, 1970). 6-OHDA is a neurotoxin that selectively accumulates in the dopaminergic neurons of the substantia nigra and causes cellular dysfunction and neuron death through exacerbating oxidative stress and impairing mitochondrial function (Simola et al., 2007). The standard approach for creating a 6-OHDA animal model (e.g.,

in mice, rats, cats and primates) was first developed by Ungerstedt in 1968, who injected 6-OHDA bilaterally into the substantia nigra of rats and observed features of PD such as akinesia and high mortality rate. This approach was soon followed by the development of a unilaterally-lesioned 6-OHDA rat model of PD, where the toxin was injected into the medial forebrain bundle (MFB), resulting in akinesia and typical rotational behaviour "away" from the lesion (e.g., contralateral rotational behaviour) in response to dopamine mimetic agents (e.g., apomorphine) (Ungerstedt and Arbuthnott, 1970). In contrast, the response to drugs which enhanced DA levels, such as amphetamine, caused ipsilateral rotational behaviour directed towards the side of the body which was depleted of DA (Simola et al., 2007). This property of drug-induced rotational behaviour of the 6-OHDA model has become a useful tool for investigating the effects of different pharmacological therapies for PD. In particular, it has been well established that the ability of a compound to induce contralateral rotational behaviour in the unilaterally-lesioned 6-OHDA model directly correlated with its ability to improve PD symptoms and motor impairments (Dauer and Przedborski, 2003). Thus, animal models represent a useful tool for investigating the biochemical pathogenesis of PD and may lead to development of new disease-modifying therapies.

1.4 Proteins of Interest: Molecular chaperones

1.4.1 Molecular chaperone proteins and heat-shock proteins

Molecular chaperone proteins are essential for multiple cellular functions including protein quality control and maintenance of protein homeostasis (Chang et al.,

2007). In the cell, proteins are susceptible to changes in conformation which may alter their function and cause them to aggregate into cytotoxic complexes. Molecular chaperones function by preventing protein aggregation by using adenosine triphosphate (ATP) as energy to drive conformational changes that are necessary for refolding their particular targets (Soti et al., 2005). Furthermore, molecular chaperones may solubilise initial protein aggregates and aid in the folding of nascent proteins as they are synthesized by ribosomes (Ellis, 1987). As well, they may control protein-protein interactions by influencing conformational changes. In cases where cellular proteins are extensively damaged and where molecular chaperones cannot help to refold the proteins, they may function in targeting the proteins for degradation by facilitating their transfer to proteolytic systems or sequestering the damaged proteins into larger aggregates (Soti et al., 2005).

Numerous classes of molecular chaperones have been described thus far. Many of these proteins are known as heat-shock proteins (Hsp) or stress proteins because it has been found that various cellular stresses upregulate their expression. These may include heat-shock, exposure to heavy metals, protein kinase C (PKC) activators, amino acid analogues, calcium increasing agents, ischemia, microbial infections and various hormones (Kiang and Tsokos, 1998). Different families of molecular chaperone proteins are classified according to their molecular weights and include the Hsp40, Hsp60, Hsp70, Hsp90, Hsp100, and small Hsp proteins (Kiang and Tsokos, 1998). Heat-shock proteins are expressed in the cytosol, nucleus, mitochondria the endoplasmic reticulum and typically have long half-lives of about 48 hours (Kiang and Tsokos, 1998). The heat-

shock protein 70 kDa (Hsp70) family represents one of the most ubiquitous classes of molecular chaperones. These proteins are highly conserved and may be constitutively expressed or upregulated by various stressors (Chang et al., 2007). The Hsp70 family plays a role in assisting in *de novo* folding of proteins as well as protein trafficking and targeting of misfolded proteins for proteolytic degradation (Chang et al., 2007). They function in collaboration with the Hsp40 or DnaJ family of proteins as well as various nucleotide-exchange factors in ATP-driven reactions (Mayer et al., 2000). Hsp70 assist in *de novo* folding of proteins by binding to nascent chains through allosteric coupling of its N-terminal ATPase domain (~40 kDa) with the peptide-binding domain (~25 kDa) which is located at the C-terminal region (Zhu et al., 1996). The C-terminal domain consists of a β-sandwich subdomain that recognizes hydrophobic segments of approximately 7 amino acid residues and an α-helical lid which regulates ATP-binding (Hartl and Hayer-Hartl, 2009). When ATP is bound to the Hsp70, the α-helical lid adopts an open conformation which represents low affinity for peptides. Interaction of Hsp70 with Hsp40 (e.g., the J domain of Hsp40) leads to closure of the α-helical lid by promoting the hydrolysis of ATP to adenosine diphosphate (ADP), which increases affinity and leads to stable binding of peptides (Hartl and Hayer-Hartl, 2009). Once ATP is hydrolyzed, nuclear exchange factors (e.g., Bag, HspBP1 and Hsp110 in eukaryotes) interact with the N-terminal ATPase domain of Hsp70 to catalyze the ADP-ATP exchange, which leads to lid opening and release of substrates (Hartl and Hayer-Hartl, 2009).

Molecular chaperone proteins are emerging as important factors in a number of human disorders such as Alzheimer's, PD, and Huntington's which share the common

characteristics of aberrant protein folding (Kaul et al., 2007). For example, it has been found that increasing the levels of heat-shock proteins such as those of the Hsp70 family can inhibit the formation of soluble oligomeric cytotoxic proteins which cause protein aggregation and dysfunction in these disorders (Auluck et al., 2002; Muchowski and Wacker, 2005). Further study is required to increase the understanding of cellular chaperone networks and ways in which they may be manipulated to serve as possible therapeutic factors in human diseases where protein homeostasis has been impaired.

1.4.2 Mortalin/Mitochondrial Heat-Shock Protein 70

Mortalin, also known as mortalin-2 or mitochondrial heat-shock protein 70, is an essential ubiquitously expressed molecular chaperone with multiple roles which include the following: participating in mitochondrial biogenesis, maintaining mitochondrial protein integrity, and aiding in import of mitochondrial proteins into the matrix via formation of ATP-dependent motors (Deocaris et al., 2008). Recently, mortalin has been implicated in neurogenesis and neurodegeneration processes (Deocaris et al., 2008). As well, mortalin has been linked to diseases such as Parkinson's, Schizophrenia, Alzheimer's and Huntington's (Deocaris et al., 2008). Also, since mortalin has been found to exert various cytoprotective functions that permit cell survival under stressful conditions, it has been implicated in cancer and aging systems (Kaul et al., 2007).

Mortalin consists of 649 amino acids and is encoded by the nuclear gene HSPA9B located on chromosome 5q31.1.1 (Kaul et al., 2007). Mortalin localization depends on the proliferative state of the cell; in normal cells, mortalin is distributed in a pancytoplasmic

manner, while in immortal cells, mortalin is found in the perinuclear zone (Deocaris et al., 2008). There have been numerous studies that have examined the possible functions of mortalin. It has been suggested that mortalin may have the potential of causing cellular proliferation through its interaction with the tumour suppressor protein (p53) via its N-terminal domain (Deocaris et al., 2008). Further, mortalin expression was found to be elevated in many human cancers including brain cancer, colon cancer and leukemia (Kaul et al., 2007). As well, it has been shown that increased levels of mortalin increase malignancy of breast carcinoma cells (Wadhwa et al., 2006). Mortalin has recently been implicated in the aging process. Studies have shown reduced levels of mortalin expression in senescent human fibroblasts and in aged worms, suggesting that the ability of mortalin to perform its various functions as well as to control cellular proliferation declines in the aging process (Deocaris et al., 2008; Kimura et al., 2007). Mortalin has also been studied as a possible biomarker for brain ischemia, as it is upregulated following brain injury (Deocaris et al., 2008). It is suggested that mortalin may serve a protective function in ischemia by limiting the accumulation of reactive oxygen species (ROS) in neurons (Liu et al., 2005). Furthermore, studies have shown that mortalin has the ability to interact with the apoptosis-inducing factor (AIF) (Sun et al., 2006). Normally, when AIF is released from the mitochondria, it may be translocated to the nucleus where it can cause caspase-independent apoptosis. It has been suggested that mortalin sequesters AIF and thus suppresses cell death (Sun et al., 2006). Interestingly, this protective ability of mortalin was not retained in Hsp70 deletion mutants lacking the C-terminal (Ravagnan et al., 2001). The functionality of the C-terminal of mortalin was

further confirmed in studies by Sun and colleagues (2006) who found that Hsp70 mutants lacking the entire amino-terminal domain and Hsp70 ATPase-deficient point mutants retained the ability to protect primary astrocytes against ischemic insults in vitro as well as to inhibit AIF translocation to the nucleus; this indicated that the C-terminal was indeed sufficient for protection against ischemic brain injury (Sun et al., 2006).

Evidence for the involvement of mortalin in several human diseases has been accumulating over the past decade. Gabriele and colleagues (2010) studied the possible involvement of mortalin in the pathogenesis of Schizophrenia. This study showed that antisense knockdown of mortalin in the medial prefrontal cortex (mPFC), which has been implicated in Schizophrenia, resulted in decreased levels of mortalin in this area, followed by an increase of mortalin in the nucleus accumbens (Gabriele et al.,2010). Since mortalin interacts with DA, reduced concentrations of mortalin in the mPFC correspond to reduced DA activity, while increased concentrations of mortalin in subcortical brain regions such as the nucleus accumbens correspond to DA overactivity (Gabriele et al., 2010). The corresponding behavioural alterations that were observed as a result of knockdown of mortalin in the mPFC were significant deficits in DA-dependent behaviours such as pre-pulse inhibition (PPI) (Gabriele et al., 2010). PPI assesses the startle response evoked by a loud acoustic pulse tone and it has been previously used to measure sensorimotor gating deficits in patients with Schizophrenia (Gabriele et al., 2010). Further, similar deficits in PPI have also been observed in established animal models of Schizophrenia (Gabriele et al., 2010). Mortalin is thus responsible for regulating DA-dependent behaviours in the

brain and may play an important role in the pathogenesis of Schizophrenia (Gabriele et al., 2010).

Mortalin has also been implicated in several neurodegenerative diseases such as Alzheimer's disease, and PD, which are thought to be associated with old age. As well, these diseases are associated with abnormal polypeptides which can form insoluble neurotoxic protein aggregates leading to cell death (Kaul et al., 2007). Also, there are notable defects in ubiquitin-proteasome degradation systems and responses to oxidative stress (Kaul et al., 2007). Osorio and colleagues (2007) showed differential expression of mortalin isoforms in hippocampi of Alzheimer's patients. In another study using an animal model of Alzheimer's disease, the ApoE knockout mouse model, it was shown that mortalin sustained Alzheimer's-associated oxidative damage, suggesting the involvement of this protein in the pathogenesis of this disease (Choi et al., 2004).

There is also substantial evidence for the involvement of mortalin in PD. Jin and colleagues (2006) demonstrated that mortalin expression was significantly reduced in the SNc of PD patients. As well, *in vitro* experiments with MES cells, which express features of dopaminergic neurons, showed a significant decrease in mortalin levels when the cells were exposed to the mitochondrial Complex 1 inhibitor rotenone (Deocaris et al., 2008). Further *in vitro* studies by Van Laar and colleagues (2008) showed that treatment of PC12 cells with a DA quinone resulted in degeneration of dopaminergic terminals and a decrease in mortalin levels as well as reduction of mitochondrial proteins that may play important roles in PD.

Recent studies by Shi and colleagues (2008) showed decreased levels of mortalin levels in mitochondria from post-mortem PD patients' substantia nigra brain samples. It is suggested that these reductions in mortalin may be a result of oxidative modification and protein damage that occurs in PD. Mortalin has even been found to associate with DJ-1, a gene responsible for a familial form of PD, and translocate to mitochondria in response to oxidative stress (Li et al., 2005). These observations were further confirmed in studies by Jin and colleagues (2007), who found that mortalin associates with not only DJ-1, but α-synuclein as well. These observations are significant because it is known that α-synuclein causes certain forms of sporadic PD (Jin et al., 2007).

Studies using 6-OHDA animal models of PD have also linked mortalin as an important factor in the disease progress. Weiss and colleagues (2006) injected human umbilical cord matrix stem cells into the striatum of 6-OHDA lesioned rats and observed that this manipulation was able to elicit complete alleviation of rotational symptoms that were previously induced by injection of apomorphine. Interestingly, upon proteonomic analysis, the authors found that mortalin was highly expressed in the umbilical cord matrix stem cells, lending support to the involvement of mortalin in PD pathology (Weiss et al., 2006). Despite the crucial roles of mortalin that have been demonstrated in these studies, it is difficult to conjure up a possible therapeutic role of mortalin in PD due to its functions in cell cycle regulation and its evident association with human cancers.

1.4.3 Catecholamine-Regulated Protein 40 (CRP40)

Early studies from our laboratory on catecholamine-regulated proteins reported the presence of three distinct brain-specific chaperone-like proteins with molecular weights of 26, 40, and 47 kDa, which were isolated based on their ability to bind DA and structurally related catecholamines (Ross et al., 1993; Ross et al., 1995). Further investigation confirmed the novel nature of these proteins as pharmacological and biochemical studies did not reveal similarities to other known catecholamine binding proteins or receptors in the brain (Modi et al., 1996). In 2001, Nair and Mishra cloned CRP40 from the bovine brain (GenBank #AF047009) and it was found that the novel protein shares significant structural homology with the human Hsp70 family of proteins including Hsp70 or mortalin (Genbank #BC024034) and Hsc70 (GenBank #NM006389) as well as proteins from other species including the rat and SH-SY5Y cells. Further, immunolocalization studies using SH-SY5Y cells revealed CRP40 colocalization with DA in vesicles (Nair and Mishra, 2001). Indeed, CRP40 has functional specificity for catecholamines as it associates with DA, epinephrine, and norepinephrine but not with other amines such as serotonin. Nair and Mishra (2001) also revealed that bovine CRP40 expression is induced following exposure to heat-shock in SH-SY5Y cells, as seen with Hsp70. Further, CRP40 expression was also increased when SH-SY5Y cells were treated with excess DA, suggesting that CPR40 may share crucial properties with other heat-shock proteins such as mortalin, including protective roles in oxidative stress (Nair and Mishra, 2001). These hypotheses were further strengthened by the fact that treatment of cells with CRP40 following heat-shock resulted in decreased protein denaturation and

aggregation compared to non-treated controls (Nair and Mishra, 2001). As well, immunofluorescence analyses showed that exposure of SH-SY5Y cells to detrimental DA oxidation caused CRP40 translocation to the nucleus, further implicating CRP40 as a protective, catecholamine-specific heat-shock protein (Nair and Mishra, 2001).

Early studies to determine the specific localization of CRP40 in the brain were performed by Ross and colleagues (1995) using covalent affinity labelling techniques. A newly formulated substance, the 6-hydroxy-[^{125}I]iodo-[*N*-(*N*-2′,4′-dinitrophenyl)aminopropyl]-2-amino-1,2,3,4-tetrahydronaphthalene, was used to specifically label catecholamine-related proteins (Ross et al., 1995). The experiments showed that the concentration of catecholamine-regulated proteins in the brain was the greatest at the striatum, followed by nucleus accumbens, olfactory tubercle, frontal cortex, hypothalamus, hippocampus, and lastly the cerebellum. Interestingly, catecholamine-regulated protein labelling studies on other non-CNS tissues such as skin, muscle, heart, liver, kidney, and spleen showed no expression of these proteins in these areas (Ross et al., 1995). Goto and colleagues (2001) also performed localization studies, specifically on CRP40, and detected the protein in the majority of SNc and striatal neurons. As well, CRP40 was found to colocalize with TH, the rate limiting enzyme in DA synthesis (Goto et al., 2001). These observations suggest that CRP40 may mediate a variety of functions in the nervous system and may be a key player in dopaminergically-driven diseases such as PD through its modulation of DA.

In 2009, Gabriele and colleagues cloned and characterized CRP40 from the human brain. It was found that the human 40 kDa CRP40 belongs to a family of heat-

shock proteins and is a splice variant of mortalin (Gabriele et al. 2009). The human CRP40 displays 100% homology to human mortalin and is expressed from downstream exonic sequences of mortalin (e.g., exons 10-17). Bioinformatic analysis indicated that a promoter region for CRP40 may be contained at intron 9 of mortalin and that the human CRP40 is expressed from the HSPA9 gene (Gabriele et al., 2009). Further studies are required to identify the specific transcription factors and regulatory components necessary for CRP40 expression.

Gabriele and colleagues (2009) also discovered that the human CRP40 shares similar functions to the bovine CRP40 protein. Specifically, CRP40 was found to possess the following chaperone and catecholamine function characteristics: 1) CRP40 prevented thermal aggregation of firefly luciferase, suggesting its ability to protect cells from oxidative stress; 2) Overexpression of CRP40 in heat-shocked cells decreased protein denaturation and aggregation and increased cellular viability, indicating molecular chaperone-like functions; 3) CRP40 was found to bind DA with a low affinity and high capacity profile, which is characteristic of molecular chaperones involved in maintaining cellular protein homeostasis.

Several studies were performed in order to elucidate the function of the human CPR40. Gabriele and colleagues (2009) showed that treatment of cells with a D_2 receptor antagonist commonly used for Schizophrenia (e.g., haloperidol) caused the predicted increase in free synaptic DA, along with modulation of CRP40 levels, which increased significantly following haloperidol treatment in comparison to untreated cells. These results were also consistent with those observed in animal models. Sharan and colleagues

(2001) showed differential modulation of CRP40 by DA D1 and D2 receptor antagonists following chronic treatment of rats with haloperidol and a D1 receptor antagonist, SCH23390. They found that haloperidol treatment induced marked increases in striatal CPR40, while treatment with the D1 receptor antagonist caused a decrease in striatal CPR40 (Sharan et al., 2001). These studies suggested that the CRP40 is differentially modulated by DA receptor antagonists.

Subsequent studies also discovered that CRP40 may be modulated by DA receptor agonists and psychotropic drugs. Gabriele and colleagues (2002) found that chronic, but not acute, d-amphetamine treatment of rats increased the expression of CRP40 in the striatum and the nucleus accumbens brain areas. Furthermore, when the expression levels of Hsp70 were examined following a similar treatment with d-amphetamine, no significant changes in Hsp70 expression were observed, indicating that the modulatory effects of d-amphetamine were specific to the CPR40 protein (Gabriele et al., 2002). These findings were supported by studies examining the differential effects of cocaine treatment on CPR40 expression versus Hsp70 expression, which again showed specificity towards the CPR40 protein. Sharan and colleagues (2003) found that acute cocaine treatment increased CRP40 expression in the nucleus accumbens and striatum of rats, whereas chronic cocaine treatment increased CRP40 expression in the nucleus accumbens only. In contrast, cocaine treatment did not affect Hsp70 levels (Sharan et al., 2003). Further, it was hypothesized that the rise in CRP40 expression was due to increased protein synthesis, and not protein translocation, since pre-treatment with a protein synthesis inhibitor (e.g., anisomycin) inhibited the increase in CRP40 levels following

cocaine treatment (Sharan et al., 2003). Increased CRP40 expression in response to cocaine, which induces oxidative stress, may indicate that this protein may play a neuroprotective role in the brain.

The differential effects on CRP40 expression in the nucleus accumbens following acute and chronic treatment regimens were further examined by Gabriele and colleagues (2007). It was shown that chronic, but not acute, haloperidol treatment induced an increase in CPR40 levels in the nucleus accumbens core region (e.g., the region that expresses mainly D2 receptors). When the same authors tested the effects of chronic versus acute treatment with quinpirole, a high affinity D2/D3 receptor agonist, they found increased CRP40 levels in the nucleus accumbens shell region (e.g., the region that expresses D1 receptors) following chronic treatment only (Gabriele et al., 2007). Again, the results suggested that modulation by haloperidol and quinpirole was specific to the CRP40 protein, with no effects observed on Hsp70 (Gabriele et al., 2007).

Localization studies on the human form of CRP40 were recently performed by Gabriele and colleagues (2009). Using immunohistochemical techniques, the authors reported cytoplasmic localization of CRP40 in the ventral striatum of healthy post-mortem as well as in drug naïve Schizophrenic patients' brain samples (Gabriele et al., 2009). In contrast, the localization of CRP40 shifted to the nucleus in post-mortem brain samples of haloperidol-treated Schizophrenic patients, which is consistent with mortalin function following cell stress (Gabriele et al., 2009). In this instance, it is hypothesized that the shifted localization of CRP40 to the nucleus may have been due to oxidative stress induced by increased DA concentrations resulting from haloperidol treatment

(Gabriele et al. 2009). The specific role of CRP40 in the nucleus remains to be discovered, however, bioinformatic analysis suggests that CRP40 may possess a leucine zipper motif, which may serve as an activator of transcription (Gabriele et al., 2009).

Several studies have found that CRP40 is expressed solely in the CNS and blood, unlike mortalin which is found ubiquitously (Gabriele et al., 2009; Ross et al., 1995). As well, the CRP40 sequence is identical to the C-terminal region of mortalin and lacks the p53-binding domain which is located on the N-terminus of mortalin (Gabriele et al., 2009). Since CRP40 does not seem to possess the functional properties of mortalin, which regulates cell proliferation, it may be possible to consider CRP40 as a potential therapeutic agent in neurodegenerative diseases.

Along with its potential therapeutic role in neurodegenerative disorders, it is also important to consider the possible use of CRP40 as a biomarker for dopaminergically-driven diseases. In 2005, Gabriele and colleagues measured CPR40 concentrations in schizophrenic, bipolar/depressed, and normal post-mortem brain samples of the ventral striatal area from the Stanley Foundation Neuropathology Consortium and found the following: 1) CRP40 levels were significantly reduced in the brains of schizophrenic patients compared to the healthy control group; 2) There were no significant differences between the CRP40 concentrations in the bipolar, or depressed patients' brain samples when compared to the control group; 3) Un-medicated Schizophrenia patients showed the lowest concentrations of CRP40; 4) CRP40 levels in brain samples of subjects treated with clozapine or haloperidol were slightly higher than those of un-medicated patients, however the levels were still reduced in comparison to normal, healthy controls.

This chapter has illustrated a summary of several studies that suggest that CRP40 may be implicated in neurological disorders. The set of studies presented here sought to determine the potential roles of CRP40 as a biomarker and therapeutic in PD, and further elucidate the functional roles of this molecular chaperone protein.

Chapter 2: The Therapeutic Potential of Catecholamine-Regulated Protein 40 – Cloning and Characterization of CRP40 and its fragments and elucidation of the smallest functional piece of CRP40

2.1 Introduction/Rationale/Hypotheses

Hsp are an emerging area of research in neurodegenerative disorders characterized by aberrant protein folding, mitochondrial dysfunction, and oxidative stress (Soti et al., 2005). A number of studies using *in vitro* and *in vivo* models of PD have already shown that increasing the expression of Hsp, such as Hsp70, can reduce protein misfolding, aggregation, and inhibit apoptosis that leads to the degeneration of dopaminergic neurons (Auluck et al., 2002; Pan et al., 2005; Shen et al., 2005). Hsp are involved in regulating the apoptotic response and protein degradation pathways, including the ubiquitin-proteasome pathway (Kaul et al., 2007). However, the biological functions of these Hsp are largely unknown. There is a critical need to uncover the mechanisms of action of Hsp in order to determine their potential application in neurodegenerative diseases.

Mortalin, the protein related to CRP40 through alternative gene splicing, has been explored as a potential therapy for cancers (Kaul et al., 2007). This protein has been shown to participate in carcinogenesis, through interactions with the p53 tumour suppressor protein (Kaul et al., 2007). Mortalin overexpression in cancer leads to the sequestration of p53 in the cytoplasm and inhibition of its transcriptional activation, causing uncontrolled cellular proliferation (Kaul et al., 2007). It has been proposed that inhibition of mortalin through the use of mortalin-derived synthetic peptides, mortalin immunotherapy, and functional ribonucleic acid (RNA) inhibition using antisense RNA or small interfering RNA could be explored as a therapeutic avenue in various cancers (Kaul et al. 2007). Evidence has also accumulated for mortalin's potential role in neurodegenerative diseases such as PD (Burbulla et al., 2010; Deocaris et al., 2008; Kaul

et al., 2007). However, the potential application of mortalin as a therapy in PD has not been studied extensively. Perhaps efforts in this area have been halted by the knowledge that mortalin regulates cellular proliferation and is involved in cancer (Kaul et al., 2007). The discovery of the related protein, CPR40, and its involvement in PD, has opened up additional avenues for exploration of the biological roles of this protein and its potential applications in neurodegenerative diseases.

Recently, experiments conducted by my colleague Sarah Groleau demonstrated that injection of 100μg of CRP40 into the striatum of hemi-lesioned 6-OHDA rats corrected behavioural impairments, implicating CRP40 as a possible therapeutic for PD and other movement disorders (unpublished data). The 6-OHDA animal model was chosen for this study since this model is characterized by oxidative stress and degeneration of DA neurons, similar to the condition in human idiopathic PD patients (Perese et al., 1989). 6-OHDA animals were prepared by hemi-lateral lesioning of the A9 dopaminergic pathway by injection of the 6-OHDA toxin in the SNc region of the rat brain. This unilateral nigrostriatal degeneration caused asymmetry in motor behaviour due to imbalanced dopaminergic activity between striata (Ungerstedt and Arbuthnott, 1970). The 6-OHDA hemi-lesioned rats displayed a characteristic full-body rotational behaviour in response to dopaminergic agonists, including apomorphine, unlike non-lesioned controls which did not rotate following apomorphine challenge. Baseline rotational behaviour and locomotor testing was performed before surgical intervention. The cloned recombinant CRP40 fusion protein and CRP40 plasmid deoxyribonucleic acid (DNA) were directly injected into the striatum of the 6-OHDA lesioned rats via

stereotaxic surgery. The results clearly showed correction of rotations following apomorphine challenge, relative to sham control animals, at various time-points (Figure 2.1). Previously, our group has shown that 6-OHDA lesioned rats (n=6) display a significant reduction of CRP40 expression in the striatum relative to sham controls, as evidenced by Western immunoblotting (unpublished data). We predict that the correction of behavioural impairments may have been due to the restoration of CRP40 concentrations in the rat brain. Furthermore, injected recombinant mortalin protein and mortalin plasmid DNA also corrected rotations in hemi 6-OHDA rats, but, to a lesser degree, suggesting that the alternate spliced variant CRP40 is more specific for acting on dopaminergic movement disorders (unpublished data; Figure 2.1).

These preliminary findings are important and have the potential to transform future PD therapeutics. However, our group has realized that the large size of CRP40 (e.g., 350 amino acids) will present significant challenges for non-invasive delivery across the blood-brain barrier, which is only permeable to small lipid soluble molecules of ~600 Daltons (Banks, 1999). The current study was designed to circumvent this potential future issue. The objective of this study was to determine whether the CRP40 protein can be cloned into smaller fragments that would be therapeutically-effective in correcting the movement impairments in the 6-OHDA model. This was a complementary study where the design of methods to elucidate the smallest functional piece of CRP40 and subsequent *in vitro* experiments to create potential functional fragments were performed by myself, Jovana Lubarda, and therapeutic efficacy testing *in vivo* was performed by Sarah Groleau. My hypothesis for this study was that using bioinformatics

approaches would identify smaller fragments of CRP40 that could eventually be used to create a therapeutically-effective protein fragment of ~8-10 amino acids that would have the ability to cross the blood-brain barrier. The results of this study describe the development of the methodology to determine the smallest functional fragment of CRP40. Bioinformatics and cloning approaches that were optimized to achieve this initiative (See Figure 2.2 for study plan).

The importance of this study cannot be overstated. The detailed investigation of CRP40 properties that was performed herein has shed light on the potential roles of this protein and has opened up avenues for future investigation of its involvement in signalling roles, and structure-activity relationships, which may have a relevance to PD.

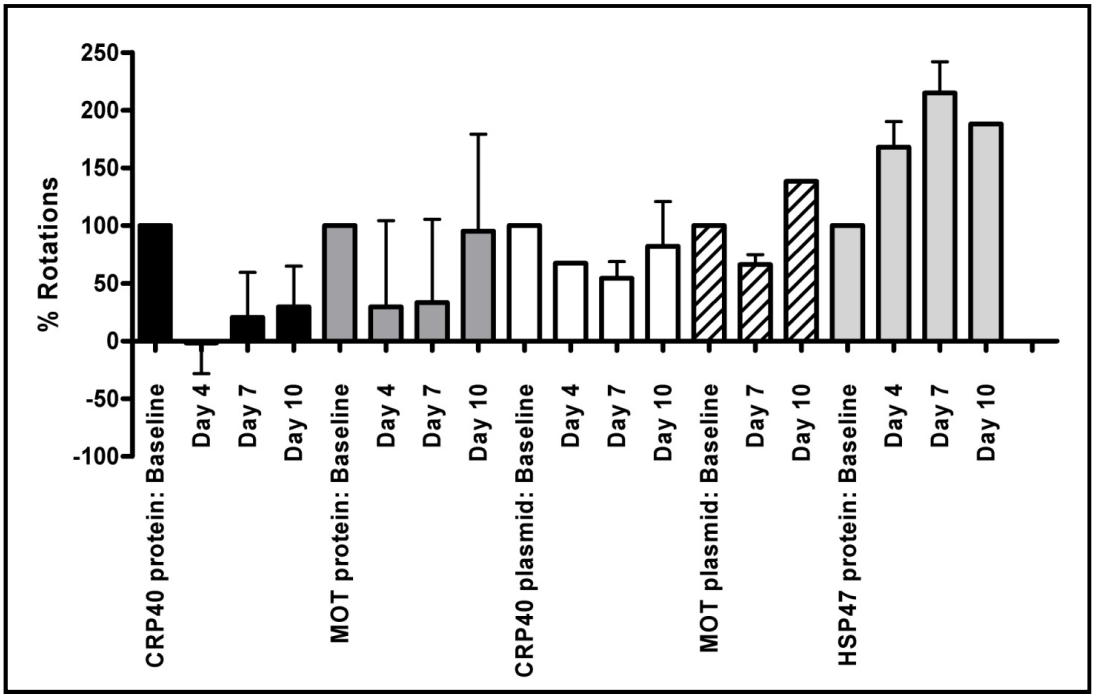

Figure 2.1 Significant reduction in rotational behaviour in animals treated with CRP40 fusion protein or CRP40 plasmid DNA in preclinical animal model (6-hydroxydopamine) of dyskinesia.

FIGURE LEGEND

Figure 2.1: Animals treated with CRP40 protein or CRP40 plasmid DNA displayed significantly less turning behaviour than at baseline, compared to animals treated with negative control protein (Hsp47) ($p<0.05$). CRP40 protein n=2; CRP40 plasmid n=3; mortalin (mot) protein n=2; mot plasmid DNA n=3; Hsp47 protein n=3. Animals treated with mot protein or mot plasmid DNA displayed a pattern of reduced turning behaviour, but this trend was not significant. To view an additional video of experiments, please follow the link: http://cathcart.70ms.com/2011/CRP40/index.html

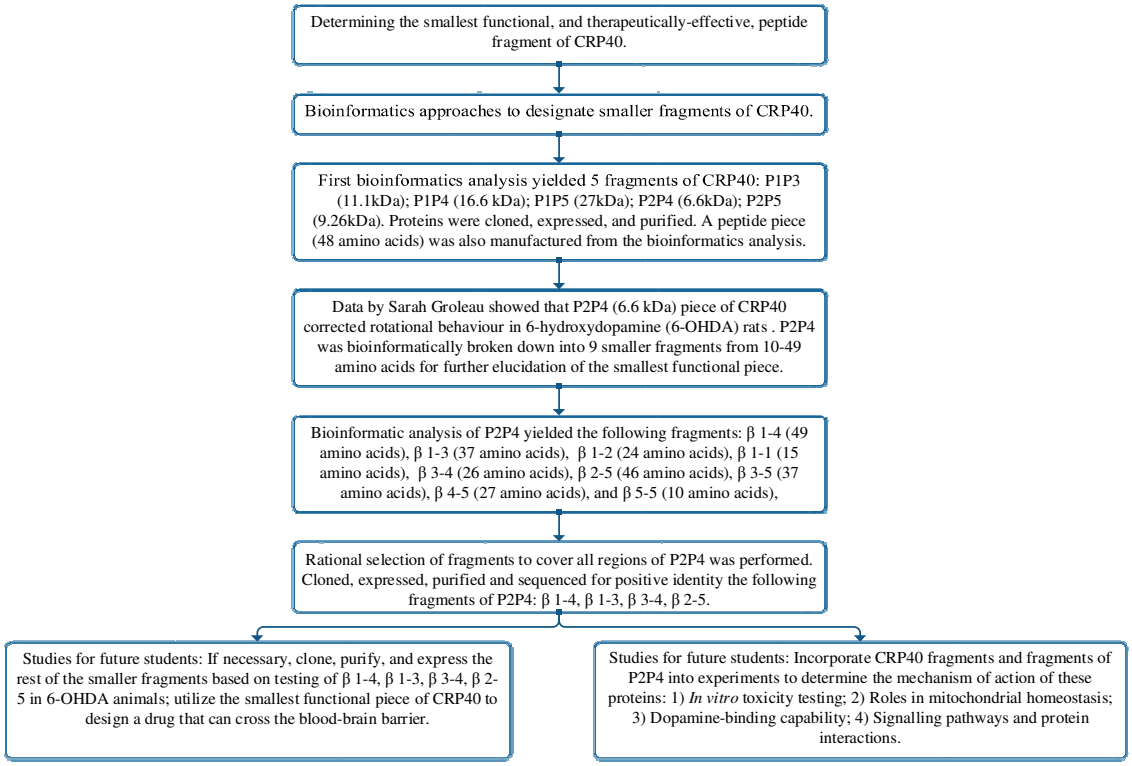

Figure 2.2 Study design summary of experiments for characterization, cloning, and elucidation of smaller functional protein fragments of CRP40.

2.2 Materials and Methods

2.2.1 Determining the smallest functional fragment of the human CRP40: Bioinformatics approaches

In order to determine the smallest functional fragment of CRP40, bioinformatics approaches, in collaboration with Dr. Zdenek Pristupa, were carried out to identify possible regions of functional significance within the CRP40 protein sequence. Protein structure prediction through bioinformatics approaches was used to predict the secondary structure (e.g., β-sheet composition) and potential sites of interaction, such as phosphorylation sites, with other proteins including cellular kinases. The full length CRP40 nucleotide sequence (accession #DQ480334) and protein sequence were previously determined by our laboratory (Gabriele et al., 2009). The protein sequence was compared with known structures present in the Protein Data Bank. It was found that CRP40 shares significant sequence homology with the DnaK, an evolutionarily conserved molecular chaperone. DnaK is a bacterial member of the Hsp70 protein family that shares 40-50% sequence identity with its eukaryotic homologues (Zhu et al., 1996). The crystal structure of DnaK has already been determined (Zhu et al., 1996). The rationale underlying the use of DnaK to predict the structure of CRP40 through a process known as comparative modeling is that many proteins sharing a common evolutionary origin have been shown to have similar backbone structures and 3D folds (Edwards and Cottage, 2003). Due to the sequence similarity of amino acids between these two proteins (over 30% is considered homologous for structural analysis), CRP40 structure was modeled at

the level of accuracy of a medium resolution X-ray or nuclear magnetic resonance structure (Edwards and Cottage, 2003). It was postulated that similar sequences in DnaK and CRP40 may perform similar functions.

To perform bioinformatics analysis, we used tools from the website ExPASy (http://www.expasy.org/), a bioinformatics resource portal. Structural information of CRP40 was assessed using the online service PredictProtein (http://www.predictprotein.org/) for predictions such as secondary structure and possible β-sheets, coiled-coil regions, potential protein phosphorylation sites, potential cysteine bonds and disulphide bridges. The SWISS-MODEL (http://swissmodel.expasy.org/workspace/index.php) portal was used to predict secondary structure of CRP40 based on homology modeling to the known crystal structure of DnaK.

The initial bioinformatics analysis identified five possible functional fragments within the 40 kDa CRP40, which were named according to their forward and reverse primer pairs: P1P3 (11.1 kDa), P1P4 (16.6 kDa), P2P4 (6.6 kDa), and P2P5 (9.26 kDa), and P1P5 (27 kDa) (Figure 2.2; Figure 2.3). A small peptide (48 amino acids) was also manufactured to be tested as the possible functional piece. This peptide was derived from the results of the bioinformatics analysis.

The five initial fragments of CRP40 were cloned, expressed and purified as per methods outlined later in the Methods section of Chapter 2 (Figure 2.3). In order to continue dividing CRP40 into smaller fragments, our group performed testing with the initially cloned smaller fragments of size 6.6-27 kDa in 6-OHDA rats (studies were

performed by Sarah Groleau). These experiments demonstrated that injection of the smaller cloned fragments of CRP40 (27 kDa P1P5, 16.6 kDa P1P4, and 6.6 kDa P2P4), but not a synthetic peptide piece (48 amino acids) completely corrected the rotational behaviour in the preclinical hemi-lesioned 6-OHDA rat model of PD at day 4 post-injection (Figure 2.4). Since P2P4 was the smallest amino acid fragment that corrected rotational behaviour (e.g., 6.6 kDa; 60 amino acids) in the 6-OHDA rat, it was rationalized that this peptide piece may contain the functional region of CRP40. The peptide piece, P2P4, was further analyzed by bioinformatics and structural approaches which were used to predict its secondary structure and putative substrate binding sites (Figure 2.5). Interestingly, it was found that P2P4 had significant homology to the substrate-binding region of the DnaK protein, the same member of the bacterial 70 kDa heat-shock protein family, that CRP40 was first compared to (Zhu et al., 1996). The bioinformatic analysis of P2P4 exploited information from the crystal structure of DnaK, including properties such as location of β-sheets and the location of its substrate-binding region. The substrate binding region of DnaK is comprised of a compact β-sandwich (from amino acid residues 393-502) which binds the substrate, and α helical elements that serve as a lid to encapsulate the substrate. Our comparison of P2P4 and DnaK revealed the following properties: 1. Sequence alignment of P2P4 and DnaK (e.g., amino acids 284-443) showed 83.3% identity; 2. Secondary structure analysis of P2P4 predicted 5 β-strands within the protein sequence which overlap with β1, β2, β3 and β4 strands in the crystal structure of the DnaK protein (Zhu et al., 1996); 3. Only short segments within the β1 and β2 strands of DnaK are in the sandwich of the substrate binding site, and loops 1,2

(amino acid residues 402-409) and loops 3,4 (amino acid residues 428-433) from the β-sandwich domain form the binding channel of DnaK—these regions align with the protein sequence of P2P4, suggesting that P2P4 may contain the functional segment within the CRP40 peptide.

The results of further bioinformatics analysis of the 60 amino-acid P2P4 yielded 9 possible functional fragments named according to the predicted β strands of P2P4 (e.g., β strands 1 to 5), which were the following: β 1-4, β 1-3, β 1-2, β 1-1, β 3-4, β 2-5, β 3-5, β 4-5, and β 5-5 (Figure 2.5). The smaller fragments were sized between 10-49 amino acids and were postulated to contain the functional piece of CRP40 based on the location of β-sheets and their structural properties. The β 1-3, β 1-4, β 3-4, β 2-5 were chosen for cloning and cloned as per methods described later in this chapter. Future studies will incorporate the testing of these small fragments for their ability to correct behavioural impairments in 6-OHDA rats; the results of these studies will determine the smallest functional piece, and if necessary, determine which of the smaller β-fragments should be explored further in an effort to find the smallest functional fragment of CRP40 (Figure 2.2).

2.2.2 Cloning of human CRP40 protein fragments and design and preparation of primers for cloning

The following protein fragments were cloned: P1P3, P1P4, P1P5, P2P4, P2P5, β 1-3, β 1-4, β 3-4, and β 2-5. It was previously determined by Gabriele et al., 2009, that human CRP40 contains 1, 047 base pairs (bp). The expected lengths of the CRP40

fragments that were cloned were the following: P1P3 (300 bp); P1P4 (450 bp); P1P5 (730 bp); P2P4 (180 bp); P2P5 (450 bp); β 1-3 (108 bp), β 1-4 (147 bp), β 3-4 (78 bp), and β 2-5 (138 bp). Primers for cloning were designed and synthesized by MOBIX Laboratory (McMaster University, Hamilton, ON, Canada). The forward primers (i.e., sense primers) used to clone P1P3, P1P4, P1P5, P2P4, and P2P5 were the following: P1, 5' TAG GGA TCC ATG GAT TCT TCT GGA CCC AAG CAT 3'; P2, 5' TAG GGA TCC TTG GCC GGC GAT GTC ACG GAT GTG 3'. The reverse primers (i.e., antisense primers) used were the following: P3, 5' CTA GAA TTC TCA CAC ATC CGT GAC ATC GCC GGC CAA 3'; P4, 5' CTA GAA TTC TCA ACA CAC TTT AAT TCC CAC TTG CGT 3'; P5, 5' CTA GAA TTC TCA TCG TTC CTT CTT TGG CCG GTT TTT 3'.

The forward primers (i.e., sense primers) used to clone β 1-3, β 1-4, β 3-4, β 2-5 were the following: for β 1-3 and β 1-4, P2 5' TAG GGA TCC TTG GCC GGC GAT GTC ACG GAT GTG 3', for β 3-4 5' TAG GGA TCC GGA GGT GTC TTT ACC AAA CTT ATT AAT AG 3', and for β 2-5 5' TAG GGA TCC CCC CTG TCT CTG GGT ATT GA 3. The reverse primers (i.e., antisense primers) used were the following: for β 3-4 and β 2-5, P4, 5' CTA GAA TTC TCA ACA CAC TTT AAT TCC CAC TTG CGT 3'; for β 1-4, 5' CTA GAA TTC AGC GGC AGT AGA GAA TAC CTG 3'; and for β 1-3, 5' CTA GAA TTC AGT GGT ATT CCT ATT AAT AAG TTT GGT AAA 3'.

All primers were re-constituted with nuclease free water to a concentration of 200 μM and diluted with nuclease free water to 5 μM for the polymerase-chain reaction (PCR).

2.2.3 Polymerase-Chain Reaction of CRP40 fragments

Each CRP40 DNA fragment was amplified using its respective sense and antisense primers (e.g., the sense primer used for P1P3 was P1 and antisense primer used was P3). Human brain Alzheimer's cDNA was used in the PCR reaction.

PCR was performed as per manufacturer's detailed protocol (Invitrogen Life Technologies, Burlington, ON, Canada). The contents of the PCR reaction mixture for the proteins P1P3, P1P4, P1P5, P2P4, P2P5, β 1-3, β 1-4, β 3-4, and β 2-5 were the following: 10x High-Fidelity Buffer (5 µL); 10 mM dNTP (1 µL); 50 mM $MgSO_4$ (2 µL); High-Fidelity Taq Polymerase (0.2 µL); nuclease free H_2O (NF H_2O) (27.8 µL); human brain Alzheimer's cDNA (6 µL); forward primer (4 µL); and reverse primer (4 µL). The PCR was carried out under the following conditions: initial denaturation was carried out at 95 °C for 2:25 seconds followed by 40 cycles of 95 °C for 15 seconds, 60 °C (this step was 57 °C for β 3-4, and β 2-5) for 30 seconds, and 72 °C for 5 seconds, followed by a final extension step at 72 °C for 7 minutes.

2.2.4 Agarose Gel Electrophoresis

Following the PCR reaction, P1P3, P1P4, P1P5, P2P4, and P2P5 fragments were run on a 1% agarose gel. The β 1-3, β 1-4, β 3-4, and β 2-5 fragments were run on a 2% agarose gel. To make the 2% agarose gel, 0.8 g of agarose was dissolved in 40 mL of 1X TAE containing a mixture of Tris base, acetic acid and Ethylenediaminetetraacetic acid (EDTA). Mixtures were then heated by microwaving for 2 minutes, with gentle shaking after one minute to prevent overheating. The solutions were allowed to cool to room

temperature and 2 µL of ethidium bromide was added. The solutions were poured into their respective electrophoresis tanks with a comb in place for the production of designated lanes, and allowed to dry for approximately 45 minutes. Next, 1X TAE buffer was added to completely submerge the set agarose gels and the comb was carefully removed. The different CRP40 fragments (P1P3, P1P4, P1P5, P2P4, P2P5, β 1-3, β 1-4, β 3-4, and β 2-5) products were prepared for their respective agarose gels by adding 1 part of 6X loading buffer to 5 parts of the fragment PCR products and pipetting the mixtures to the designated lanes in the gel. In the last two lanes, 10 µL of a 100 bp ladder standard (Fermentas Canada Inc., Burlington, ON, Canada) was incorporated in the gel. Electrophoresis was then run at 100 V for approximately 20 minutes and bands were observed under U.V. light. The following bands relative to the 100 bp ladder were cut out, purified using a gel extraction kit, and sequenced: P1P3 (300 bp); P1P4 (450 bp); P1P5 (730 bp); P2P4 (180 bp); P2P5 (450 bp); β 1-3 (108 bp), β 1-4 (147 bp), β 3-4 (78 bp), and β 2-5 (138 bp).

2.2.5 DNA extraction

The CRP40 fragments P1P3, P1P4, P1P5, P2P4, P2P5, β 1-3, β 1-4, β 3-4, and β 2-5 were extracted and purified from agarose gels using the QIAEX II Agarose Gel Extraction kit as per the manufacturer's protocol (Qiagen Inc., Mississauga, ON, Canada). Briefly, the DNA band for each of the fragments was cut from the agarose gel using a clean, sharp scalpel, placed in a 1.5 mL micro-centrifuge tube and weighed. 3 volumes of Buffer QX1 were added to 1 volume of gel for each of the fragments. Since the DNA concentration of each of the fragments was estimated to be less than 2 µg, 10 µL of re-

suspended and vortexed QIAEX II was added to each micro-centrifuge tube. The fragments were incubated at 50°C for 10 minutes to solubilise agarose and bind the DNA. The samples were centrifuged at 13 000 rpm for 30 seconds and supernatants were removed. Pellets were washed with 500 µL of Buffer QX1 and centrifuged for 30 seconds, removing all the traces of supernatant with a pipette. The pellets were then washed twice with 500 µL of Buffer PE, centrifuged, and supernatants were removed. The pellets were air-dried until they became white for approximately 20-30 minutes. 20 µL of buffer TE (10 mM Tris, pH 8.0, 1 mM EDTA) was used to re-suspend the pellet, and pellets were incubated at room temperature for 5 minutes. The mixture was centrifuged at 13 000 rpm for 1 minute and the supernatants containing the purified DNA were pipetted into clean, clearly-labelled 1.5 mL micro-centrifuge tubes.

DNA concentration was determined in all of the samples by measuring optical densities at an absorbance ratio of 260 nm and 280 nm on a CU-640 spectrophotometer (Beckman-Coulter, Mississauga, ON, Canada). If sufficient DNA concentration was achieved (e.g., close to 100 µg/mL), the CRP40 plasmid DNA fragments were sent for sequencing at MOBIX laboratory (McMaster University, Hamilton, ON, Canada) to confirm their identity. The sequencing results from each of the fragments were subjected to BLAST analysis in the National Center for Biotechnology Information (NCBI) database and compared to mortalin or HSPA9, whose C-terminal portion was previously found to be identical to the entire human CRP40 nucleotide and amino acid sequences. Sequencing analysis for all the fragments showed at least a 97% nucleotide homology to mortalin.

2.2.6 Restriction-enzyme digestion and vector-ligation

A *BamHI* restriction enzyme site was introduced at the 5' end of all of the forward or sense primers and an *EcoRI* restriction enzyme site was introduced at the 5' end of the reverse or antisense primers to facilitate the cloning process. The pGEX-2T vector (GE Healthcare Life Sciences, Piscataway, NJ, USA) and the protein fragments P1P3, P1P4, P2P4, P1P5, β 1-3, β 1-4, β 3-4, and β 2-5 were digested using FastDigest *EcoRI* and FastDigest *BamHI* (Fermentas Canada Inc., Burlington, ON, Canada) according to the manufacturer's recommended protocols. The PCR digestion reaction was performed at 37 °C for 20 minutes and enzymes were inactivated by heating at 80 °C for 5 minutes. The use of FastDigest restriction enzymes on protein fragment P2P5 did not produce protein bands when run on an 0.7% agarose gel. Instead, the P2P5 fragment along with fresh pGEX-2T vector was digested using slow restriction enzymes *EcoRI* and *BamH1* (Invitrogen Life Technologies, Burlington, ON, Canada) at 37 °C for 1 hour and inactivation of the enzymes was performed by heating at 75 °C for 15 minutes. The digested pGEX-2T vector and CRP40 protein fragments (P1P3, P1P4, P1P5, P2P4, P2P5) were run on an 0.7% agarose gel and purified using QIAEX II Agarose Gel Extraction kit as per manufacturer's protocols. The digested pGEX-2T vector and CRP40 protein fragments (β 1-3, β 1-4, β 3-4, and β 2-5) were run on a 2% agarose gel and purified using the QIAEX II Agarose Gel Extraction kit. DNA concentration was determined using the CU-640 spectrophotometer (Beckman-Coulter, Mississauga, ON, Canada) at an absorbance ratio of 260 nm versus 280 nm to determine if there was sufficient DNA to perform the ligation reaction (e.g., at least 25 µg/mL of DNA). Each of the respective

CRP40 protein fragments were then ligated to the pGEX-2T vector using T4 DNA ligase (Fermentas Canada Inc., Burlington, ON, Canada) overnight at 14 °C in a PCR machine.

2.2.7 Luria Bertani (LB)-medium

The following reagents were needed to make LB-media: 1% tryptone, 0.5% Yeast Extract, 1% NaCl, at pH 7.0. 10 g of tryptone and 5 g yeast extract was dissolved in 1000 mL distilled water and pH was adjusted to 7.0. The solution was then autoclaved and stored at room temperature. The LB-media when used was always handled under antiseptic conditions (use of 75% alcohol and flamed burner).

2.2.8 Preparation of LB-Agar plates

1.5 g of Agar was added to 500 mL LB-media, stirred and autoclaved. After the solution had cooled, 100 µL of stock ampicillin (100 mg/mL) was added to the mixture so that the final concentration of ampicillin was 100 µL/mL. The medium was swirled gently and was poured into plastic plates (approximately 30 mL per plate). Plates were opened and incubated at 37ºC to settle and dry.

2.2.9 DNA Transformation/Plating/DNA Extraction

The ligated pGEX-2T vector and CRP40 protein fragments were transformed into One Shot TOP10 chemically competent BL-21 *E. coli* cells (Invitrogen Life Technologies, Burlington, ON, Canada) according to the manufacturer's protocols. Briefly, One Shot TOP10 cells were thawed and 2 µL of ligated mixes for each of the CRP40 protein fragments were added to one vial of competent cells each and incubated

on ice for 30 minutes. Cells were heat-shocked by incubating the vials for 30 seconds in a 42 °C water bath. 250 µL of pre-warmed SOC medium was added to each of the vials and incubated in a shaking incubator at 37 °C for one hour at 225 rpm. Two different volumes, 50 µL and 150 µL of each of the CRP40 fragments were plated on LB-media with ampicillin (100 µg/mL) overnight at 37 °C. Five colonies from each fragment (P1P3, P1P4, P1P5, P2P4, P2P5, β 1-3, β 1-4, β 3-4, and β 2-5) were picked and re-grown in 3 mL of LB-media containing 3 µL of ampicillin (100 µg/mL) and incubated in a shaking incubator at 225 rpm overnight at 37 °C.

DNA was extracted from the 3 mL cultures of individual protein fragments using the QIAprep Spin Miniprep Kit (Qiagen Inc., Mississauga, ON, Canada) according to protocols described previously in this thesis. In order to verify the identity of the clones and incorporation into the pGEX-2T vector, all of the clones (e.g., P1P3, P1P4, P1P5, P2P4, P2P5, β 1-3, β 1-4, β 3-4, and β 2-5) were digested with restriction enzymes as specified previously. The digested fragments were run on an 0.7% agarose gel for the bigger fragments and 2% agarose gel for the smaller fragments, as described previously, and analyzed visually against a 100 bp DNA ladder (Fermentas Canada Inc., Burlington, ON, Canada) for correct fragment sizes and presence of the pGEX-2T vector. Optical densities for each of the fragments were also measured as previously described to ensure that the DNA concentration was close to 100 µg/mL, which further confirmed the success of the cloning. Clones which had the highest DNA concentration were sent for sequencing at the MOBIX Laboratory (McMaster University, Hamilton, ON, Canada).

2.2.10 Expression & purification of CRP40 fragments

For expression of the CRP40 protein fragments (e.g., P1P3, P1P4, P1P5, P2P4, P2P5, β 1-3, β 1-4, β 3-4, and β 2-5), 10 mL cultures of all of the fragments were prepared according to the following protocol: 100 µL of the 3 mL overnight-cultures were added to 10 mL of LB-media containing 10 µL ampicillin (100 µg/mL) and incubated in a shaking incubator at 225 rpm overnight at 37 °C. Next, the 10 mL overnight cultures (P1P3, P1P4, P1P5, P2P4, P2P5, β 1-3, β 1-4, β 3-4, and β 2-5 cultures) were each added to 1 L vials of LB-media containing 1 mL ampicillin (100 µg/mL). The bacterial cultures were grown at 37 °C in a shaking incubator set to shake at 250 rpm until optical density at 600 nm was at least 0.6, which took approximately 4 hours to reach. Cultures were subsequently induced with isopropyl β-D-1-thiogalactopyranoside (IPTG) by adding 1 mL of 100 mM to 1 L cultures and incubating overnight at 14 °C in a shaking incubator (250 rpm) to initiate transcription of the Glutathione S-transferase (GST)-CRP40 fragment fusion proteins. Bacterial cultures of the five fragments were spun down at 4000 rpm for 15 minutes at 4 °C in an SL-6000 rotor in a Sorvall Revolution Rc centrifuge (Thermo Scientific, Burlington, ON, Canada). The supernatants were discarded and the bacterial pellets of the individual fragments were washed with 100 mL of phosphate-buffered saline (PBS) and spun again at the same conditions. Supernatants were discarded and pellets of the individual fragments were resuspended in 10 mL of PBS with Complete Mini Protease Inhibitor tablets (Roche Canada, Mississauga, ON, Canada). The PBS that was used in this step was prepared by dissolving 2 Complete Mini Protease Inhibitor

tablets in 500 mL PBS. The cells containing the 10 mL fragments were lysed with a French press at a pressure of 15 000 psi.

Lysates of the individual fragments P1P3, P1P4, P1P5, P2P4, P2P5, β 1-3, β 1-4, β 3-4, and β 2-5 were diluted to a volume of 15 mL. 50 µL samples of each of the fragments were saved for SDS-PAGE electrophoresis. Subsequently, the fragments were diluted to a volume of 30 mL with PBS. The protein fragment preparations were then spun down at 12 000 rpm for 20 minutes in a JA20 rotor in a Beckman-Coulter centrifuge (Beckman-Coulter, Mississauga, ON, Canada) and clear supernatants were transferred to clean 50 mL BD Falcon tubes (BD-Canada, Mississauga, ON, Canada) and saved for addition to a 50% glutathione sepharose 4B slurry (Amersham, Picataway, NJ, USA). As well, 50 µL samples of each of the fragments were saved for sodium dodecyl sulfate polyacrylamide gel electrophoresis (SDS-PAGE). Prior to mixing with clear supernatants, the glutathione sepharose beads were prepared as per the following protocol: 1.25 mL of the beads were added into 50 mL Falcon tubes and spun down at 500 g for 5 minutes; the supernatant was discarded and 5 mL of PBS was added; and, the beads were then spun down again at 500 g for 5 minutes and the supernatant was discarded. The prepared GST-bound protein fragments P1P3, P1P4, P1P5, P2P4, P2P5, β 1-3, β 1-4, β 3-4, and β 2-5 were added to the corresponding labelled preparations of equilibrated sepharose beads and incubated at 4 °C overnight with shaking. The following morning, the protein fragment and sepharose bead mixtures were added to columns for protein purification. Each column was then washed with 20 mL of wash buffer containing 1x PBS containing a Complete Mini Protease Inhibitor tablet, 0.1 % Triton X-100 (Roche Canada,

Mississauga, ON, Canada), and 0.5 M sodium chloride. Following the washes, the bound fusion proteins were liberated from the glutathione sepharose beads by adding 1 mL of mixture containing thrombin protease (100 units or 50 µL) and 950 µL of PBS containing a Complete Mini Protease Inhibitor tablet. The columns were then sealed with Parafilm and incubated overnight at room-temperature to complete the reaction. The proteins P1P3, P1P4, P1P5, P2P4, P2P5, β 1-3, β 1-4, β 3-4, and β 2-5 were eluted from the column into 8, 1.5 mL Eppendorf tubes per protein. The first protein fractions were eluted directly from the column, and subsequent fractions were eluted by washing with 1 mL of wash buffer as specified above. Protein concentration was determined using the Bradford (1976) method and the first four fractions of each protein (e.g., the fractions that gave the highest protein concentrations) were pooled together. Phenylmethylsulfonyl fluoride (PMSF; 0.35 mM) was added to each pooled fraction of proteins and incubated at 37 °C for 15 minutes.

Proteins were dialyzed by passive diffusion through a semi-permeable membrane to remove unwanted small molecular weight molecules (e.g. salts). Dialysis bags of 3.5 kDa and 1 kDa were used to purify P1P3 (11.1 kDa), P1P4 (16.6 kDa), P2P4 (6.6 kDa), and P2P5 (9.26 kDa). P1P5 (27 kDa) was purified using a 10.0 kDa dialysis bag (VWR, Mississauga, ON, Canada). Dialysis bags of 0.5-1 kDa were used to purify the smaller protein fragments β 1-3, β 1-4, β 3-4, and β 2-5. All dialysis bags were cut to a length of approximately 30 cm and soaked in water. Water was passed though the bags to check for leaks, and subsequently, the bags were tied at one end and clamped. Protein solutions were added to each of the five bags and tied and clamped at the other end. The dialysis

bags containing the individual proteins were placed in beakers containing 500 mL of 1x PBS and incubated at 4 °C for 36 hours, changing the PBS solution three times during this time period.

2.2.11 Sodium dodecyl sulfate polyacrylamide gel electrophoresis: P1P5

To further confirm the cloning of proteins, SDS-PAGE was carried out as previously described by Gabriele et al., 2003 and Gabriele et al., 2005 on the largest protein fragment P1P5, in addition to sequencing. SDS-PAGE was not performed with the other larger proteins (e.g., P1P3; P1P4; P2P4; and P2P5) and the smaller fragments β 1-3, β 1-4, β 3-4, and β 2-5 as they were sequenced to confirm positive identity. Since the P1P5 protein was of a larger size compared to all of the other proteins, gel electrophoresis was performed using precast 10% Mini-PROTEAN TGX gel with Tris/Glycine buffer (Bio-Rad Laboratories, Hercules, California, USA). Briefly, 1 µg of the protein sample was mixed with 6x-loading dye (0.625 M Tris, 2% SDS, 0.05% β-mercaptoethanol, 10% glycerol, 0.01% bromophenol blue, pH 6.8) and heated in boiling water for 7 minutes in order to denature the protein (Bradford 1976). As well, spun and lysed fractions of the P1P5 protein sample were prepared in the same manner. The PiNK Plus Prestained Protein Ladder (GeneDirex, distributed by FroggaBio Inc., Toronto, ON, Canada) was utilized to verify the molecular weight of P1P5. The protein was separated using an SDS-PAGE 10% separating gel with running buffer (0.025 M Tris, pH 8.3, 0.3M glycine, 0.1% SDS). An electrical voltage of 80 V was applied for approximately 2 hours until the bands were resolved. Coomassie Brilliant Blue-250 gel staining was used following electrophoresis for 45 minutes. Destain solution (30% methanol; 10 % glacial acetic acid)

was applied overnight to the gel. The gel was scanned and pictures were taken on the computer. The gel was also dried and saved.

2.3 Results

2.3.1 Bioinformatics analysis identified 14 possible functional proteins within the 40 kDa CRP40 peptide

Bioinformatics analysis of the CRP40 protein sequence (accession number: BQ224193) using ExPASy tools (http://www.expasy.org/) and homology modeling to the evolutionarily conserved molecular chaperone**,** DnaK (Primary accession number: P0A6Y8)**,** revealed five possible functional fragments, and an additional small peptide piece, within the CRP40 peptide which were named according to their forward and reverse primer pairs: P1P3 (11.1kDa); P1P4 (16.6 kDa); P1P5 (27kDa); P2P4 (6.6kDa); P2P5 (9.26kDa), and a 48 amino acid peptide fragment (Figure 2.3). These proteins were cloned, expressed, and purified. Experiments were performed by Sarah Groleau in 6-OHDA rats that revealed that P1P4, P1P5, and P2P4, but not the 48 amino acid fragment, corrected behavioural impairments. The results of the initial bioinformatics analysis, cloning, and animal testing produced a functional fragment of CRP40, which was the P2P4 fragment that was ~6 times smaller than the original protein (e.g., 6.6 kDa).

P2P4 was further analyzed using bioinformatics approaches and compared to the substrate-binding region of the crystallized DnaK protein, which showed an 83.3% sequence identity between the two proteins (Zhu et al., 1996). Further, the positions of the 6 β-sheets in the DnaK protein aligned with the 5 predicted β-sheets in the P2P4 peptide (Figure 2.5). Since segments of the β1 and β2 strands of DnaK are in the sandwich of this protein's substrate binding site, and align with the protein sequence of P2P4, this

information suggests that P2P4 may contain the functional segment within the CRP40 divided peptide. In order to elucidate this further, P2P4 was divided into 9 possible functional fragments, named according to the predicted β strands within the P2P4 structure. For instance, the peptide piece β 1-4 included predicted β strands 1 to 4 within the P2P4 structure. The 9 possible functional fragments contained between 10-49 amino acids and were as follows: β 1-4 (49 amino acids), β 1-3 (37 amino acids), β 1-2 (24 amino acids), β 1-1 (15 amino acids), β 3-4 (26 amino acids), β 2-5 (46 amino acids), β 3-5 (37 amino acids), β 4-5 (27 amino acids), and β 5-5 (10 amino acids) (Figure 2.5). β 1-3, β 1-4, β 3-4, and β 2-5 were cloned, expressed, and purified.

Figure 2.6 displays additional bioinformatic information obtained from the analysis of the CRP40 peptide in the PredictProtein (http://www.predictprotein.org/) database. CRP40 predicted secondary structure is composed of 42.57% α-helix, 19.43% β-folded, and 38.00% random coils, and indicates a protein of mixed secondary structure. The secondary structure of a protein is significantly related to its function, with a greater α-helix and β-folded composition contributing to bonds that have a higher chemical energy, and residues that usually stay in the internal regions of a protein. The CRP40 protein contains a moderately high percentage of random coils, which make up a looser structure that is more prone to distortion, with residues that may be exposed on the surface of the protein – these properties may contribute to its potential interaction with other proteins. The predicted solvent accessibility composition of the protein indicates that the ratios of residues exposed more than 16% of their surface is 62.00%, and the rest residues is 38.00%; therefore, most amino acids of CRP40 are

exposed to the solvent interface, with only a few amino acids embedded in the protein's interior. In terms of the disulphide bonding predictions, there were no disulphide bonds detected within CRP40; however, the confidence of possible disulphide boding prediction was high for 3 cysteine residues within the CRP40 sequence (Ceroni et al., 2006). The lack of disulphide bonds in CRP40 is consistent with the idea that molecular chaperones tend to have a very high conformational flexibility that would allow them to function and fold/refold as well as assemble/reassemble (Rao et al., 1998). Thus, the flexibility in function offered by molecular chaperones has been linked to the lack of disulphide bonding in their structure (Rao et al., 1998).

In terms of protein-protein interactions, bioinformatics analysis of CRP40 predicted several interaction sites, including an N-glycosylation site, a cAMP or cyclic guanosine monophosphate (cGMP) dependent kinase phosphorylation site, 6 PKC phosphorylation sites, 10 casein kinase II phosphorylation sites, 1 tyrosine kinase phosphorylation site, and 3 N-myristoylation sites (Figure 2.6). A leucine zipper pattern and an Hsp70 family signature, previously identified by our laboratory, were also confirmed in the sequence of CRP40 (Figure 2.6). Investigating the interactions of CRP40 with cellular kinases and other proteins will be an important endeavour in future studies that would help to further elucidate the roles of this molecular chaperone.

2.3.2 Cloning, expression and purification of CRP40 protein fragments was confirmed using DNA sequencing and SDS-PAGE analysis

The following P1P3 (300 bp); P1P4 (450 bp); P1P5 (730 bp); P2P4 (180 bp); P2P5 (450 bp); β 1-3 (108 bp), β 1-4 (147 bp), β 3-4 (78 bp), and β 2-5 (138 bp) were cloned, expressed, purified and DNA was sequenced for positive identity at the MOBIX Sequencing Facility (McMaster University, Hamilton, ON, Canada).

The protein fragments of CRP40 were amplified through PCR by using their respective forward and reverse primers identified in Methods section 2.2.2. The following proteins were cloned: P1P3 (300 bp); P1P4 (450 bp); P1P5 (730 bp); P2P4 (180 bp); P2P5 (450 bp); β 1-3 (108 bp), β 1-4 (147 bp), β 3-4 (78 bp), and β 2-5 (138 bp). Figure 2.7 (1% agarose gel) and Figure 2.8 (2% agarose gel) display the bands of the proteins compared to DNA ladders (100 bp), that were stained with ethidium bromide, and visualized under U.V. light. The respective bands were eluted and sent for sequencing at MOBIX (McMaster University, Hamilton, ON, Canada). The sequences were analyzed and they showed over 97% nucleotide homology to mortalin, indicating positive identity of the peptide fragments.

To further confirm that the cloning process was successful, a 10% SDS-PAGE gel was run on the biggest protein fragment, P1P5 (27 kDa), of CRP40 (Figure 2.9). The fragment was stained with Coomassie Brilliant Blue-250, and the gel revealed a 27 kDa protein band, indicating successful cloning of the P1P5 piece of CRP40 (Figure 2.9).

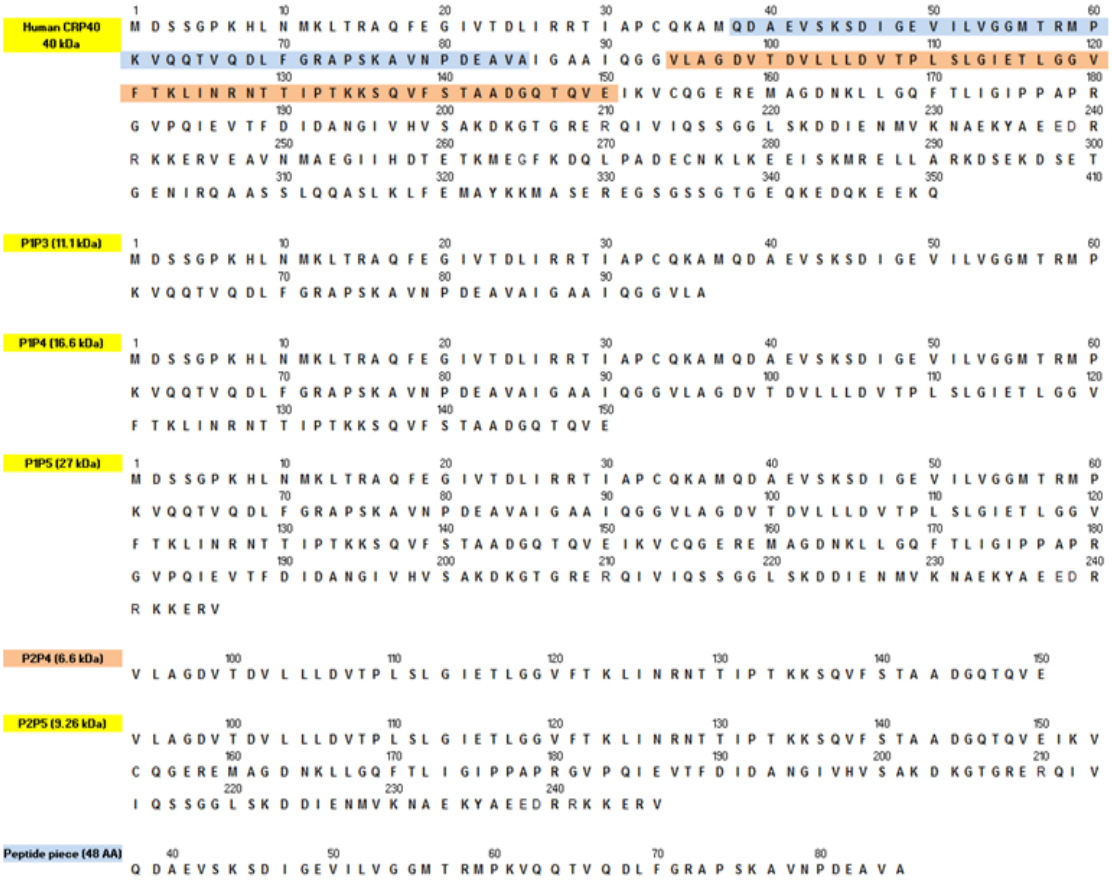

Figure 2.3 Sequences and locations of putative functional fragments of CRP40.

FIGURE LEGEND

Figure 2.3: The full peptide sequence of human CRP40 is displayed along with the first five fragments that were cloned in the experiment to elucidate the functional piece of CRP40: P1P3 (11.1kDa); P1P4 (16.6 kDa); P1P5 (27kDa); P2P4 (6.6kDa); P2P5 (9.26kDa). A synthetic peptide piece (48 amino acids) that was manufactured is displayed as well. P1P4, P1P5, P2P4, and the synthetic peptide piece were assessed for ability to correct rotational behaviour in 6-OHDA rats. P1P4, P1P5, and P2P4, but not the peptide piece, corrected behavioural impairments in the 6-OHDA model of dyskinesia. The location of P2P4 is marked in orange on the human CRP40 peptide sequence and the location of the peptide piece is marked in blue on the human CRP40 peptide sequence.

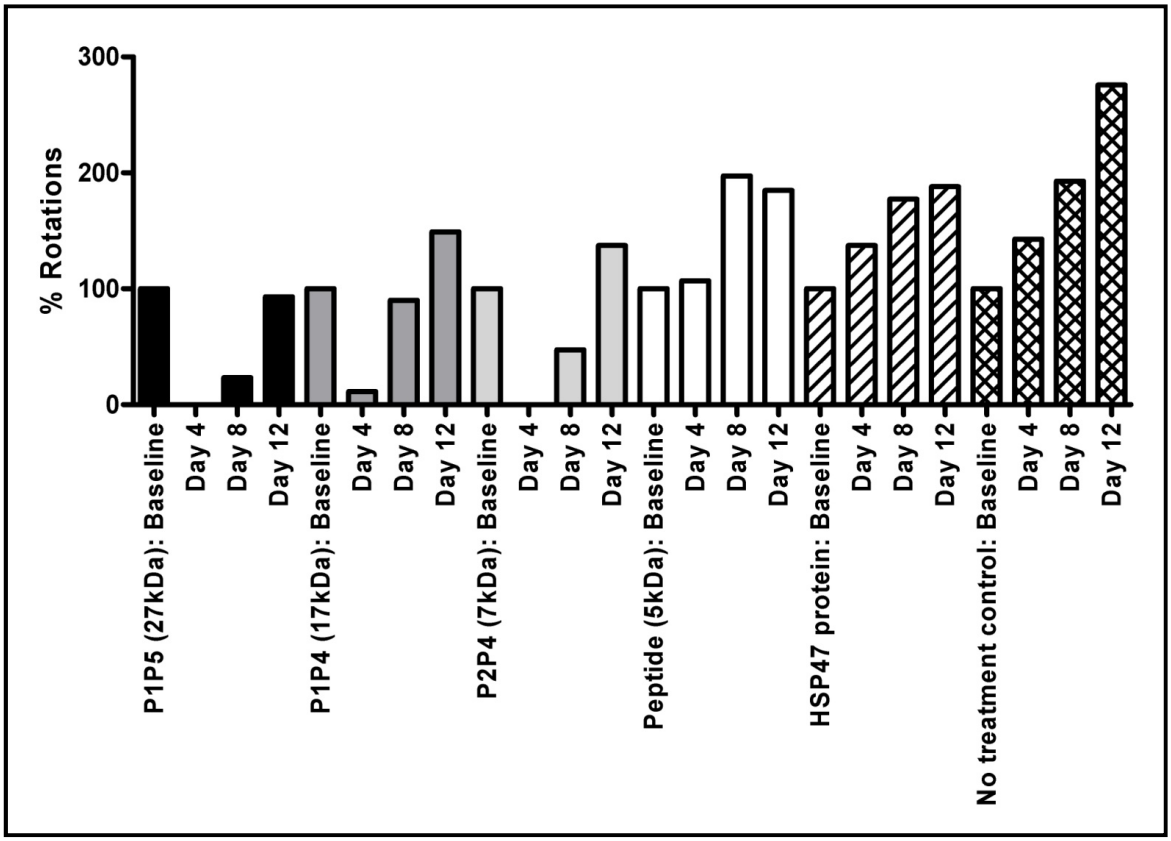

Figure 2.4 Reduction of rotational behaviour in animals treated with fragments P1P5, P1P4, and P2P4 in preclinical animal model (6-hydroxydopamine) of dyskinesia (n=1).

FIGURE LEGEND

Figure 2.4: Animals treated with CRP40 fragments P1P5, P1P4, and P2P4 displayed less turning behaviour than at baseline, compared to animals treated with the synthetic peptide and untreated controls (experiments performed by Sarah Groleau). These experiments in 6-OHDA rats identified the 6.6 kDa P2P4 peptide, which was the smallest functional fragment. P2P4 was further subdivided into smaller functional fragments using bioinformatics analysis.

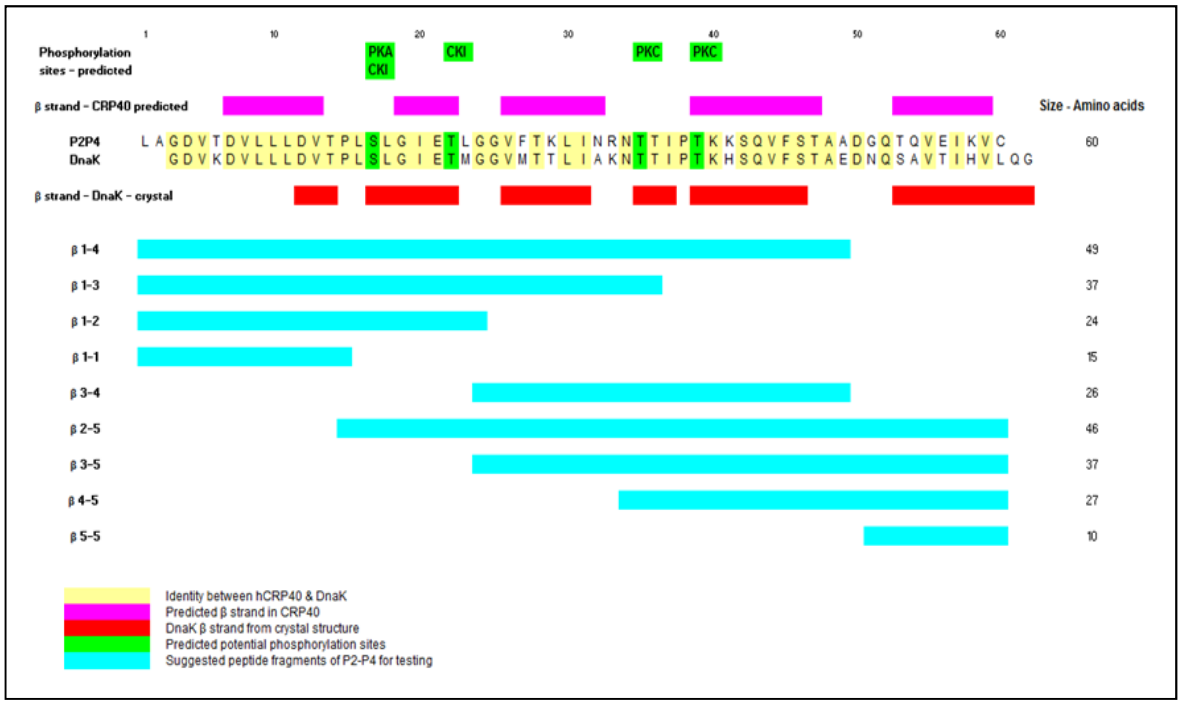

Figure 2.5 Bioinformatic analysis of P2P4 and putative functional fragments used to identify 9 smaller fragments of P2P4.

FIGURE LEGEND

Figure 2.5: Alignment of the protein sequence of the P2P4 fragment of CRP40 with the sequence of DnaK, a member of the 70kDa heat shock protein family, showed an 83.3% identity. Secondary structure prediction of P2P4, in pink, displays the location of 5 β strands, which show a high level of similarity in size and location to the 6 β-strands obtained from the crystal structure of DnaK displayed in red. Additional information shown in green indicates predicted phosphorylation sites on P2P4 by protein kinase A, protein kinase C, and casein kinase I — this information will be important in elucidating the signalling pathway responsible for therapeutic efficacy of P2P4 and its fragments in future studies. Protein fragments of P2P4 shown in blue (e.g., β 1-4, β 1-3, β 1-2, β 1-1, β 3-4, β 2-5, β 3-5, β 4-5, and β 5-5), which were identified based on these structural and bioinformatic analyses will be cloned, expressed, purified and tested for functional effects in 6-OHDA rats.

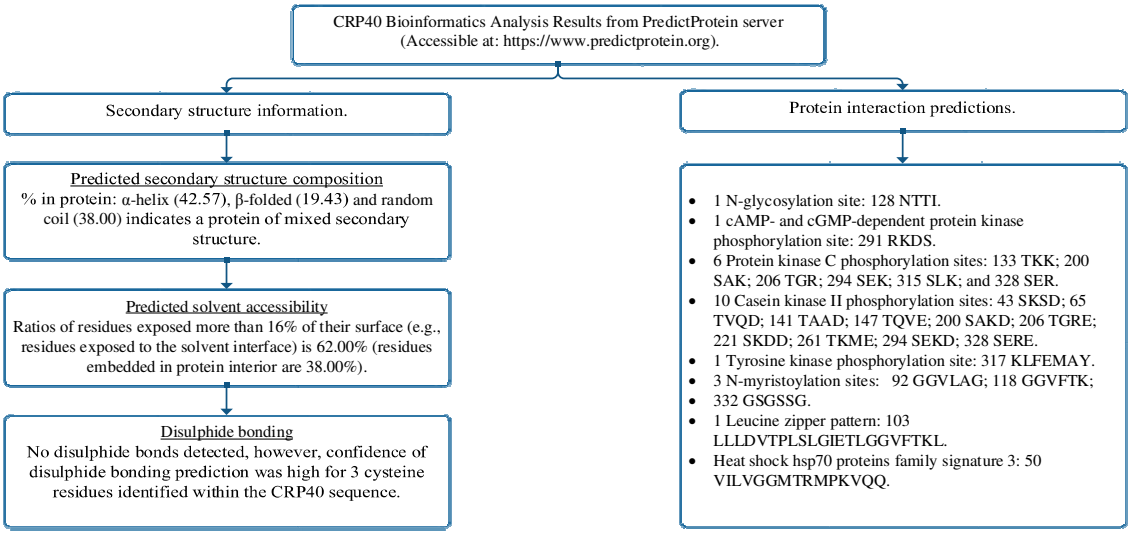

Figure 2.6 Results of bioinformatic analysis of CRP40 reveal important secondary structure and protein interaction predictions.

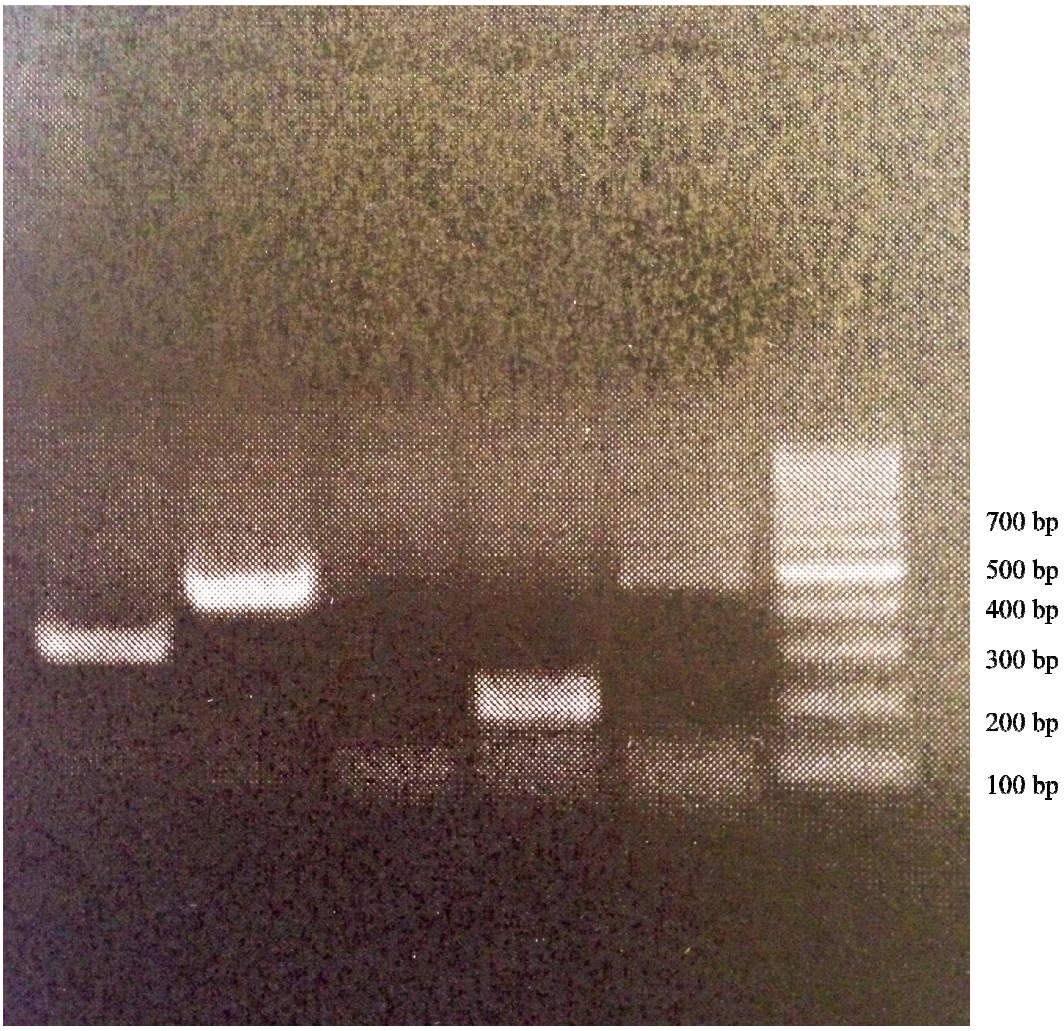

Figure 2.7 1% agarose gel identifies cloned CRP40 fragments P1P3, P1P4, P1P5, P2P4, and P2P5.

FIGURE LEGEND

Figure 2.7: This is a photograph of a 1% agarose of the CRP40 fragments P1P3, P1P4, P1P5, P2P4 and P2P5. The DNA of each fragment was amplified using PCR and the agarose gel was prepared and loaded as per protocols described in Chapter 2 Methods. The last lane incorporated a 100 bp DNA ladder for size comparison.

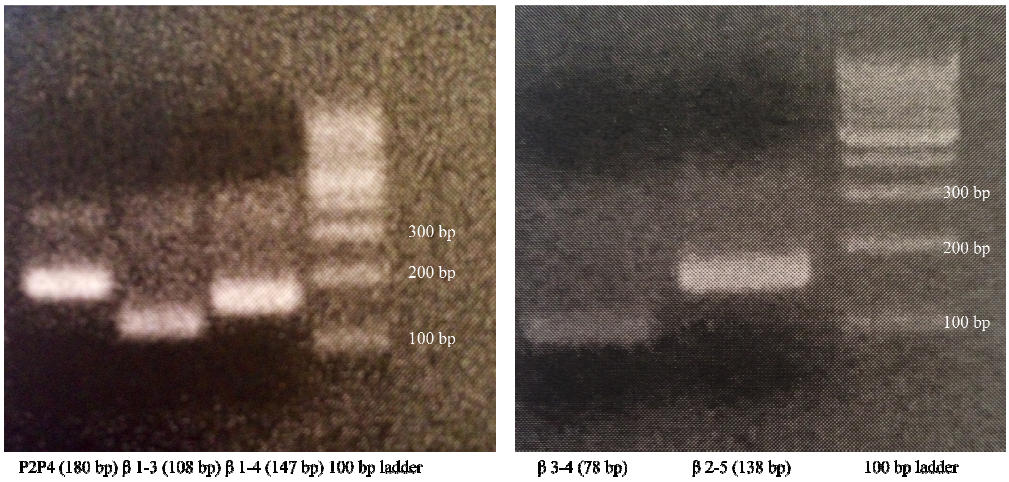

Figure 2.8 2% agarose gel identified cloned P2P4 fragments of CRP40, which were the following: β 1-3, β 1-4, β 3-4, and β 2-5.

FIGURE LEGEND

Figure 2.8: This is a photograph of 2% agarose gels of the P2P4 fragments β 1-3 (108 bp), β 1-4 (147 bp), β 3-4 (78 bp), and β 2-5 (138 bp) (P2P4 was used as a control). The DNA of each fragment was amplified using PCR and the agarose gel was prepared and loaded as per protocols described in Chapter 2 Methods. The last lane incorporated a 100 bp DNA ladder for size comparison.

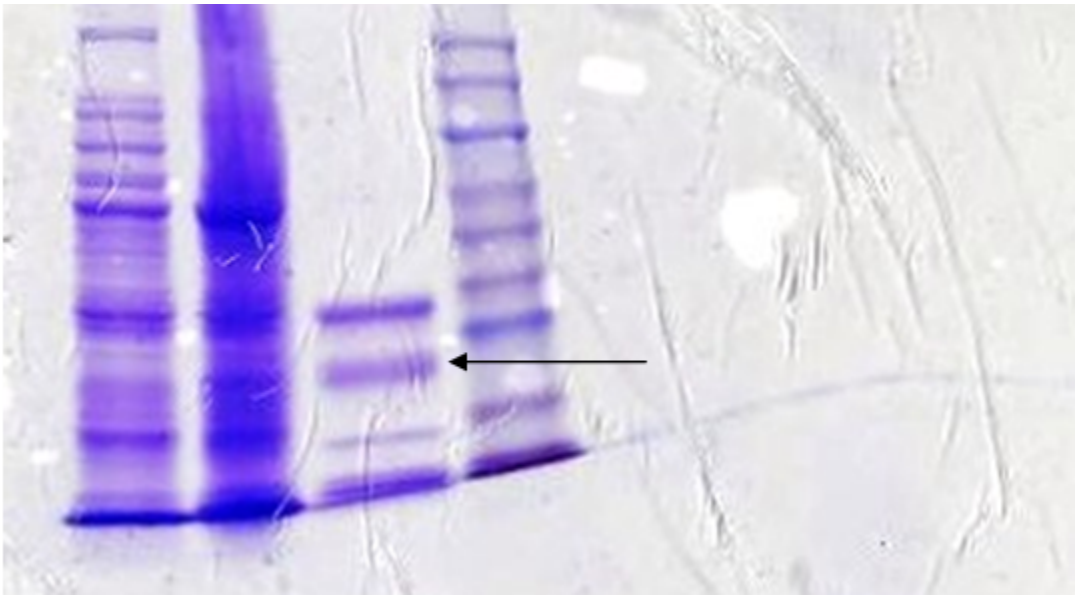

Figure 2.9 SDS-PAGE gel revealed a protein band near 27 kDa corresponding to the successful cloning of the P1P5 fragment of CRP40.

FIGURE LEGEND

Figure 2.9: A scan showing a 10% SDS-PAGE gel of pure P1P5 (27 kDa) stained with Coomassie Brilliant Blue-250. From left to right: Lane 1, spun fraction; Lane 2, lysed fraction; Lane 3, pure P1P5 (see arrow); Lane 4, protein molecular weight marker.

2.4 Discussion

PD is complex neurodegenerative movement disorder that has been linked to oxidative stress, resulting from occupational exposure to neurotoxic pesticides, genetic mutations, mitochondrial dysfunction, and protein misfolding (Schapira, 2009; Schapira and Jenner, 2011). However, despite major research advances over the past few decades, the etiology of PD is still incompletely understood. This is reflected by the lack of neuroprotective treatments and valid diagnostic tests. Moreover, the current treatments for PD are over four decades old and unsustainable for long-term use due to severe side-effects (Schapira and Jenner, 2011). The development of drugs presents a challenging aspect of this disease and new therapies have been largely unsuccessful due to problems with bioavailability, controlled delivery into affected brain regions, and the lack of discovery of optimal drug targets which are both safe and effective (Schapira and Jenner, 2011). Molecular chaperone proteins have emerged as an interesting target for research in the realm of neurodegenerative disorders due to their diverse functionalities and roles in cells.

Since the discovery of the novel CRP40 molecular chaperone in our laboratory, we have produced conclusive evidence suggesting that this protein may play important roles in CNS disorders, as a potential biomarker and diagnostic in PD (Gabriele et al., 2009; Lubarda et al., 2013). As well, we have recently uncovered a potential dual function of CRP40 in PD, as both a diagnostic and therapeutic for PD sufferers. Our findings of the reductions of CRP40 expression in post-mortem human brain specimens, live PD patients, and the 6-OHDA rat model of dyskinesia have prompted us to design an

animal study to examine the behavioural effects achieved by restoration of CRP40 levels (Gabriele et al., 2009; Lubarda et al., 2013). Recently, animal experiments performed by Sarah Groleau demonstrated that the cloned CRP40 recombinant fusion protein injected into the striatum of hemi-lesioned 6-OHDA rats, an animal model that has been traditionally used to test PD therapies, completely corrected the rotational behaviour impairments for approximately 10 days (unpublished data)**.** This was a compelling finding that was explored further in this study.

Therefore, the current study was designed to explore the potential functional roles of CRP40, its mode of action, and its relevance to PD. We have taken an innovative path towards developing methods to investigate the potential functional role of CRP40. Our group had realized early on that that the large size of the CRP40 protein (40kDa) may present challenges for its delivery across the blood-brain barrier, combined with bioavailability issues and targeting the drug in sufficient quantities to reach the specific brain regions affected in PD. Taking this into consideration, we designed methods to elucidate the smallest functional fragment of CRP40 to increase success for crossing the blood-brain barrier. The blood-brain barrier is composed of endothelial cells with continuous tight junctions, and is surrounded by astrocyte foot processes that contribute to its low permeability and structural stability (Abbott, 2002; Wolburg and Lippoldt, 2002). CRP40, a large peptide, and other large or hydrophilic compounds such as vitamins and sugar compounds would not be able to penetrate the plasma membrane of endothelial cells. Instead, the blood-brain barrier is only permeable to small, lipophilic and non-polar molecules of 400 to 600 Daltons that enter through a passive diffusion

mechanism aided by the concentration gradient between the internal and external space of endothelial membranes (Ohtsuki and Terasaki, 2007). The blood-brain barrier is composed of various carriers that transport glucose, amino acids, and nucleosides by active transport mechanisms. Small proteins or peptides can also be transported across by receptor-mediated endocytosis, or adsorptive-mediated transcytosis through electrostatic interactions with the endothelium (Ohtsuki and Terasaki, 2007). However, this type of transport necessitates that the size of the peptide is between 8-10 amino acids or smaller, and would not be suitable for a 40 kDa protein such as CRP40. Other strategies for crossing the blood-brain barrier include the following: direct administration of drugs or peptides into the brain, which would require an invasive approach; transient disruption of the blood-brain barrier to increase permeability; design of prodrugs; and employing different formulations such as solid lipid nanoparticles, polymeric nanoparticles, liposomal colloidal carriers, and polymeric micelles and dendrimers (Denora and Trapani, 2009).

This study used bioinformatics approaches to predict the structure and possible functional regions of CRP40. The possible functional regions were then used to identify smaller fragments of CRP40 in order to reduce the size of the functional peptide and increase its chances for crossing the blood-brain barrier. The structure of CRP40 was compared to the crystallized and evolutionarily conserved bacterial Hsp70 chaperone, DnaK (Zhu et al., 1996). Based on homology modeling using effective tools from the bioinformatics resource portal ExPASy (http://www.expasy.org/), five fragments of CRP40 sized between 6.6-27 kDa [P1P3 (11.1 kDa), P1P4 (16.6 kDa), P2P4 (6.6 kDa),

and P2P5 (9.26 kDa), P1P5 (27 kDa), and a small synthetic peptide of 48 amino acids were identified, cloned, purified, and expressed into functional proteins (Figure 2.2; Figure 2.3; Figure 2.7; Figure 2.9). Identification of P2P4 as the smallest functional peptide prompted further bioinformatics analysis that decreased the possible functional region of CRP40 to 10-49 amino acids (Figure 2.4; Figure 2.5). Subsequently, 9 smaller peptides of CRP40 between 10-49 amino acids were identified as the possible functional regions, and the biggest of those peptides were cloned, expressed, and purified [β 1-3 (37 amino acids), β 1-4 (49 amino acids), β 3-4 (26 amino acids), and β 2-5 (46 amino acids)] (Figure 2.5; Figure 2.8). Future experiments will be performed to test these smaller peptides in 6-OHDA animals and if possible, to identify even smaller functional peptides of CRP40. Collectively, these unique approaches would help to validate the functional potential of CRP40 and its smaller fragments, and possible relevance to PD. As well, these experimental methods would increase the potential for rational drug design through developing a functional fragment that is small enough to cross the blood-brain barrier, combat bioavailability challenges, and allow for the possibility of drug development using advanced formulations and drug delivery strategies.

In addition, the bioinformatics analyses undertaken in this study will help to shed light on the mechanistic roles of CRP40. The identification of protein interaction sites and secondary structure properties presents opportunities for further studies that will uncover the relevance of kinase phosphorylation sites in CRP40 and its fragments (Figure 2.6). As well, elucidation of functional fragments of CRP40 may help to uncover the specific region of the protein that is involved in binding DA, a critical neurotransmitter in PD.

Such information may help to elucidate the specific signalling pathways involved in the therapeutic action of CRP40 and its smallest functional fragments, including P2P4.

Indeed, there is a critical need for discovery of neuroprotective and sustainable therapies to treat PD. This is especially important in developed countries that are expected to experience an increase in the prevalence of neurodegenerative disorders as populations continue to age. The current gold standard drug, $_{L}$-DOPA has been used for over four decades, and represents a symptomatic therapy for PD. However, $_{L}$-DOPA treatment has been shown to contribute to motor complications and dyskinesias when used as an initial therapy in PD. Other symptomatic therapies for PD have been based on the use of DA receptor agonists such as cabergoline and pramipexole, in order to reduce dyskinesia and wearing-off of medications; however, while DA agonists may serve as $_{L}$-DOPA-sparing agents for some time, the incorporation of $_{L}$-DOPA is eventually required in order to manage severe motor symptoms in patients (Hayes et al., 2010). The symptomatic treatments for PD that include dopaminergic medications have been linked to severe side-effects including gastrointestinal symptoms, nausea, hypotension, cognitive symptoms, and drowsiness (Hayes et al., 2010). In addition, certain DA agonists have been associated with the development of fibrosis (Hayes et al., 2010). The knowledge of the side-effects and wearing off effects of PD medications has led to many patients in the past being treated at late stages of the disease, when functional disability was already been incurred (Hayes et al., 2010). However, current practices and standards for symptomatic therapy in PD have been altered to initiate treatment at early stages to improve the quality of life of patients. As well, initial $_{L}$-DOPA treatment has been prescribed to older patients

over the age of 60, while DA agonists have been prescribed in early-onset PD cases or in patients under the age of 60 (Hayes et al., 2010). However, a recent longitudinal study following patients who have been initially treated with either $_{L}$-DOPA or DA agonists for fourteen years failed to show that either of those treatment strategies provided any ultimate advantages over the other (Katzenschlager et al., 2008).

Along with symptomatic treatments, there have been significant advances in neurosurgical strategies that have taken place over the past few years. Deep brain stimulation surgery has taken precedence over older strategies of lesioning, or pallidotomy, when it was approved by the United States Food and Drug Administration in 2002 for application in advanced cases of PD (Okun, 2012). Patients are considered as candidates for deep brain stimulation if multiple treatment options such as carbidopa-$_{L}$-DOPA therapy, and treatment with DA agonists and monoamine oxidase failed to ameliorate symptoms of PD (Okun, 2012). Deep brain stimulation therapy is achieved by surgical subcutaneous implantation of a pulse generator composed of a connecting lead and electrodes that are positioned at targeted brain sites such as the subthalamic nucleus or globus pallidus interna (Okun, 2012). This therapy has been shown to be effective and improve the quality of life of patients who experience symptoms such as tremors, on-off fluctuations of medication, and dyskinesia; however, this therapy has not shown any benefits towards improvement of gait dysfunction, balance and speech (Okun, 2012; Weaver et al., 2009). However, deep brain stimulation is costly and there are currently many unanswered questions including the benefits of targeting one brain site over

another, whether to incorporate bilateral or unilateral therapy, and the usefulness of this therapy in younger patients and less advanced cases of PD (Okun, 2012).

Despite the availability of symptomatic treatments and new applications such as deep brain stimulation, there is currently a lack of neuroprotective therapies for PD. Thus, there is a critical need for research to find disease-modifying treatments. The approaches used in the current investigation are innovative and may transform future drug development for PD by exploiting mitochondrial heat-shock proteins as novel targets and providing improved methods for drug design. Indeed, therapeutic approaches using proteins that assist in refolding of misfolded or aggregated proteins are now extensively being studied in a variety of diseases, including PD, Alzheimer's disease, amyotrophic lateral sclerosis, and the polyglutamine diseases. Although molecular chaperones including Hsp70 and Hsp40 have shown some therapeutic effects in animal models of neurodegenerative disease, the majority of these approaches are still in their early investigational stages and may take years to develop (Broadley and Hartl, 2009). As well, there are additional hurdles in drug development using molecular chaperones such as crossing the blood-brain barrier and targeting treatments to the specific brain regions that are affected. Our approach to elucidate the smallest functional fragment of CRP40 using bioinformatics approaches will increase success for crossing the blood-brain barrier. In addition, elucidation of a small functional piece of CPR40 of ~8-10 amino acids would allow our group to explore multiple viable options for the delivery of this therapeutic into the brain, including plasmid-delivery or delivery aided by implantable devices. The protein plasmid may be attached to small polymeric nanoparticles of size 1 to 100 nm

using different methods such as adsorption, entrapment or covalent attachment (Malavolta and Romero-Cabral, 2011). In addition, nanoparticles provide the practical advantages of being able to incorporate specific molecular-targeting factors to ensure that drugs reach the specific brain regions that are affected, and provide a controlled-release mechanism for their cargo (Malavolta and Romero-Cabral, 2011).

Another interesting option for delivery of CRP40 or its smallest functional peptide into the brain could involve an implantable pump-delivery system. This would be a suitable mode of delivery for larger proteins, such as the full length CRP40. The pump delivery system consists of a pump and catheter which are surgically placed under the skin, with a thin flexible tube (e.g., the catheter) that extends to the affected area to deliver medications in a targeted manner that minimizes the risks of unwanted side-effects. Recently, the pharmaceutical giant Ely Lilly has teamed up with Medtronic, the largest maker of drug pump delivery devices in the world, in efforts to explore this novel technology to deliver the modified glial-cell derived neurotrophic factor into the brain for treatment of PD (Cartwright, 2011). The glial-cell derived neurotrophic factor is a 20 kDa glycosylated polypeptide that has been suggested to promote neuronal survival; however, the evidence for the neuroprotective effects of this protein is still unclear (Decressac et al., 2011). The technology developed by Medtronic will explore the possibility of pump-based delivery of the glial-cell derived neurotrophic factor into the brain, and if successful, this type of technique could be applied in the future to deliver larger peptides such as CRP40 and/or its fragments into the brain for targeted and specific treatment of PD.

Further, the current study will yield a greater understanding on the mechanism of action of CRP40 that may allow for the incorporation of specific transcription factors to induce heat-shock function. Indeed, small chemical activators of heat shock transcription factors 1, including geldanamycin and 17-AAG, are now being investigated for their ability to induce multiple endogenous molecular chaperones, which may be a useful strategy in developing future treatments for neurodegenerative diseases with abnormal protein folding (Herbst and Wanker, 2007).

In conclusion, the results of this study, aided by a combined effort of molecular biology, bioinformatics, and *in vivo* animal validation, have helped to identify a small functional fragment of CRP40, which aas the 6.6 kDa P2P4 fragment. The preliminary behavioural observation of correction of rotational behaviour in P2P4-treated 6-OHDA rats presents an exciting opportunity for further elucidation of the smallest functional fragment of CRP40 using the β-fragments indentified from the bioinformatics analysis of P2P4. As well, this initial investigation should be followed up by a multitude of studies that will aid in the validation of the functional potential of CRP40 as well as its mechanisms and roles in cellular signalling, with an emphasis on expanding knowledge of the pathology of PD and other diseases related to oxidative stress and mitochondrial dysfunction.

Once our group have successfully found the smallest functional and specific peptide fragment of CRP40, experiments should be performed in future studies to determine the lowest dose required to obtain the maximal and most robust effects on

correction of behavioural impairments in 6-OHDA rats. In addition, experiments should be done to test toxicity and determine the optimal concentrations of peptide needed to enter the striatum region of the brain and sustain the therapeutic effects.

Overall, this study has illustrated the potential functional roles of a novel heat-shock protein, CRP40, and has created a basis for future studies to determine its putative role in PD. Increased understanding of the roles of crucial heat-shock proteins will help to establish their relationship and potential applications in a variety of protein misfolding disorders.

Chapter 3: Validation of Heat-shock protein 47 (Hsp47) – a negative control for testing the functional efficacy of Catecholamine-Regulated Protein 40 (CRP40)

3.1 Introduction/Rationale/Hypotheses

The goal of this project was to identify and validate a negative control for future experiments for testing the effect of CRP40 and its functional fragments on rotational behaviour in the unilaterally lesioned 6-OHDA rat model of PD. Heat-shock protein 47 (Hsp47), a collagen-specific chaperone previously cloned by Thomson and Ananthanarayanan (2001), was chosen as a potential negative control due to its similar size to CRP40 (e.g., the size of Hsp47 is 47 kDa, while the size of CRP40 is 40 kDa) and its role as a molecular chaperone.

Since Hsp47 is a collagen-specific chaperone, it was hypothesized that this protein would not interact with DA and/or regulate the dopaminergic pathway; these properties would make Hsp47 an appropriate negative control for use in experiments testing the functional effects of CRP40 in unilaterally-lesioned 6-OHDA rat models of PD. Thus, methods were designed to determine whether Hsp47 may be a valid negative control (Figure 3.1). All of the experiments for Hsp47 validation contained herein were performed *in vitro* before testing in animal studies.

Hsp47 was cloned and expressed as per previous methods by Thomson and Ananthanarayanan (2001). Validation of Hsp47 as a negative control for CRP40 experiments was performed by testing its DA-binding ability. Since we have previously shown that CRP40 binds DA with high capacity, low affinity, a negative control that does not bind DA and has no role in regulating the dopaminergic system was necessary. We performed a series competitive radio-labelled ligand binding studies using tritiated DA

([^{3}H]-DA), which assessed the ability of Hsp47 to bind [^{3}H]-DA in the presence of different concentrations of unlabelled or cold DA. CRP40 was used as a positive control because of its previously determined DA-binding ability.

Following the *in vitro* experiments that showed that Hsp47 had no effect on the DA system, this protein was eventually incorporated into *in vivo* animal experiments in 6-OHDA rats, performed by colleague Sarah Groleau. These experiments showed that Hsp47 did not have an effect on correction of behavioural impairments as CRP40 did (unpublished data).

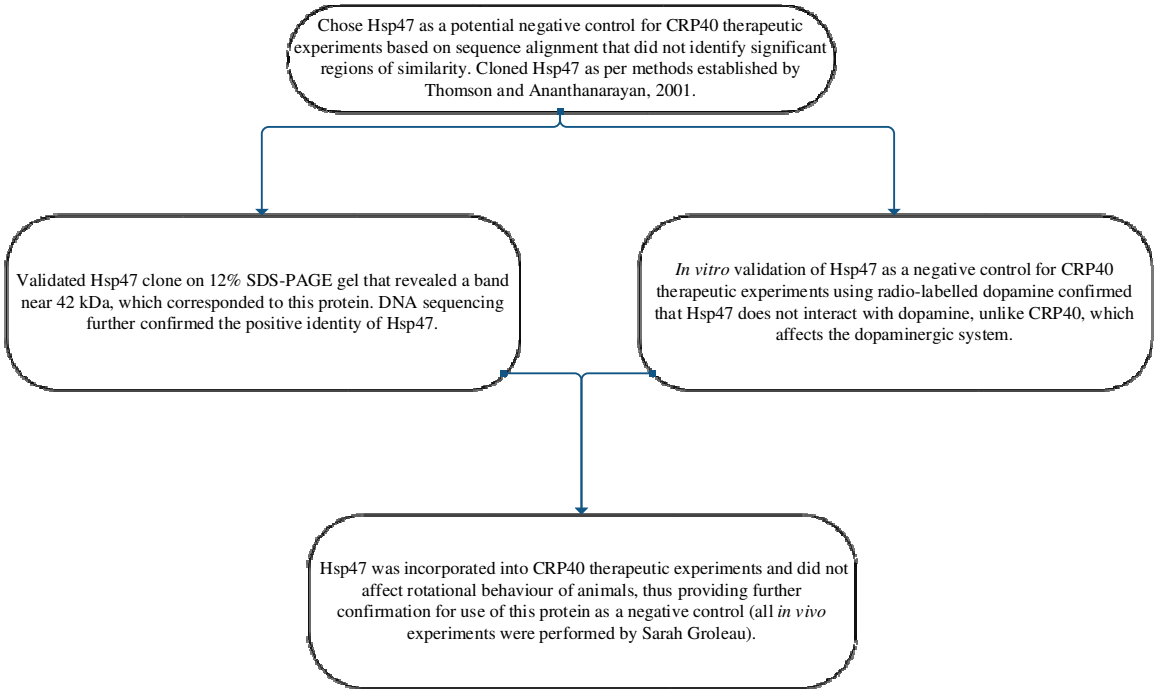

Figure 3.1 Study design summary of experiments for validation of Heat-Shock Protein 47 as a negative control for testing the functional effects of CRP40 and its fragments.

3.2 Materials and Methods

3.2.1 Cloning of Heat-Shock Protein 47

Hsp47 was cloned and validated as a negative control for CRP40 in *in vivo* animal experiments. Hsp47, a 47-kDa protein was an attractive candidate as a negative control for CPR40 experiments because of its similar size to CRP40, which is a 40-kDa protein. As well, it is known that both proteins share similar roles as molecular chaperones, including the ability to recognize protein polypeptide chains during biosynthesis and aid in proper folding, sorting, assembly and disassembly of polypeptides. While CRP40 is thought to be involved in the regulation of the neurotransmitter DA, Hsp47 has been well established as a molecular chaperone involved in the biosynthesis of collagen (Nagata, 1996; Nagata, 1998). Even though CRP40 and Hsp47 may share similar roles as molecular chaperones, they have distinct functions and target different substrates. To further demarcate this difference in function between the two proteins, we performed a series of radiolabelled DA binding experiments to test whether Hsp47 binds DA (methods and results described below). These experiments have aided in the validation of Hsp47 as a suitable negative control for use in future studies involving CRP40.

Hsp47 was previously expressed in *E. coli* using the IMPACT expression system (New England Biolabs, Ipswich, Massachusetts, USA) as per the protocol from Thomson and Ananthanarayanan, 2001. Briefly, the IMPACT system used by Thomson and Ananthanarayanan, 2001 allowed for one-step purification of Hsp47 through its facile

cleavage from its fusion adduct, intein. The vector that was used to clone Hsp47 was pTYB4 because this vector incorporated a T7 promoter which was advantageous for expressing this protein in high quantities. As well, the T7 promoter added a single glycine residue to the C-terminus of Hsp47, which was used to facilitate its cleavage from intein in the presence of thiols. Hsp47 was amplified using PCR methods from its original expression vector, pTrc46K, which initially yielded low levels of expression of the recombinant protein. The primers incorporated an *NcoI* restriction site at the N-terminus and a *SmaI* site at the C-terminus of the Hsp47 cDNA. The PCR product was subsequently digested, ligated into the pTYB4 vector, sequenced to confirm its identity, and transformed into the competent BL21 (DE3) strain of *E.coli*. These *E. coli* cells expressing Hsp47 were generously donated to our laboratory by Dr. Ananthanarayanan (Department of Biochemistry, McMaster University, Hamilton, ON, Canada). As the *E. coli* cells were approximately 10 years old, we did not use them to grow cultures. Instead, we began our cloning process by extracting the Hsp47 plasmid DNA using the QIAprep Spin Miniprep Kit (Qiagen Inc., Mississauga, ON, Canada) according to manufacturer's protocols.

3.2.2 DNA extraction using QIAprep Spin Miniprep Kit

Briefly, cultures of E.*coli* in LB-medium were spun at 500 g for 10 minutes. Pelleted bacterial cells were re-suspended in 250 μL of Buffer P1 and transferred to microcentrifuge tubes. 250 μL of Buffer P2 was added and tubes were inverted gently 4-6 times to mix. 350 μL of Buffer N3 was added and tubes were inverted and mixed again,

4-6 times. Reaction tubes were centrifuged for 10 minutes at 10 000 g (or 13 000 rpm). Supernatants were applied to QIAprep spin columns by decanting and centrifuged twice for 30-60 seconds, discarding the flow-through. The QIAprep spin columns were washed by adding 0.5 mL of Buffer PB and centrifuged 30-60 seconds. Flow-through was discarded, and QIAprep spin columns were washed by adding 0.75 mL of Buffer PE and centrifuging twice for 30-60 seconds, making sure to discard the flow-through after each spin. QIAprep spin columns were placed in clean 1.5-mL Eppendorf tubes and DNA was eluted by adding 50 µL of EB buffer to the center of each QIAprep column, incubating for 1 minute at room temperature and centrifuging for 1 minute in order to obtain DNA at the bottom of the Eppendorf tubes. Following DNA extraction, we re-transformed DNA into fresh *E.coli*-competent cells and grew the transformants on ampicillin-resistant agar plates at 37ºC overnight. Unused extracted DNA was stored in glycerol stock at -80°C.

3.2.3 DNA Transformation/Plating of Transformants on Agar Plates

Extracted Hsp47 DNA was transformed into One Shot TOP10 *E.coli* competent cells (Invitrogen Life Technologies, Burlington, ON, Canada) as per the following protocol. Competent cells were thawed on ice and 2 µL of the extracted Hsp47 DNA was added to the competent cells and mixed gently by tapping. The competent cells were incubated on ice for 30 minutes. A water bath was set to 42°C and the competent cells were heat-shocked for exactly 30 seconds. Vials of competent cells were removed from the water bath and placed on ice. 250 µL of pre-warmed S.O.C medium composed of 2% Tryptone, 0.5% Yeast Extract, 10mM NaCl, 10mM $MgSO_4$ and 10mM $MgCl_2$ was added

to each vial via sterile techniques (e.g., disinfecting work area with ethanol, performing experiments under a flame). The vials were placed on a secured rack and shook at 37°C for exactly 1 hour at 225 rpm in a shaking incubator. 50 µL and 150 µL from each transformation vial were spread on separate, labelled LB-agar plates which were inverted and incubated at 37°C overnight. The next day, single colonies were selected, usually from the 50 µL plates, and used for large scale preparation of proteins.

3.2.4 Large-scale preparation: Expression and purification of Hsp47 protein

In order to make large-scale quantities of the Hsp47 protein, two isolated colonies were inoculated into 3.0 mL LB-ampicillin, incubated at 37ºC and 250 rpm overnight in a shaking incubator. The next morning, 100 µL of each of the 3.0 mL overnight cultures were added to separate Falcon tubes containing 10.0 mL of LB-media and 10 µL of 100 mg/mL ampicillin. The 10.0 mL cultures were incubated at 37ºC and 250 rpm overnight in a shaking incubator. The next day, 10.0 mL of overnight cultures were inoculated into two 1 L flasks of LB-ampicillin (e.g., 1 mL of 100 mg/mL ampicillin in 1 L of sterile LB-media) and incubated at 37ºC for 3 to 4 hours until OD600 was 0.6. OD was measured using a Beckman DU-640 spectrophotometer, where the blank was 1 mL of sterile LB-media and the sample was 1 mL of culture taken from one of the 1 L flasks. Cultures were subsequently induced by adding 1 mM IPTG and incubated at14ºC for 3 hours. The mixture was then centrifuged at 4000 rpm for 15 minutes with an SLC-6000 rotor in a Sorval Evolution Rc Centrifuge (Thermo Scientific, Burlington, ON, Canada). Supernatants were discarded and the pellets were re-suspended in 500 mL of lysis buffer containing 0.1 M Tris, pH 7.6, 500 mM NaCl, and 0.5 mM EDTA. Cells were spun down

again at 4000 rpm for 15 minutes, supernatants were discarded, and pellets were pooled and re-suspended in 50 mL of lysis buffer containing two protease inhibitor tablets. Cells were lysed twice using the French press method at 15 000 psi until the lysate appeared clear. The lysate was frozen at -20°C until further purification.

3.2.5 Purification of Hsp47

Hsp47 was purified based on the construction of its expression vector pTYB4, which consisted of Hsp47 fused to the N-terminus of intein and a chitin-binding domain fused to the C-terminus of intein. First, Hsp47 lysate that was stored previously was thawed and spun down at 12,000 rpm for 20 minutes in a Beckman-Coulter centrifuge (Beckman-Coulter, Mississauga, ON, Canada) using the JA-20 rotor setup. In order to perform affinity purification of the fusion protein via the chitin-binding domain, the supernatant was bound to 10 mL of equilibrated chitin-containing affinity beads. The equilibration was performed by spinning down the chitin-beads at 500 g for 5 minutes, removing supernatant, applying 20 mL of lysis buffer (0.1 M Tris, pH 7.6, 500 mM NaCl, 0.5 mM EDTA, 0.1% Triton X-100), spinning again at the same speed, and re-suspending the pellet in 20 mL of Hsp47 lysate. The lysate and chitin-beads were then mixed, end over end, for 1 hour at 4°C. The mixture was then spun at 500 g for 5 minutes and the unbound material was collected. The mixture was divided and poured into four separate columns (1 x 10 cm) and washed extensively with buffer containing 20 mM Tris, pH 7.4, 1.0 M NaCl, 0.5% Triton X-100, followed by a wash with buffer containing 20 mM sodium phosphate, pH 7.4, containing 50 mM NaCl. Finally, 3 mL of cleavage buffer containing 100 mM β-mercaptoethanol, 20 mM sodium phosphate, pH 7.4, and 50 mM

NaCl was added to each column in order to initiate the self-cleavage reaction of intein at its N-terminus. The solution was incubated at 4°C overnight in order to complete the cleavage of Hsp47 from intein. Following the cleavage reaction, Hsp47 was collected as an eluent from the chitin column using wash buffer containing 20 mM sodium phosphate, pH 7.4, with 50 mM NaCl.

3.2.6 Determination of the Protein Concentration-Bradford Method

Protein concentration was determined using the Bio-Rad Protein Assay (Bio-Rad Laboratories, Mississauga, ON, Canada) kit which is based on the Bradford method. The standard curve on the Beckman DU-640 spectrophotometer was previously created by preparing five dilutions of bovine standard albumin (BSA) (e.g. linear range of the assay for bovine standard albumin is 0.2 to 0.9 mg/mL). The Dye Reagent Concentrate was prepared for the reaction by diluting 1 part concentrate with 4 parts distilled, deionized (DDI) water and filtering though Whatman #1 filter to remove particulates (e.g., this reagent was stored or used for a maximum of two weeks at room temperature before being discarded). 100 µL of each BSA standard was pipetted to test tubes (e.g., each protein standard was assayed in triplicate) and 5.0 mL of diluted dye reagent was added to each tube, vortexed and incubated at room temperature for 5 minutes. Absorbance was measured at 595 nm and the standard curve for protein concentrations was saved on the computer connected to the spectrophotometer and used in all subsequent measurements of protein concentration.

In order to measure the protein concentration of eluted Hsp47 fractions, 100 μL of each protein sample was added to 900 mL of diluted Bradford assay dye, vortexed, and incubated at room temperature for 10 minutes. Absorbance was measured at 595 nm and protein concentration was determined based on the previously constructed standard curve of protein concentrations. The cloning protocol for Hsp47 yielded adequate amounts of protein for radio-labelled ligand binding assays as well as future animal experiments.

3.2.7 Sodium Dodecyl Sulfate Polyacrylamide Gel Electrophoresis

10 μg of Hsp47 protein was pipetted, mixed with sample buffer (0.625 M Tris, 2% SDS, 0.05% β-mercaptoethanol, 10% glycerol, 0.01% bromophenol blue, pH 6.8) and heated in boiling water for 7 minutes in order to denature the proteins. The proteins were separated using SDS-PAGE (12% acrylamide) using running buffer (0.025 M Tris, pH 8.3, 0.3 M glycine, 0.1% SDS). An electrical voltage of 80 V was applied until the bands moved past the stacking gel, and then increased to 100 V for the remaining run. The gels were stained using Coomassie Brilliant Blue-250 and de-stained using a solution of 30% methanol and 10% glacial acetic acid. The gels revealed a band near 42 kDa indicating a fragment of Hsp47. Although Hsp47 is a 47 kDa protein, there may have been some degradation due to freezing of the protein. This staining pattern was also observed in the paper by Thomson and Ananthanarayanan, 2001. The plasmid Hsp47 DNA was sent for sequencing at MOBIX Laboratory (McMaster University, Hamilton, ON, Canada) and the identity of Hsp47 was confirmed, indicating a successful cloning experiment.

3.2.8 Validating Hsp47 as a negative control — Radio-labelled ligand binding studies

Hsp47 was cloned as a putative negative control for use in CRP40 animal experiments. The purpose of the negative control for such experiments was to clone a protein similar in size but not in function to the CRP40 protein. It was previously found that CRP40 binds DA with high capacity and low affinity. Thus, the ability to bind DA was not expected from an ideal negative control for CPR40 animal experiments. In order to validate Hsp47 as a negative control in CRP40 animal experiments, radio-labelled ligand binding studies were performed using [^{3}H]-DA. These studies assessed the ability of Hsp47 (as well as CRP40, which was used as a control) to bind DA by competitively binding [^{3}H]-DA in the presence of different concentrations of unlabelled or cold DA (0.1 % ascorbic acid).

All assays were performed in triplicate using 10 µg of proteins Hsp47 and the human CRP40. The final reaction volume was 200 µL which was made up with assay buffer consisting of 50 mM TRIS, 5.0 mM $MgCl_2$, 1.0 mM EDTA, 0.1 mM DTT, 0.1 mM PMSF, 100 mg/mL Bacitracin and 5.0 mg/mL soybean trypsin inhibitor at a pH of 7.4. DA (189.6 g/mol) was dissolved in 0.1% ascorbic acid. A 100 mM cold DA stock solution (e.g., this concentration represented non-specific binding) was made by dissolving 19 mg of DA in 1 mL of 1% ascorbic acid from which a 100 µM and a 100 nM solution of cold DA was subsequently made. The concentration of radioligand [^{3}H]-DA added to each reaction tube was 5 nM. The chart below describes the concentrations and/or amounts of reagents which were utilized for each protein:

Reaction tube	Protein (e.g., either Hsp47 or human CRP40)	[^{3}H]-DA	Cold DA	Assay Buffer
1.	10 µg (reaction tubes 1-12)	5 nM final concentration; 10 µL added (reaction tubes 1-12)	-	Volume of each reaction tube was made up to 200 µL.
2.			-	
3.			-	
4.			10 µL of 100 mM	
5.			10 µL of 100 mM	
6.			10 µL of 100 mM	
7.			10 µL of 100 µM	
8.			10 µL of 100 µM	
9.			10 µL of 100 µM	
10.			10 µL of 100 nM	
11.			10 µL of 100 nM	
12.			10 µL of 100 nM	

Following the addition of all solutions to each labelled test-tube, tubes were vortexed briefly and incubated in a shaking water bath at 37ºC, for 2 hours. Next, the cell harvester was prepared (Brandel, USA) by washing the lines 3 times with distilled water. The plastic lines were then cleaned by repeated washing in assay buffer using 50 nM TRIS, 1 mM EDTA, pH 7.4. Fiberglass filter paper was added and the samples were passed through filter paper with 3 consecutive washes. The filter paper was cut and placed in labelled scintillation tubes and 5.0 mL Biodegradable Counting Scintillant was added (Amersham, Picataway, NJ, USA). The tubes were then placed in racks and analyzed using a scintillation counter (Beckman LS5000TA), which measured the disintegrations per minute of [^{3}H]-DA or the radioactive counts. Briefly, it was previously found that CRP40 was binding with DA. However, no significant DA-binding was

detected for Hsp47. These results were further confirmed by repeating radio-labelled ligand binding experiments for Hsp47 using the indicated concentrations of unlabelled or cold-DA: 5mM (e.g., this represented non-specific binding); 5 μM; and 5 nM.

3.2.9 Data Analysis

Statistical analysis of the data was performed utilizing Graph Pad Prism 6.0 software. A one-way analysis of variance (ANOVA) with a confidence interval of 95% was utilized to analyze the data; the post-test used was Tukey's test.

3.3 Results

3.3.1 Sequence alignment of CRP40 and Hsp47 did not identify significant regions of similarity – a preliminary rationale for differential roles of two heat-shock proteins of similar size

We performed a sequence alignment of CRP40 and Hsp47 proteins and we have shown a very low level of sequence similarity (Figure 3.2). Thus, this was the rationale for choosing Hsp47 to be further tested as a potential negative control for CRP40 functional experiments. Sequence alignment alone does not reveal clues about potential overlapping functions of proteins, and due to the similar size of these two heat-shock proteins (40 kDa for CRP40 and 47 kDa for Hsp47), further testing needed to be performed to verify that these proteins did not have similar roles. In particular, it was important to verify that CRP40 and Hsp47 would not exert a similar function in 6-OHDA animals, and that Hsp47 could be used as a valid negative control in functional experiments. Thus, along with an artificial cerebrospinal fluid standard negative control, Hsp47, a Hsp that is similar in size to CRP40 would add another level of control to the *in vivo* experiments. The goal of subsequent experiments was to clone Hsp47 and develop methods to determine its mechanism of action and compare it to CRP40. The following results demonstrate the successful cloning of Hsp47, as well as a functional comparison to CRP40 using radio-labelled DA binding studies.

3.3.2 SDS-PAGE gel and DNA analysis determine successful Hsp47 cloning

The cloning of Hsp47 was performed as per previously established methods (Thomson and Ananthanarayanan, 2001). Briefly, expression and purification of Hsp47 was performed in *E.coli* using the IMPACT expression system, aided by the adduct intein that contains the gene of interest as well as a chitin-binding domain for purification. In order to verify cloning, a 12% SDS-PAGE gel of Hsp47 stained with Coomassie Brilliant Blue-250 was performed. The results of this experiment revealed a protein band near 42 kDa (Figure 3.3). Although Hsp47 is a 47 kDa protein, there may have been some degradation due to freezing of the protein. This staining pattern was also observed in the paper by Thomson and Ananthanarayanan, 2001. The plasmid Hsp47 DNA was sent for sequencing at MOBIX Laboratory (McMaster University, Hamilton, ON, Canada) and the identity of Hsp47 was confirmed.

3.3.2 In vitro validation of Hsp47 as a negative control reveals that Hsp47 does not interact with [^{3}H]-DA, and confirms the previous observation for the ability of CRP40 to bind DA

The ability of CRP40 to bind DA with high capacity and low affinity was previously reported by Gabriele et al., 2009. In order to determine whether Hsp47 may serve as a negative control in CRP40 functional experiments, the ability of this protein to bind DA was assessed by competitively binding [^{3}H]-DA in the presence of different concentrations of unlabeled DA. Unlike CRP40, the radio-labelled binding experiments with Hsp47 revealed that this protein does not bind DA. Thus, Hsp47, a molecular

chaperone involved in collagen synthesis, does not bind DA. In contrast, CRP40, which has a similar molecular weight and chaperone function, binds DA with high capacity and low affinity *in vitro*, and alters behaviour in 6-OHDA rats *in vivo*. Therefore, Hsp47 was shown to be a suitable negative control for experiments investigating the functional roles of CRP40 (Figure 3.4).

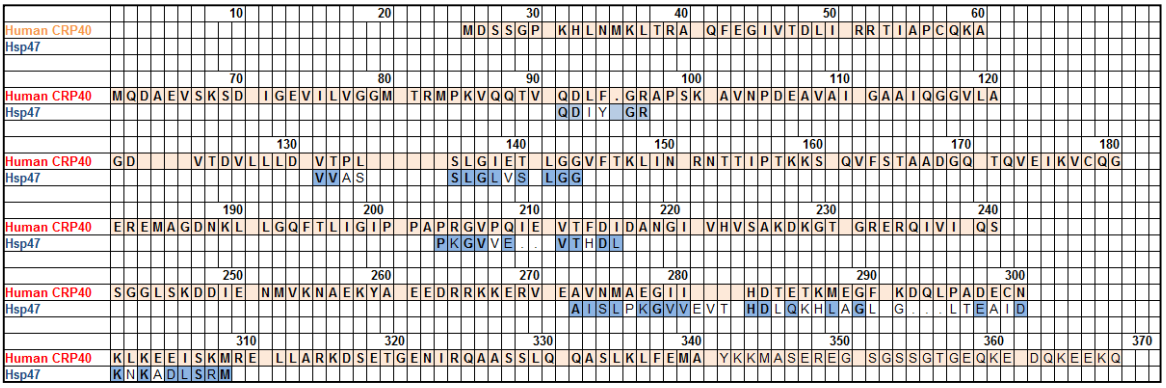

Figure 3.2 Sequence alignment of human CRP40 and Hsp47 shows no significant overlap of the amino acid sequences of the two proteins.

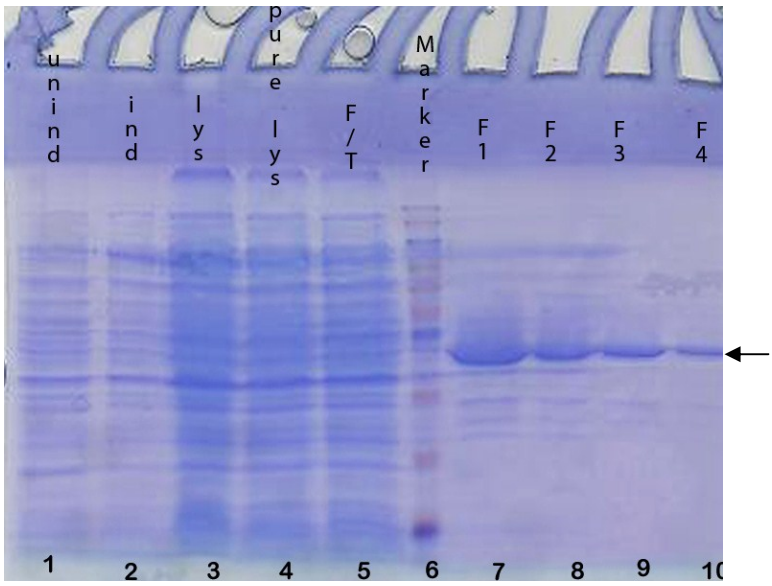

Figure 3.3 Purification of recombinant Hsp47 and 12% SDS-PAGE analysis of samples under reducing conditions using Coomassie Brilliant Blue-250 revealed a protein band near 42 kDa (lanes 7-10). Arrow shows band that corresponded to cleaved Hsp47.

FIGURE LEGEND

Figure 3.3: 12% SDS-PAGE gel of pure Hsp47 stained with Coomassie Brilliant Blue-250. Lane 1, uninduced fraction; Lane 2, induced fraction; Lane 3, lysed fraction; Lane 4, pure lysed fraction; Lane 4, F/T; Lane 5, protein marker; Lanes 7-10, purified Hsp47 fractions.

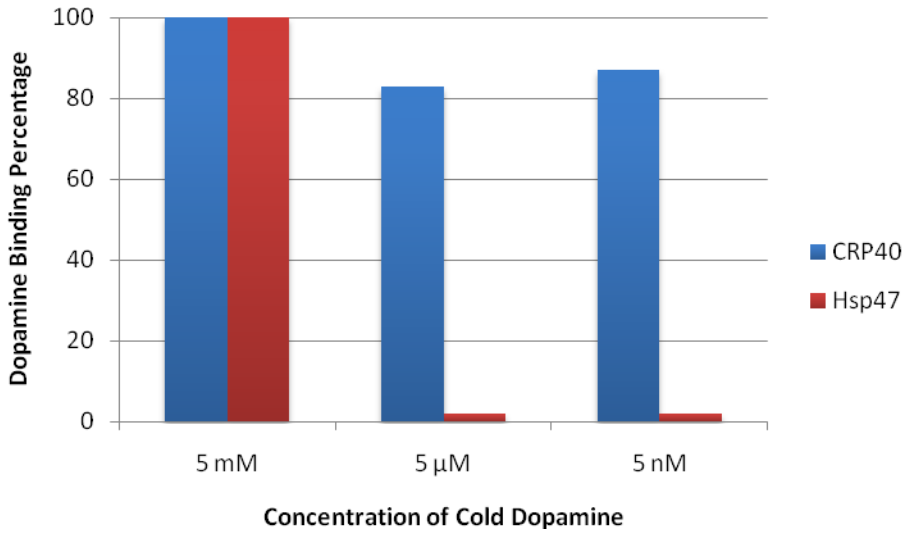

Figure 3.4 Radiolabelled [^{3}H]-DA binding results for CRP40 and Hsp47 in the presence of excess cold dopamine (5 mM, 5 µM, and 5 nM). The results indicate that Hsp47 does not bind DA, while CRP40 binds DA with high capacity and low affinity.

3.4 Discussion

The current study was designed in order to identify proteins that would act as a potential negative control for use in CRP40 functional experiments. The protein identified, Hsp47, may also be applied in future *in vitro* studies to explore the mechanism of action of CRP40. Hsp47, a collagen-specific protein, was chosen for testing and validation as a potential negative control, due to its comparable size to CRP40 (47 kDa versus 40 kDa, respectively) and similar role as a molecular chaperone. Hsp47 and CRP40 were examined for similarity of protein sequences, and it was determined that there was no significant overlap between these two proteins (Figure 3.2). Subsequently, Hsp47 was cloned and expressed as per previously established methods by Thomson and Ananthanarayanan, 2001 and the identity of the protein was confirmed through SDS-PAGE analysis and DNA sequencing (Figure 3.3). Competitive radio-labelled binding with [^{3}H]-DA was used to assess the function of Hsp47 and this was compared to CRP40. It was determined that Hsp47 does not possess DA binding ability (Figure 3.4). Thus, it was hypothesized that Hsp47 will not interact with the DA system, and therefore be useful as a negative control in *in vivo* animal studies in 6-OHDA rats, where CRP40 has been shown to correct rotational behaviour (unpublished data). These animal studies, performed by Sarah Groleau, used mortalin as a positive control, since it shares a high degree of sequence similarity to CRP40 (~99%). Thus, future *in vitro* studies on the mechanism of action of CRP40 could incorporate both mortalin as a positive control and Hsp47 as a negative control.

Indeed, careful design of scientific studies with proper controls plays a very important role in laboratory experiments, and allows investigators to reach a higher degree of certainty in their results. In particular, the routine use of negative controls in experiments allows for detection of sources of bias and other uncontrolled confounding factors (Hernan et al., 2004). As well, negative controls are useful in instances where there is a small sample size, to account for any imbalances between treatment groups. The correct choice of a negative control in experiments requires an in depth knowledge of the subject area. In this case, due to the extensive testing of CRP40 and knowledge on its interaction with the DA system, Hsp47 was tested for its ability to bind DA and was also later identified as an appropriate negative control *in vivo*. However, if the investigator does not possess an in depth knowledge of subject area, there is considerable risk in identifying negative controls based on incorrect assumptions, thus leading to incorrect analysis and misleading experimental results. Thus, negative controls may be used as sensitive tools to ascertain the credibility of a scientific study only if they are properly identified and carefully selected based on reasonable assumptions and an in depth knowledge of test material.

Hsp are classified based on their molecular weights and are involved in various functions (Hartl et al., 2011). For instance, the Hsp70 family of proteins is comprised of at least eight members, which are expressed in a tissue-specific manner, suggesting distinct individual functions that may be related to regulation of protein folding, or other non-chaperone-like functions (Daugaard et al., 2007). Hsp47, a protein that is closely related in size to CRP40, has been described as the only substrate-specific chaperone

discovered to date (Mala and Rose, 2010). The hypothesis of this study was that Hsp47 and CRP40 perform diverse functions in terms of their DA-interaction abilities.

Hsp47 was first identified based on its interaction with type IV collagen in murine parietal endoderm cells (Mala and Rose, 2010). Later, it was discovered that Hsp47 is localized to the endoplasmic reticulum of collagen-secreting cells and that it may participate in collagen biosynthesis. Hsp47 has been classified as a member of the Serpin superfamily that is composed of protease inhibitors, although Hsp47 does not have the ability to inhibit proteases (Nagata, 1998). However, unlike other members of the Serpin superfamily, Hsp47 contains a characteristic Arg residue in its C-terminal domain (Nagata, 1998). Also, Hsp47 contains an N-terminal signal sequence, and a retention signal RDEL sequence specific to the endoplasmic reticulum that is similar to the KDEL endoplasmic-reticulum retention signal of other chaperones (Mala and Rose, 2010). The protein contains a total of two high mannose type glycosylation sites and is constitutively expressed in non-stressed cells during collagen synthesis (Mala and Rose, 2010). Unlike CRP40, which is blood and brain specific, Hsp47 has been found in connective tissue, the heart, placenta, and in vascular tissue (Mala and Rose, 2010). Along with the results of the experiments presented here, a literature search on the functions of Hsp47 did not reveal any involvement in the DA system or PD. Hsp47 function thus far has been restricted to collagen processing. Specifically, Hsp47 binds nascent procollagen as it enters the endoplasmic reticulum and forms a triple helix that facilitates the transport of the bound collagen into the *cis*-Golgi (Mala and Rose, 2010). The dissociation of procollagen from Hsp47 in the *cis*-Golgi is aided by a change in pH and/or prolyl-4-

hydroxylation (Mala and Rose, 2010). Hsp47 is then recycled back into the ER and the subsequent hydroxylated procollagen goes on to the medial and *trans*-Golgi that aid in the secretion of mature collagen into the cytosol (Mala and Rose, 2010). In terms of its chaperone-like functions Hsp47 has been shown to be essential in procollagen secretion by preventing the formation of protein aggregates, assisting in modifications of procollagen, and preventing degradation of procollagen (Mala and Rose, 2010). Interestingly, Hsp47 does not possess the ability to bind ATP, which is characteristic of most molecular chaperones. In contrast to Hsp47, the chaperone-like functions of CRP40 are based on its significant amino acid sequence homology with the Hsp70 family. Preliminary studies have revealed that CPR40 has the ability to prevent thermal aggregation of firefly luciferase and enhance cell viability when overexpressed – these findings suggest chaperone-like functions of this protein (Gabriele et al., 2009). In addition, CRP40 binds DA with high capacity and low affinity; this is a feature of molecular chaperones (Gabriele et al., 2009). As well, the examination of the amino acid sequence of CRP40 has identified a characteristic leucine zipper motif that may be important in transcriptional activation (Gabriele et al., 2009).

In conclusion, Hsp47 and CRP40 are two similar sized proteins, with vastly different roles. This is demonstrated by the difference in their amino acid sequence, localization, differential binding of catecholamines such as DA, as well as numerous studies that have specifically and solely linked Hsp47 to collagen biosynthesis in comparison to CRP40 that has been associated with dopaminergic CNS disorders. Thus, Hsp47 was an appropriate negative control for use in CRP40 functional experiments.

Chapter 4: Roles of Catecholamine-Regulated Protein 40 in mitochondrial homeostasis and oxidative stress: Implications for Parkinson's disease

4.1 Introduction/Rationale/Hypotheses

Mitochondria are an important source of energy necessary to fuel crucial processes in neurons. Mitochondrial dysfunction has been reported in the SNc of deceased PD patients, as well as in skeletal muscle, platelets and lymphoblasts (Schapira et al., 1990; Schapira, 1994). Further, it has been found that the products of DA oxidation can decrease mitochondrial complex I activity and induce various functional defects (Bisaglia et al., 2010). It is now believed that there is a direct relationship between the combined effects of increased oxidative stress and impaired mitochondrial function in PD pathogenesis.

Recently, mortalin, the protein related to CRP40 through expression from a common gene and alternative splicing, has been identified as a protective protein in the mitochondria. Knockdown of mortalin in various human cell models, including HeLa cells and HEK293 cells, resulted in increased intramitochondrial ROS production, collapse of mitochondrial membrane potential important for energy production and cell viability, as well as alterations in mitochondrial morphology (Burbulla et al., 2010; Yang et al., 2011). In turn, overexpression of mortalin in neuronal cells and astrocytes preserved mitochondrial function, decreased ROS, and increased cell viability (Liu et al., 2005; Volobоueva et al., 2008). *In vivo* studies in an ischemia model of oxidative stress reported that mortalin overexpression improved neurological outcomes, mitochondrial function, reduced free radical generation, and preserved ATP concentrations (Xu et al., 2009). Further, mortalin has been found to participate in biogenesis of mitochondria as

the only ATPase component of the mitochondrial protein import machinery (Burbulla et al., 2010).

Recently, mutations in the substrate-binding domain of mortalin, from which CRP40 is expressed, have been identified in PD patients (Burbulla et al., 2010). Studies with these variants of mortalin in various neuronal and non-neuronal cell lines have been associated with impaired mitochondrial function, increased oxidative stress, and altered morphology—these mitochondrial parameters were rescued only by wild-type mortalin (Burbulla et al., 2010). Interestingly, two of the mortalin variants identified in this study by Burbulla et al. (2010), in German and Spanish PD patients, are located within the CRP40 sequence. One of these variants is specifically located within the 6.6kDa P2P4 protein that was found to be functionally effective in 6-OHDA rats. Based on these observations, it is hypothesized that CRP40 and P2P4 may have roles in the protection of mitochondria.

The present study was undertaken to investigate whether CRP40 plays a role in maintaining mitochondrial function. The goal of this study was to shed light on the mechanistic roles of this novel molecular chaperone, and to determine specifically whether the CRP40 portion of mortalin plays a role in maintaining mitochondrial homeostasis. SH-SY5Y neuronal cells were chosen for this study because this cell line has been reliably applied for studying oxidative stress, and thus represents an ideal model for investigation of CRP40 function *in vitro* (Burbulla et al., 2010). The study was designed to investigate whether mitochondrial parameters such as ROS and ATP concentrations were preserved in SH-SY5Y cells that overexpress the CRP40 protein and

mortalin as a control, following induction of cell stress using proteasomal inhibitors and ROS (see Figure 4.1 for study design). Future studies should be designed to complement these *in vitro* investigations. For example, mitochondrial parameters should also be examined in brain tissues of sacrificed 6-OHDA rats that have been treated with CRP40 and CRP40 fragments. As well, the specific function of CRP40 fragments in the mitochondria may serve as a future research target to complement these initial investigations.

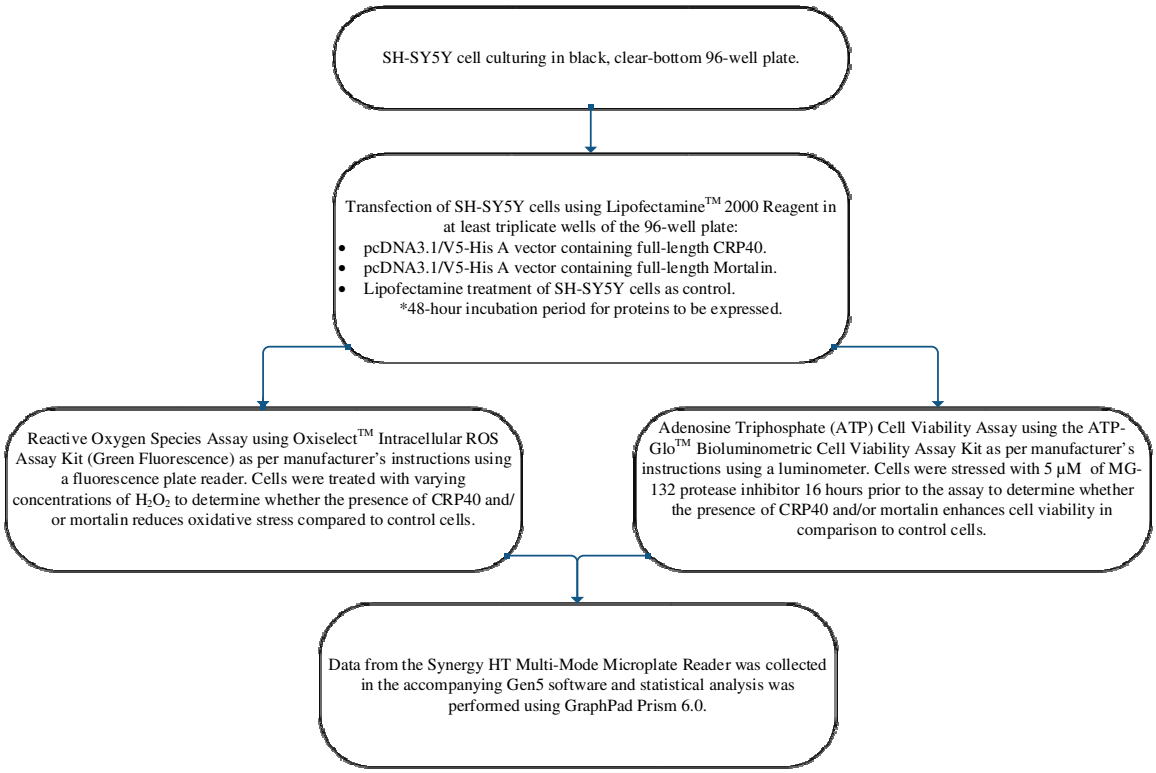

Figure 4.1 Study design summary of experiments to determine the mechanism of action of CRP40 in the mitochondria tested *in vitro* in SH-SY5Y cells.

4.2 Materials and Methods

4.2.1 Plating the cells

SH-SY5Y human neuroblastoma cells were a gift obtained from Dr. Niles' laboratory (McMaster University, Hamilton, ON, Canada). Cells obtained from liquid nitrogen storage that were previously frozen in 90% fetal bovine serum (FBS) and 10% dimethyl sulfoxide, were rapidly thawed at 37°C. 0.5 mL of thawed cells were added to 4.5 mL of pre-warmed Roswell Park Memorial Institute (RPMI) media and centrifuged at 2000 rpm for 5 minutes. The cell pellet was then re-suspended in 10 mL fresh RPMI in 10-cm cell culture dishes (Corning Life Sciences, Tewksbury, Massachusetts, USA). The RPMI that the cells were cultured in was supplemented with 10% FBS, 1% penicillin/streptomycin, and 1% L-glutamine, which made up the cell culturing media. Cells were incubated at 37°C in a 5% CO_2 incubator.

4.2.2 Passing and plating the cells (serial dilution)

Cells were passed when 80-90% confluence was reached. The RPMI was aspirated from the cell culture plates, and cells were detached from plates by addition of 5 mL of 1X Trypsin (diluted in PBS). After 5 minutes, 10-15 mL of fresh RMPI was added to the plates to inhibit the toxic effects of Trypsin. This mixture of cells, RPMI and trypsin was aspirated from the plates and centrifuged at 2000 rpm for 5 minutes. The cell pellet was then resuspended in 10 mL of fresh RPMI. The cells were then counted using a standard haemocytometer (e.g., 0.1 mm counting chamber depth). Briefly, 25µL of the cell mixture was loaded onto the haemocytometer and covered with a glass cover slip.

Cells were counted under the microscope in 4 grids of the haemocytometer and the number of cells per mL was calculated using the following formula:

(# of cells counted in 4 grids) x (4x10^4) x (any dilution factor applied)

= # of cells/mL

For the mitochondrial assays, cells were plated into black, clear-bottom 96-well plates (ThermoFisher Scientific, Burlington, ON, Canada) at a density of 3 x 10^5 cells per well, in a total volume of 100 µL cell culturing media. The number of cells obtained per mL, from the calculation above, was adjusted through dilution in media to obtain the desired number of cells per well (e.g., 3 x 10^5 cells per well) in a total volume of 100 µL per well. Cells were then incubated at 37°C in a 5% CO_2 incubator.

4.2.3 Transfection of SH-SY5Y cells

SH-SY5Y cells were cultured in 96-well plates until 80-90% confluent, and transfections were performed using Lipofectamine™ 2000 reagent (Invitrogen Life Technologies, Burlington, ON, Canada) according to the manufacturer's instructions. Briefly, 3 x 10^5 cells per well were transfected with the pcDNA3.1/V5-His A vector containing full-length CRP40 or mortalin. Lipofectamine treatment of SH-SY5Y cells at the same concentration as for the CRP40 and mortalin transfections was used as a control.

First, the medium for cells in 96-well plates was replaced with 100 µL of fresh cell culture medium and cells were incubated 37°C in a 5% CO_2 incubator for the duration of the experiment. Next, different ratios of DNA:Lipofectamine were used to

transfect cells. A ratio of 1 DNA:1 Lipofectamine was used according to the manufacturer's instructions as well as a ratio of 1.66 DNA:1 Lipofectamine. The following calculations and concentrations of reagents are presented per 1-well of the 96-well plate. For both of these ratios, 0.5 μg mortalin or CRP40 plasmid DNA was mixed with 5 μL RMPI media without FBS, antibiotics or glutamine. For the 1 DNA:1 Lipofectamine ratio, Lipofectamine was mixed gently before use and 0.5 μL of Lipofectamine was diluted with 5 μL RMPI media. Similarly, for the 1.66 DNA:1 Lipofectamine ratio, 0.3 μL Lipofectamine was mixed with 5 μL RMPI media. The DNA of mortalin or CRP40 was mixed with their respective Lipofectamine solutions within 5 minutes and incubated at room temperature for 20 minutes to allow for the DNA and Lipofectamine complexes to form. Following this 20 minute period, 10 μL of the respective DNA and Lipofectamine complexes were added per each well of the 96-well plate, mixed gently by rocking the plate back and forth, and incubated for 12 hours at 37°C and 5% CO_2. After 12 hours, the media containing Lipofectamine was replaced with 100 μL of fresh cell culture media per each transfected well. Mitochondrial assays were performed 48 hours following transfection to allow for the mortalin and CRP40 proteins to be expressed.

4.2.4 Mitochondrial assays using SH-SY5Y cells

The SH-SY5Y cell line used in this study has been extensively characterized and previously utilized to study the role of mortalin in mitochondria (Burbulla et al., 2010; Nair and Mishra, 2001). This cell line is derived from the human neuroblastoma and is

commonly used as an *in vitro* model for neurodegenerative disorders. Thus, the SH-SY5Y cell line was used as a neuronal modeling system to perform experiments to determine whether CRP40 is involved in maintaining mitochondrial homeostasis.

4.2.4.1 Adenosine Triphosphate Assay

Relative ATP concentrations that reflect cell viability were measured under different conditions (SH-SY5Y cells; SH-SY5Y cells transfected with CRP40; and SH-SY5Y cells transfected with mortalin) using the ATP-Glo™ Bioluminometric Cell Viability Assay Kit (Biotium, Hayward, California, USA) according to the manufacturer's instructions. To induce proteolytic stress, SH-SY5Y cells were treated with 5 μM MG-132 protease inhibitor (Sigma-Aldrich, Oakville, ON, Canada) for 16 hours prior to the assay as per previously established protocols from Burbulla et al., 2010. MG-132 was prepared by dissolving the powder in dimethyl sulfoxide (DMSO) solution. MG-132 has been previously shown to be a potent inducer of apoptosis through formation of ROS (Ling et al., 2003). As well, this ROS formation due to MG-132 has been suggested to cause mitochondrial dysfunction due to release of *cytochrome c* from the mitochondria and lead to loss of cell viability (Ling et al., 2003). Thus, incorporation of this reagent for the assay was used to determine whether the CRP40 and/or mortalin transfected cells have improved cell viability versus control cells when treated with a proteasomal inhibitor that causes oxidative stress. Specifically, in the ATP assay, cell viability is proportional to the amount of intracellular ATP.

Cell viability was investigated using the ATP-Glo™ Bioluminometric Cell Viability Assay Kit, which uses ATP as an indicator of metabolically active cells. Cell viability is therefore determined based on the amount of ATP available in cells. The kit incorporates the reaction catalyzed by Firefly luciferase, which uses ATP to oxidize D-Luciferin, resulting in production of light which is used to determine the amount of ATP availability. Cells in each well of the 96-well plate were prepared in 90 µL dH_20 and 10 µL RPMI for maximum signal output.

The reagents for the assay were prepared as per the manufacturer's instructions on the day of the assay. Briefly, a bottle of ATP-Glo Assay Buffer was thawed and 25 mL was transferred to a new clean container. 10 mg of D-luciferin was dissolved with the above assay buffer to make 25 mL of the ATP-Glo assay solution. 250 µL of Firefly luciferase was added to 25mL of the ATP-Glo assay solution to make the ATP-Glo Detection Cocktail.

Luminescence was detected for each individual well of the 96-well plate using a Synergy HT Multi-Mode Microplate Reader (BioTek, Winooski, Vermont, USA) luminometer with an injector set at a delay time of 10 seconds and an integration time of 10 seconds for appropriate sensitivity. 100 µL of the ATP-Glo Detection Cocktail was automatically injected into each well and luciferase activity was measured for 10 seconds. All conditions were assayed in triplicates.

4.2.4.2 Reactive Oxygen Species Assay

In order to examine the effects of the CRP40 on oxidative stress, intracellular ROS were assessed using the OxiSelect™ Intracellular ROS Assay Kit (Green Fluorescence) (Cell Biolabs Inc., San Diego, California, USA) as per manufacturer's instructions. Briefly, 48 hours after transfection of cells in the black, clear-bottom 96-well plate, media was removed and cells were washed 2 times with 100µL 1X PBS. Next, cells were incubated for 60 minutes at 37°C in a 5% CO_2 incubator with 100µL/well of the 1X fluorogenic probe 2', 7'-Dichlorodihydrofluorescin diacetate (DCFH-DA) that was diluted in RPMI from its original 20X solution contained in the kit. The DCFH-DA dye works by rapidly diffusing into cells and is deacetylated by esterases in cells to the non-fluorescent 2', 7'-Dichlorodihydrofluorescin (DCFH), which is then rapidly oxidized to highly fluorescent 2', 7'-Dichlorodihydrofluorescin (DCF) by ROS. The fluorescence units measured reflect the levels of ROS in the cell cytosol. After incubation with DCFH-DA, cells were washed 2 times with 100µL 1X PBS and treated with varying amounts of hydrogen peroxide (H_2O_2) (0 µM basal condition, 300 µM, 500 µM, and 1000 µM) for one hour at room temperature, which was used to induce cell stress. Fluorescence was measured using a fluorescence plate reader, Synergy HT Multi-Mode Microplate Reader (BioTek, Winooski, Vermont, USA), at 480 nm (excitation) and 530 nm (emission). All conditions were assayed in triplicates.

A standard curve of DCF standards was prepared to test out the instrumentation and whether the assay was functional. However, according to the manufacturer's instructions, the DCF standards could not be used for absolute quantitation due to the

additional treatment with H_2O_2. As well, cells are differentially permeable to H_2O_2, thus a standard curve incorporating H_2O_2 cannot be used for obtaining absolute quantitation, as advised by the manufacturer. Thus, the results of this assay reflect the relative change in ROS or fluorescence between the different cells (SH-SY5Y cells; SH-SY5Y cells transfected with CRP40; and SH-SY5Y cells transfected with mortalin) and different concentrations of H_2O_2 treatment.

4.2.4.3 Data Analysis

Data for the ROS and ATP assays respectively were collected in the Gen5 Data Analysis Software (BioTek, Winooski, Vermont, USA) and exported to GraphPad Prism 6.0 software for analysis. Statistical analysis was performed using two-way ANOVA with the Tukey's multiple comparisons test.

4.3 Results

4.3.1 Adenosine Triphosphate Assay: Cells overexpressing CRP40 and Mortalin have different intracellular ATP concentrations

The ability of CRP40- and mortalin- transfected SH-SY5Y cells to maintain mitochondrial homeostasis, specifically energy production and ATP concentrations, was examined using the ATP-Glo^{TM} Bioluminometric Cell Viability Assay Kit as described in methods. MG-132 was used to inhibit proteasomal function and cause increased oxidative stress, which would compromise mitochondrial function, as well as the processes of energy production. The quantitation of ATP conncetraitions was thus used as a measure of cell viability.

As seen under the basal condition in Figure 4.2, cell viability was significantly lower in SH-SY5Y cells that have been transfected with either CRP40 or mortalin, and that overexpress these proteins, versus normal non-transfected SH-SY5Y cells ($p<0.0001$ for both CRP40- and mortalin- transfected cells). It is expected that ATP concentrations in transfected cells would not be reduced to this extent, especially in the untreated condition. The cells overexpressing either CRP40 or mortalin should have the same viability as normal SH-SY5Y cells. The cell viability of non-transfected SH-SY5Y cells treated with MG-132 diminished significantly in comparison to the non-transfected, non-treated SH-SY5Y cells ($p<0.0001$). In terms of percentage, there was approximately a 50% drop in cell viability when non-transfected SH-SY5Y cells are treated with MG-132. When comparing the effect of MG-132 treatment on the viability of CRP40-transfected

SH-SY5Y cells, there was a slight (~24%), but statistically significant, drop in ATP following treatment with the proteasomal inhibitor (Figure 4.2). For mortalin-transfected SH-SY5Y cells, there was a statistically significant reduction in cell viability (~37%) following treatment with MG-132 (Figure 4.2). Thus, MG-132 treatment caused a reduction in cell viability of approximately 50% for normal non-transfected cells, approximately 24% for SH-SY5Y cells overexpression CRP40, and approximately 37% for cells overexpressing mortalin.

The reduction in ATP and the resulting loss of cell viability in CRP40 and mortalin- transfected cells that have been treated with MG-132 was thus not as pronounced as the loss in cell viability in the normal non-transfected cells treated with MG-132. These preliminary findings suggest that overexpression of CRP40 and mortalin in SH-SY5Y cells helps to maintain intracellular ATP concentrations and energy production from the mitochondria, and that these proteins may confer protection from cell death induced by oxidative stress. These preliminary results are hypothesis-generating and require further verification through more experimental trials and using different strategies to impair ATP production in cells, such as oxygen-glucose deprivation. As well, in the future, these experiments should be performed in primary neuronal cell lines or astrocytes, as well as using *in vivo* animal models of neurodegenerative disease.

4.3.2 Reactive Oxygen Species Assay: Cells overexpressing CRP40 and mortalin have differential mitochondrial ROS concentrations

The ability of CRP40- and mortalin- transfected SH-SY5Y cells to protect against the harmful effects of mitochondrial ROS in comparison to normal non-transfected SH-SY5Y cells was measured using the OxiSelect^{TM} Intracellular ROS Assay Kit (Green Fluorescence) as described previously. H_2O_2 treatment was used to induce oxidative stress in the assay. Increased fluorescence in this assay corresponded to greater ROS concentrations.

Overall, treatment with oxidant resulted in higher ROS production in normal (or in the un-transfected basal condition) SH-SY5Y cells, CRP40-transfected SH-SY5Y cells, and mortalin-transfected SH-SY5Y cells in comparison to the basal untreated condition (Figure 4.3). Specifically, under the basal condition, where non-transfected SH-SY5Y cells were not treated with an oxidant, the levels of ROS were significantly lower than in the treated conditions for non-transfected SH-SY5Y cells ($p= 0.0343$ for 300 μM H_2O_2 treatment and $p<0.0001$ for 500 μM H_2O_2 treatment) (Figure 4.3). Also, CRP40-transfected SH-SY5Y cells treated with 300 μM H_2O_2 treatment had significantly higher concentrations of ROS than untreated CRP40-transfected SH-SY5Y cells ($p=0.0343$). Mortalin-transfected SH-SY5Y cells in the basal condition displayed a similar tendency for decreased ROS concentrations in comparison to mortalin-transfected SH-SY5Y cells treated with either 300 μM H_2O_2 or 500 μM H_2O_2, however statistical significance for these differences was not reached.

Furthermore, in the untreated condition, the normal SH-SY5Y cells showed a tendency towards slightly higher ROS concentrations than both the CRP40-transfected SH-SY5Y cells, and the mortalin-transfected SH-SY5Y cells; however this difference was not statistically significant (Figure 4.3). Similarly, when different cells (normal SH-SY5Y cells; CRP40-transfected SH-SY5Y cells; and mortalin-transfected SH-SY5Y cells) were treated with 300 μM H_2O_2, there was a tendency towards higher ROS concentreations in the normal un-transfected SH-SY5Y cells compared to the transfected conditions, however this difference was not statistically significant. The protective role of CRP40 and mortalin was observed in the 500 μM H_2O_2 treatment condition, where there was a statistically significant difference between normal SH-SY5Y cells treated with 500 μM H_2O_2 versus CRP40-transfected SH-SY5Y cells treated with 500 μM H_2O_2 ($p=0.0056$), and normal SH-SY5Y cells treated with 500 μM H_2O_2 versus mortalin-transfected SH-SY5Y cells treated with 500 μM H_2O_2 ($p=0.0343$). Therefore, normal SH-SY5Y cells had increased concentrations of ROS in comparison to CRP40- and mortalin-transfected SH-SY5Y cells that were more pronounced when a high amount of oxidant was used to induce oxidative stress. Also, in the 500 μM H_2O_2 treatment condition, there was no statistically significant difference in ROS concentrations between the CRP40-transfected SH-SY5Y cells and mortalin-transfected SH-SY5Y cells, although the CRP40-transfected SH-SY5Y cells displayed a tendency towards lower ROS production in this condition. Future studies should be carefully designed to examine the differential ability of CRP40 and mortalin to protect cells against oxidative stress.

Interestingly, when a greater concentration of H_2O_2 (e.g., 500 µM) was applied to CRP40-transfected SH-SY5Y cells, these cells showed a tendency towards higher ROS production than the untreated CRP40-transfected SH-SY5Y cells, which was the expected result. However, ROS production in the CRP40-transfected SH-SY5Y cells treated with 500 µM H_2O_2 was lower than for the CRP40-transfected SH-SY5Y cells treated with 300 µM H_2O_2 (results not statistically significant). While there was a statistically significant increase in ROS levels of the untreated CRP40-transfected SH-SY5Y cells in comparison to the CRP40-transfected SH-SY5Y cells treated with 300 µM H_2O_2 ($p= 0.0343$), there was no statistically significant difference between ROS levels in untreated CRP40-transfected SH-SY5Y cells in comparison to the CRP40-transfected SH-SY5Y cells treated with a higher concentration of H_2O_2 (e.g., 500 µM). This result suggests that CRP40 may have conferred a differential degree of protection against higher concentrations of the H_2O_2 oxidant, keeping ROS levels closer to those observed in the normal, untreated condition for cells transfected with CRP40. Perhaps there is a higher activation threshold (e.g., a greater amount of oxidative stress required) for CRP40 to exert its potential cytoprotective function against oxidative stress. However these are preliminary hypotheses that should be further examined.

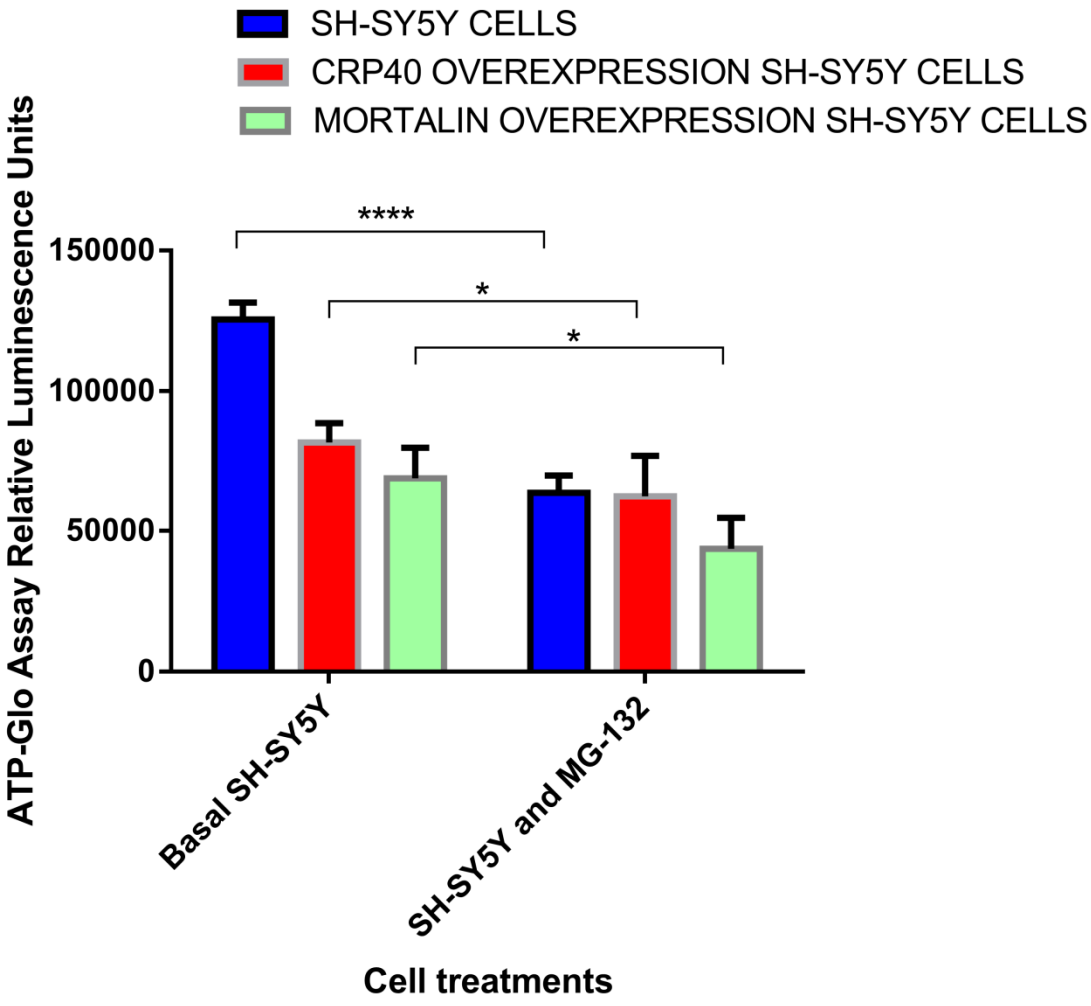

Figure 4.2 Overexpression of CRP40 and mortalin partially preserve ATP concentrations and cell viability in SH-SY5Y cells subjected to 16 hours of 5 µM MG-132 proteasomal inhibitor.

FIGURE LEGEND

Figure 4.2: The left panel shows ATP concentrations under basal conditions in normal SH-SY5Y cells, cells overexpressing CRP40, and cells overexpressing mortalin. Mortalin was used as a positive control in this assay. The right panel shows ATP concentrations under conditions of proteasomal stress induced by treatment with MG-132. After treatment with proteasomal inhibitor, cells overexpressing CRP40 and mortalin demonstrated slight, but statistically significant alterations in ATP/cell viability (*$p<0.05$; ~24% reduction of cell viability in CRP40-transfected cells; ~37% reduction of cell viability in mortalin-transfected cells). In contrast, non-transfected SH-SY5Y cells demonstrated a significant drop in ATP and cell viability after treatment with MG-132 (****$p<0.0001$; ~50% reduction in cell viability). The data are representative of mean ± S.D. of experiments for each condition performed twice, in triplicates.

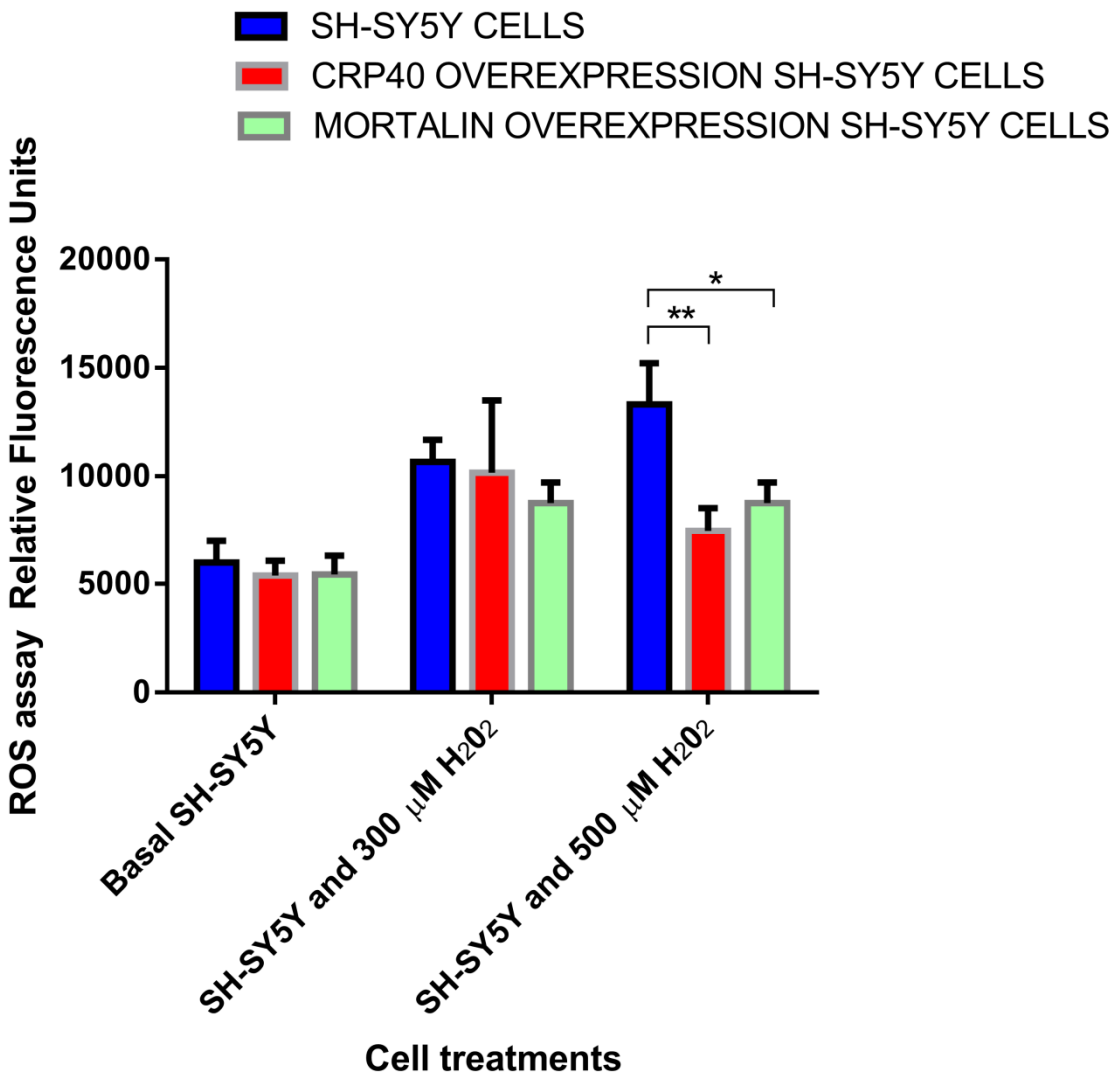

Figure 4.3 Overexpression of CRP40 and mortalin partially preserves mitochondrial homeostasis and ROS concentrations under conditions of oxidative stress induced by treatment with H_2O_2 (500 µM).

FIGURE LEGEND

Figure 4.3: An increased florescence signal correlates with a higher amount of ROS. The far left panel shows ROS concentrations under basal conditions in normal SH-SY5Y cells, cells overexpressing CRP40, and cells overexpressing mortalin. Mortalin was used as a positive control in this assay. The right panels show ROS concentrations under conditions of oxidative stress induced by treatment with 300 μM and 500 μM H_2O_2, respectively. ROS increases significantly after treatment with H_2O_2 (from left to right panels) for normal non-transfected cells, and CRP40-transfected cells, and shows a tendency towards increasing concentrations for mortalin-transfected cells (not statistically significant). After treatment with 500 μM H_2O_2, cells overexpressing CRP40 display a statistically significant decrease in ROS compared to normal SH-SY5Y cells (**p=0.0056), with cells overexpressing mortalin following a similar, but less pronounced pattern for control of ROS concentrations following oxidative stress (*p=0.0343). The data are representative of mean ± S.D. of experiments for each condition performed in triplicates.

4.4 Discussion

The present study was undertaken to investigate the functional roles of CRP40. As discussed previously, this protein has been linked to PD through reductions in both the post-mortem brain samples and blood specimens of live patients. Indeed, since the discovery of CRP40, 16 years of research have produced findings and evidence that have converged to reveal its intricate involvement in neurodegenerative disease pathology. However, the specific involvement of CRP40 in maintaining mitochondrial function and homeostasis has not been studied until now.

The results of this study provide preliminary evidence that indicates that overexpression of CRP40 in the *in vitro* cell model SH-SY5Y cells, results in protection against oxidative stress, as evidenced by maintenance of ATP concentrations and cell viability, as well as cellular homeostasis and intramitochondrial ROS concentrations under conditions causing cellular stress (Figure 4.2; Figure 4.3). Specifically, after treatment with proteasomal inhibitor, cells overexpressing CRP40 retain ~76% viability, and cells overexpressing mortalin retain ~63% viability, in comparison to normal SH-SY5Y that show ~50% cell death (Figure 4.2). These results are consistent with previous *in vitro* studies that have indicated the beneficial roles of mortalin in maintaining mitochondrial function. Mortalin overexpression has been shown to confer protection against glucose starvation- and ischemia- induced apoptosis in neuronal cells (Liu et al., 2005). As well, overexpression of mortalin in SH-SY5Y cells has been shown to inhibit mitochondrial defects caused by the beta-amyloid peptide $A\beta_{1-42}$, specifically by protecting against depolarization of mitochondrial membrane potential, reducing ROS

species accumulation and lipid peroxidation, protecting against increased cytochrome c oxidase activity, and suppressing deficits in ATP generation (Qu et al., 2011). Mortalin was also found to preserve ATP concentrations and cell viability of astrocytes under glucose deprivation that mimics ischemic-conditions and normally leads to severe ATP depletion and apoptosis (Volobоueva et al., 2008). Astrocytes are the most numerous cell type in the brain and they play critical roles in trophic support of neurons, oxidant defense, and neuronal homeostasis; these cells are able to confer neuroprotective effects when their metabolic and energy production processes are preserved, and thus represent an important area for neurodegenerative disease research (Volobоueva et al., 2008). In an *in vivo* study by Xu et al., 2009, where mortalin was overexpressed in the rat brain, the results indicated a 35% ATP depletion after induction of focal ischemia, compared to a 66% decrease in ATP production in vector-injected animals (Xu et al., 2009). Figure 4.2 demonstrates a similar degree of change in ATP concetrations in SH-SY5Y cells overexpressing mortalin. Although multiple studies have investigated the protective effects of mortalin in maintaining mitochondrial homeostasis, this is the first time to date that a potential protective effect in the mitochondria has been attributed to its splice variant, CRP40. The results of these studies are promising and hypothesis-generating. These preliminary results indicate that CRP40 may be more robust in its protection of mitochondrial ATP production, conferring greater protection from stress-induced cell death than mortalin (Figure 4.2). Further *in vitro* and *in vivo* studies are required to verify these hypotheses and to examine the ability of CRP40 to maintain mitochondrial

homeostasis and ATP concentrations, which are essential for neuronal signalling and other vital processes that are impaired in neurodegenerative diseases.

Future studies should also focus on examining the function of CRP40 in the mitochondria by measuring the activity of mitochondrial complexes; this could be carried out when CRP40 is knocked down, to determine whether the function of any of the complexes is compromised, or conversely CRP40 may be overexpressed and the activity of the mitochondrial complexes could be measured under proteolytic or oxidative insult to determine its potential protective role. Thus far, mortalin has been found to participate in protection of complex IV of the mitochondrial electron transport chain, which appears to be the most vulnerable during brain ischemia (Xu et al., 2009). Mitochondrial DNA deletions associated with complex IV and resulting oxidative damage have also been found to occur in PD, although PD patients have more clearly demonstrated defects in DNA encoding associated with complex I (Gu et al., 1998). Complex I of the mitochondria is an enzyme comprised of approximately 50 subunits, and is under the influence of both nuclear and mitochondrial genomes, making it a particularly challenging complex to study. There have been various studies that have reported inhibition of complex I in the SNc in platelets and in muscle tissue of PD patients (Schapira, 2011). These investigations were spurred by the discovery of neurotoxicity of 1-methyl-4-phenyl-1,2,3,6-tetrahydropyridine and its metabolite 1-methyl-4-phenylpyridinium, which cause permanent symptoms of PD through inhibition of complex I. 1-methyl-4-phenylpyridinium, along with rotenone and annonacin are all compounds that have shown a high degree of toxicity towards dopaminergic neurons

implicated in PD (Lannuzel et al., 2003; Ramsay et al., 1986). Defects in complex I activity have been found in only 30% of Parkinson's patients, thus investigation of the impacts of molecular chaperones such as mortalin and CRP40 on complex IV add an important dimension to unravelling the role of oxidative stress protection, mitochondrial homeostasis, and neuroprotection that may be regulated by this important group of proteins.

Along with energy production, oxidative stress is considered to be a major cause for the loss of dopaminergic neurons in PD. There have been numerous studies that have linked free radical production, for instance, from enzymatic oxidation of DA, to toxicity caused by 6-OHDA, and evidence from post-mortem and clinical studies, to neuronal death in PD (Jenner and Olanow, 2006). The evidence linking free radical generation to PD pathology has focused on measuring markers or inducers of oxidative stress. Most notably, it has been reported that free radical generation in the SNc of PD patients may be the cause of increased lipid peroxidation (4-hydroxynonenal, advanced glycation end products, malondialdehyde, and lipid hydroperoxides), DNA oxidation (8-hydroxyguanosine), and protein oxidation (protein carbonyls). While the source of oxidative stress remain an area of debate, with both neuronal and glial cells postulated to play a role, there is no question that the origin of these cellular stressors arises from the mitochondria. The oxidative stress seen in PD may also arise from altered accumulation of iron in the SNc, altered proteolysis, alterations in α-synuclein aggregation, mutations in proteins regulating the oxidative stress response (e.g., DJ-1), and changes in calcium channel activity (Schapira and Jenner, 2011). The evidence from the present CRP40

study, along with previous evidence for mortalin, suggests that molecular chaperones are crucial factors in defense against oxidative stress. The implications of these proteins may stretch beyond PD and extend to a variety of other disease states that are characterized by impairments in antioxidant defense and oxidative stress signalling.

The findings of the current study also point to a potential role of CRP40 in protecting cells against the harmful effects of mitochondrial ROS; this protective ability seems to be especially pronounced under conditions of high oxidative load induced by treatment with increased concentrations of H_2O_2 (Figure 4.3). In particular, ROS concentrations following treatment with 500 μM H_2O_2 in SH-SY5Y overexpressing CRP40 were not significantly different from untreated SH-SY5Y cells overexpressing CRP40; however, this was not the case in the 300 μM H_2O_2 treatment condition, where ROS concentrations in the cells overexpressing CRP40 were significantly higher than those in the untreated SH-SY5Y cells overexpressing CRP40 (Figure 4.3). In contrast, the protection conferred by SH-SY5Y cells overexpressing mortalin remained constant throughout treatment with different concentrations of H_2O_2, suggesting a differential degree of protection from oxidative stress between CRP40 and mortalin that needs to be further examined. The even level of protection for mortalin at different degrees of exposure to oxidative stress was previously observed in astrocytes overexpressing mortalin; these astrocytes had only slight increases in ROS concentrations over a two-hour time period of glucose-deprivation (Volobouéva et al., 2008). From previous studies as well as the preliminary evidence presented herein, there appears to be a differential activation threshold for CRP40 and mortalin that regulates their ability to protect cells

from oxidative stress. Future studies should expand upon these preliminary investigations to further elucidate the distinctions in roles and functions of these closely related proteins.

Further, the results from the ROS experiments presented here are consistent with findings reported for the related protein, mortalin, and the fact that overexpression of mortalin in SH-SY5Y cells enhances protection from proteolytic stress in the mitochondria (Burbulla et al., 2010). Increased ROS and impairments in energy production are typically observed when processes such as oxidative phosphorylation are impaired in the mitochondria. Mortalin seems to be involved in protection from ROS. Specifically, when wild-type mortalin or three of its functional variants (A476T; R126W; and P509S) were overexpressed in the dopaminergic SH-SY5Y cell model, significantly lower amounts of ROS were found in the cells with wild-type mortalin as compared to the functional variants and the empty vector control (Burbulla et al., 2010). These findings were consistent after induction of proteolytic stress using the proteasomal inhibitor MG-132, where it was found that wild-type mortalin is the most efficient in protecting cells from proteolytic stress in comparison to empty vector control or its variants (Burbulla et al., 2010). Interestingly, the levels of oxidative stress were higher in the P509S mortalin variant, which is located in the substrate-binding domain of mortalin, than the other variants (Burbulla et al., 2010). The P509S site is also contained within the CRP40 sequence, specifically within the P1P5 fragment of CRP40. As seen in the current experiments, CRP40 overexpression confers a slightly greater protection from ROS than mortalin overexpression following the 500 μM H_2O_2 treatment (Figure 4.3). Thus, it would be interesting to examine protection from ROS using different CRP40 fragments to

determine whether this P509S site plays a specific role in mitochondrial oxidative stress responses, or if CRP40 itself confers a differential degree of protection against oxidative stress than mortalin. These experiments should be designed to incorporate a CRP40 fragment that contains this site, such as P1P5, and compare the effects of its overexpression in cells versus a fragment such as P2P4 that does not contain this putative functional site.

Along with protection from ROS, wild-type mortalin has also been found to maintain mitochondrial membrane potential, which is an important marker for mitochondrial function, in comparison to mortalin variants in both basal conditions and under proteolytic stress (Burbulla et al., 2010). Along with ROS, ATP production, and mitochondrial membrane potential, changes in mitochondrial morphology are also indicative of mitochondrial impairment (Mandemakers et al., 2007). As such, researchers have assessed the involvement of wild-type mortalin in maintaining mitochondrial morphology using live-cell imaging techniques. SH-SY5Y cells were co-transfected with Mito-DsRed plasmid, mortalin or one of its variants and it was found that both mitochondrial branching and length were significantly increased in cells overexpressing wild-type mortalin in comparison to the empty vector control and mortalin variants, indicating healthier mitochondria (Burbulla et al., 2010). Furthermore, when ~50% of mortalin was knocked down in HEK293 cells, this caused an increase in mitochondrial ROS production and a reduction of mitochondrial membrane potential that could only be rescued by wild-type mortalin, but not any of the mortalin variants (Burbulla et al., 2010). Future studies could incorporate a knockdown strategy for CRP40 using small interering

RNA in cells to determine the effects on mitochondrial function. Depending on whether alterations in mitochondrial parameters are observed, the potential of CRP40 and CRP40 fragments to participate in restoration of mitochondrial function could then be examined as a further step to determine the impact of this molecular chaperone protein and/or its specific fragments in mitochondrial homeostasis.

Indeed, mitochondrial function has taken a central role in neurodegenerative disease processes. Both neuronal and glial cells contain a network of mitochondria along the neuronal axons, with maximum concentration at the perinuclear region. While the function of eukaryotic cells is dependent on a constant supply of ATP and a controlled level of ROS from the mitochondria, neuronal cells such as dopaminergic neurons have been reported to have a constitutively lower mitochondrial mass, making these cell types even more dependent on an abundant supply of energy from oxidative phosphorylation that is necessary to perform all vital processes, including synaptic remodelling (Liang et al., 2007). Defects in mitochondrial function can arise from misfolding of mitochondrial proteins that can occur due to external oxidative stress and defective mitochondrial DNA. These events may result in a reduction of mitochondrial membrane potential and lead to cell apoptosis (Gorman, 2008). Regulation of function and quality control in the mitochondria is regulated by the dynamic processes of fission, fusion, mitophagy, and lysosomal degradation (Twig et al., 2008). Impairments of the fission/fusion process result in swollen and aggregated mitochondria and loss of migration into neuritis (Chen and Chan, 2009). As well, defects in fission/fusion have been directly associated with a multitude of neurodegenerative diseases (Chen and Chan, 2009). Moreover, in the

disease-state, the process that selectively removes damaged mitochondria, known as mitophagy, is impaired, leading instead to bulk autophagy and programmed cell death. As previously described, mitochondria play a central role in the pathology of PD through complex I and complex IV deficits that have been identified in PD patients, making this organelle of particular importance in PD research (Schapira and Jenner, 2011). Other studies of PD have also identified defects in α-ketoglutarate dehydrogenase, an enzyme that is involved in the Kreb's cycle of the mitochondria that is responsible for production of ATP (Mizuno et al., 1994). Due to the important roles of mitochondria in neurodegenerative diseases, targets such as molecular chaperones that may be involved in its protection require a closer look.

However, along with environmental factors, there are a variety of genetic alterations that have been identified in the mitochondria that have been associated with neurodegenerative diseases such as PD. These involve mutations in proteins such as α-synuclein, PINK, DJ-1, and Parkin that have been linked to impaired mitochondrial function (Schapira and Jenner, 2011). Specifically, loss of function of DJ-1, and also Parkin and PINK1, has been shown to increase mitochondrial susceptibility to oxidative stress (Schapira and Jenner, 2011). As well, aberrations in Parkin and PINK1 lead to impaired mitophagy that reduces the ability of neurons to remove damaged mitochondria and leads to apoptosis, which may be clinically-relevant to degenerative diseases such as PD (Schapira and Jenner, 2011).

In conclusion, the results of the current study point to the potential protective roles of CRP40 in the mitochondria in SH-SY5Y cells. Future studies should be conducted to

examine ROS and ATP concentrations following overexpression as well as knockdown of CRP40 in a variety of in vitro models such as primary neuronal cultures and astrocytes, and *in vivo* in genetic and environmental animal models of PD.

Chapter 5: Catecholamine-Regulated Protein 40 as a biomarker in Parkinson's disease

5.1 Introduction/Rationale/Hypotheses

PD is the second most common neurodegenerative disorder in the world, affecting 4.1-4.6 million people worldwide, and is expected to double in prevalence by 2030 (Dorsey et al., 2007). Research into the mechanisms behind this debilitating disorder has taken a higher priority in recent years, with the establishment of the Michael J. Fox Foundation for Parkinson's research that has been very influential in raising public awareness of PD. Despite extensive research efforts, there are currently no validated biomarkers to diagnose PD. This disorder is currently diagnosed through a clinical interview that involves evaluation of extrapyramidal signs, including rigidity, bradykinesia and tremor (Shulman et al., 2011). However, it is difficult to accurately diagnose PD through a clinical evaluation until approximately 60-70% of dopaminergic neurons have degenerated, closing the gap for any early interventions to take place (Shulman et al., 2011). Further, PD is difficult to diagnose based on motor symptoms because they may be common to other movement disorders as well. Therefore, the specificity and validity of clinical diagnosis is limited, with certainty increasing only in the late stages of PD. Thus, there exists a critical need for discovery of sensitive, specific and reliable biomarkers for accurate and early disease detection. Such biomarkers would likely help to track disease progression and efficacy of treatments, especially the potential of new neuroprotective therapies. As well, biomarkers would increase the chances of diagnosing PD in prodromal stages, even before the appearance of motor symptoms, which would allow for early interventions and treatments to slow down disease progression. The possibility for prodromal detection has been fuelled by recent research

that has altered the idea of PD as solely being described as a motor disorder. PD is now identified by a variety of non-motor features, and prodromal symptoms such as constipation and depression, hyposmia, and rapid-eye-movement behaviour disorder (Siderowf and Lang, 2012). However, these non-motor features lack specificity and may not be informative to the physician until there is an accompanying diagnostic test to fill in the gaps. Recently, there have been some advances in the development of biomarkers for PD that are based on DA transporter imaging; however, these technologies are somewhat invasive due to the use of radioactive tracers, highly costly and not yet widely available (Siderowf and Lang, 2012). Furthermore, DA imaging techniques may not be ideal for prodromal detection as the development of DA deficiency may be preceded by other events, such as aberrations in protein folding (Siderowf 2012). Thus, a biochemical marker in the periphery that is highly sensitive and reliable would be the ideal tool for early or prodromal diagnosis, confirming clinical diagnosis, tracking of disease progression, and monitoring of efficacy of new neuroprotective therapies.

The discovery of CRP40 has presented a unique opportunity for investigation of this molecular chaperone protein as a biomarker in PD. Our laboratory has produced evidence linking this protein to PD pathology, as discussed in Chapter 1. We have shown that CRP40 protein and mRNA concentrations are significantly reduced in *in vitro* cell models of PD and in *in vivo* pre-clinical models of PD. Studies on a group of rats developed from the 6-OHDA rat model were recently performed in our laboratory. The left A9 dopaminergic pathway was hemi-laterally lesioned by injection of the 6-OHDA toxin in the SNc region of the brain. The animals showed phenotypic rotating behaviour

when injected with apomorphine, a DA agonist, which was the result of the hemi-lesion. Western immunoblotting analysis showed a significant reduction of CRP40 protein in the striatum of the 6-OHDA lesioned rats (n=6) relative to sham controls (Figure 5.1).

As well, we have demonstrated a significant reduction of CRP40/mortalin in post-mortem brain specimens of PD patients (Figure 5.2). This result was in agreement with previous studies that have also found significant reductions in the molecular chaperone mortalin concentrations in human post-mortem PD brain specimens, with progressive decreases in the later stages of the disorder (Jin et al., 2006). Following this discovery, we investigated the expression patterns of CRP40 in the body and revealed that CRP40 is unique by being expressed solely in the CNS and blood, unlike mortalin, which is expressed ubiquitously. Interestingly, brain proteins that are involved in neurotransmission are also found in the circulating blood system, and certain blood cells may be considered sentinel tissues that could reflect levels of these neuropeptides in the brain. Thus, we designed methods to verify this hypothesis and investigate whether CRP40 concentrations in the blood mirror the reductions found in post-mortem disease subjects. We used the versatile technique of real-time reverse-transcriptase polymerase chain reaction (RT-PCR) to measure CRP40 levels in the blood of live subjects. Preliminary findings from our laboratory have indicated that CRP40 blood platelet mRNA levels are not altered in other neurological disorders including Alzheimer's disease and stroke (Figure 5.3; Figure 5.4). Further, we found that CRP40 is not altered by the ageing process (Figure 5.5). In our studies, CRP40 mRNA and protein concentrations showed greater reductions than mortalin concentrations, indicating that

CRP40 is more sensitive than mortalin as a potential biomarker for PD. As well, CRP40 may also be more specific to CNS disorders due to its expression in the blood and the brain. In addition, it is well known that mortalin is associated with regulation of cellular proliferation and various types of cancer; therefore, this protein may not be sufficiently selective as a biomarker for PD diagnosis.

Our laboratory have previously found a significant decrease in CRP40 mRNA concetrations in schizophrenia post-mortem brain specimens, which were corroborated in white blood cells of first episode schizophrenia and chronic schizophrenia subjects compared to controls (Groleau, Lubarda et al., 2013). Thus, CRP40 requires further study as a biomarker for PD, and other neurological disorders such as schizophrenia.

The current study was designed to build upon our initial findings of CRP40 mRNA reductions in the blood of live PD patients and to validate CRP40 as a potential biomarker for the valid diagnosis, early detection and monitoring of progression of PD. This study is currently being supported by the Québec Consortium for Drug Discovery (Consortium Québécois sur la Découverte du Médicament – CQDM) in association with Merck, Pfizer and Astra-Zeneca. As well, the Canadian National Research Council in Prince Edward Island is supporting the potential commercialization of CRP40 as a diagnostic tool for neurological disorders through their Industrial Research Assistance Program Grant, and the Atlantic Canada Opportunities Agency Business Development Program.

The aims of this study are to further validate CRP40 as a potential biomarker for PD through investigation of CRP40 concentration in the blood platelets of human PD patients, and newly diagnosed, drug naïve patients clinically diagnosed with PD in comparison to healthy, age-matched controls. This investigation will help to establish threshold values of CRP40 concentrations to predictably diagnose PD. As well, a future aim of this study is to continue the investigation of steady-state concetrations of CRP40 mRNA in Alzheimer's and stroke patients (negative controls). It is hypothesized that CRP40 concetrations in PD patients, as well as in newly diagnosed PD patients will be significantly decreased in comparison to healthy age-matched controls, as seen in preliminary results. Further, it is predicted that CRP40 mRNA concentrations will be altered, and significantly higher in PD patients who have been chronically treated with dopaminergic drugs, in comparison to newly diagnosed, drug naïve patients. As well, it is hypothesized that the CRP40 mRNA concentrations in PD patients will be significantly lower than those found in negative controls (Alzheimer's and stroke patients), and that the negative controls will be comparable to healthy age-matched controls.

This is an ongoing study that will take several years to complete and this chapter will present the results obtained thus far that show promise for future development of a CRP40 diagnostic for PD (Figure 5.6 for study plan and summary). Since this is a project that is already in progress, I have played extensive roles in organizing patient recruitment from various centres (Toronto Western Hospital Movement Disorders Clinic, Toronto, ON; Dr. Michel Rathbone's Clinic at Juravinski Hospital, Hamilton, ON), processing of newly recruited patients' blood samples, performing platelet and white blood cell RNA

isolation, quantifying CRP40 mRNA concetrations utilizing the technique of real-time RT-PCR, and conducting statistical analysis to assess treatment groups compared to healthy age-matched subjects as well as negative controls.

This ongoing study could eventually lead to the development of a highly specific, sensitive, and affordable diagnostic test. Once CRP40 has been validated as a diagnostic biomarker for PD, this will allow for early diagnosis of PD, even in genetically predisposed people even before the development of symptoms. The CRP40 diagnostic test will ultimately result in earlier treatment and allow for lifestyle modifications to slow down the progression of PD and improve the lives of millions of people. As well, this research may open up the possibilities for the development of disease-modifying therapies based on restoration of function of essential heat-shock proteins.

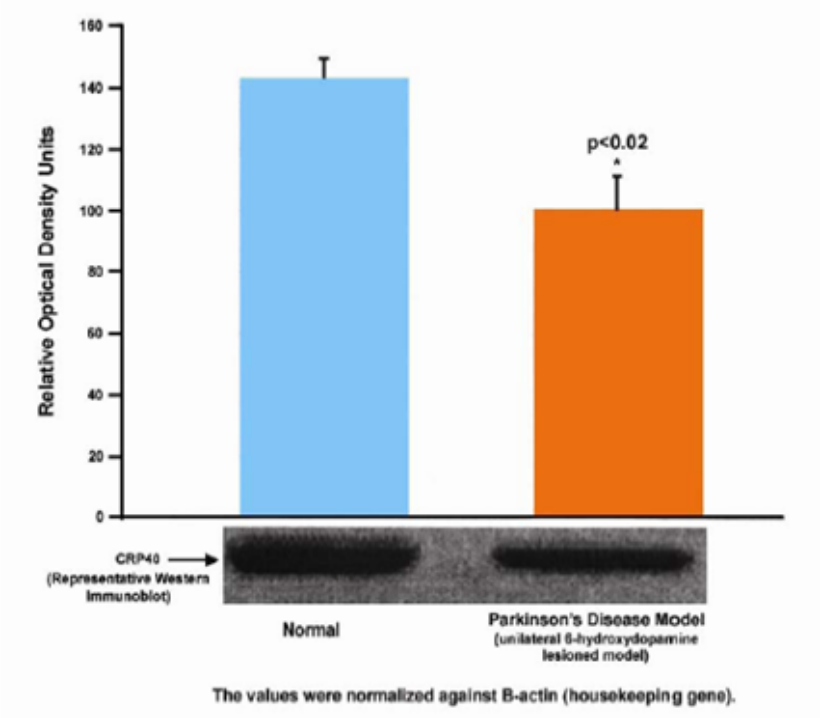

Figure 5.1 The 6-OHDA animal model of PD displays significant reductions of CRP40 protein expression in the striatum.

FIGURE LEGEND

Figure 5.1: Concentrations of striatal CRP40 protein were measured in the pre-clinical animal model (6-OHDA) of PD (n=6). Rats were sacrificed, the striatum was re-sected and homogenized and prepared for Western blotting using a polyclonal CRP40-specific antibody. Statistical analysis showed that there was a significant reduction of CRP40 protein in the striatum of the 6-OHDA rat model of PD relative to sham controls ($p<0.02$).

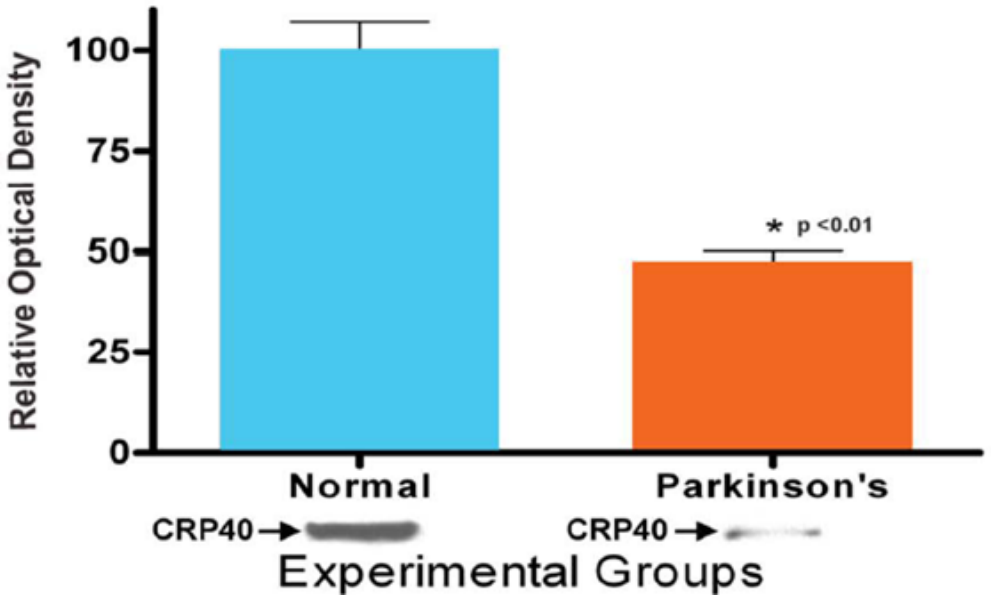

Figure 5.2 CRP40 Protein Expression is Significantly reduced in Post-Mortem Brain Specimens of PD patients compared to controls.

FIGURE LEGEND

Figure 5.2: CRP40 protein expression was examined in post-mortem PD brain samples. This figure shows reduced concentrations of CRP40 protein expression in post-mortem PD brain specimens (n=4) as compared to healthy, age-matched controls (n=6) determined by Western blotting and measured by mean optical density. Representative Western immunoblot values were normalized with the β-actin housekeeping gene. A two-tailed unpaired t-test with a confidence interval of 95% was utilized to analyze the data.

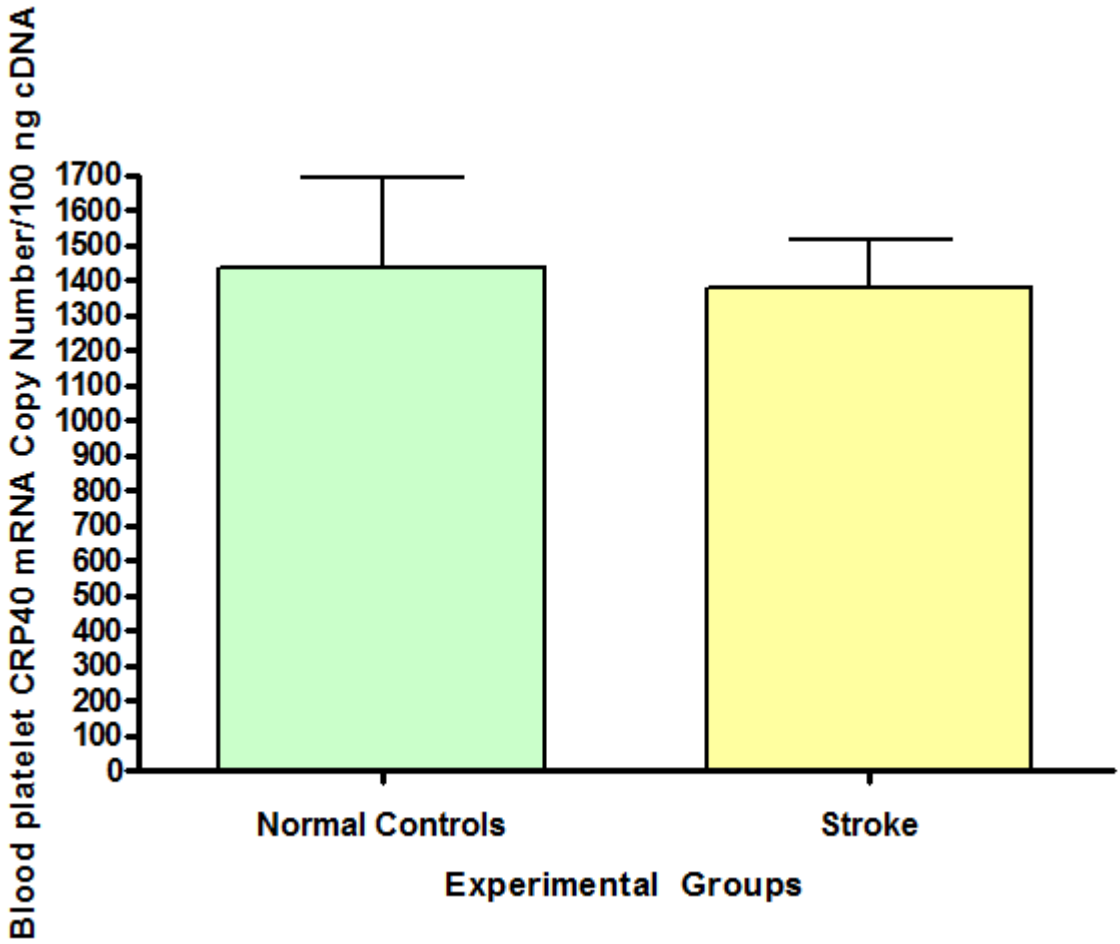

Figure 5.3 CRP40 mRNA Expression is Not Altered in platelets in Alzheimer's Disease.

FIGURE LEGEND

Figure 5.3: CRP40 mRNA expression was examined in the platelets of Alzheimer's versus age-matched healthy control subjects using real-time RT-PCR. Experimental groups were composed of n=8 normal, age-matched controls and n=8 Alzheimer's disease patients. Experiments were performed in triplicates and the results were analyzed by a two-tailed t-test, indicating no statistically significant difference in CRP40 mRNA expression between controls and Alzheimer's patients ($p>0.05$).

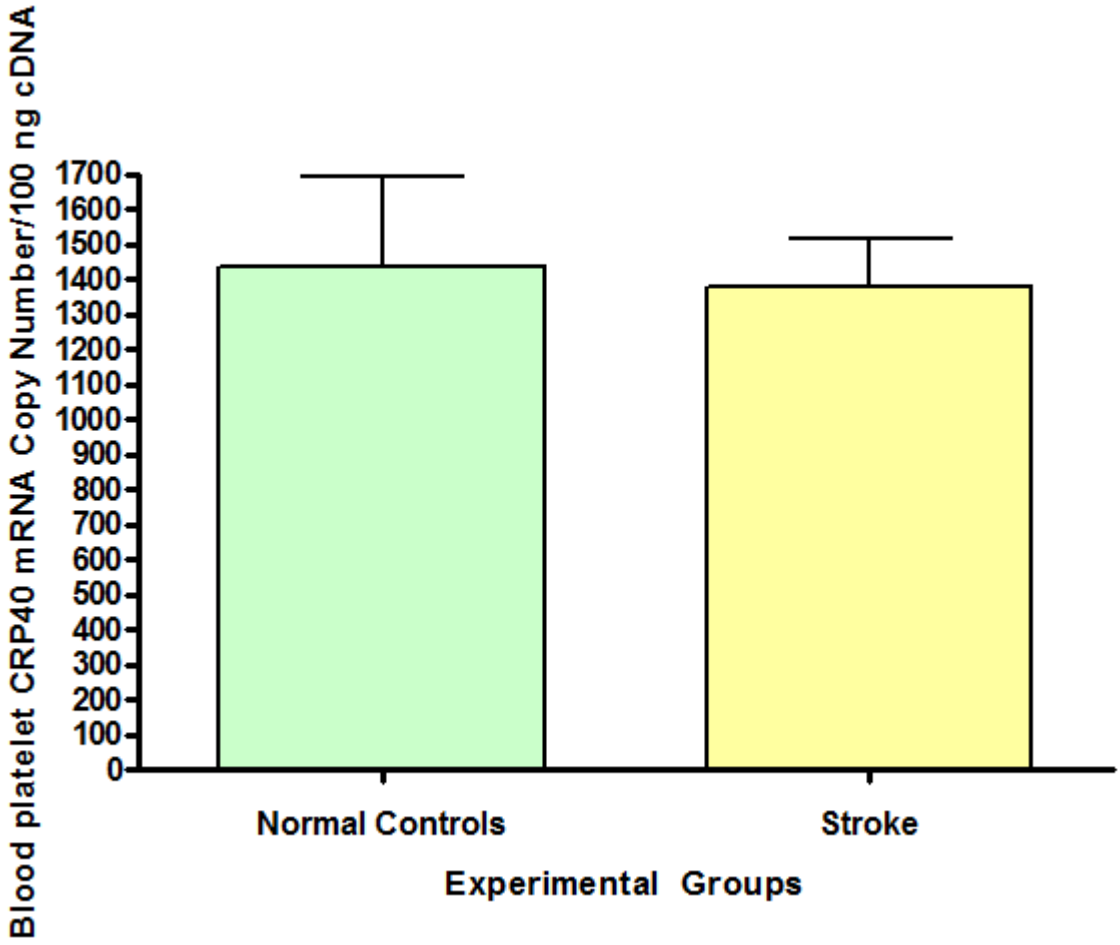

Figure 5.4 CRP40 mRNA Expression is Not Altered in Stroke.

FIGURE LEGEND

Figure 5.4: CRP40 mRNA expression was examined in the platelets of stroke patients (n=9) versus normal age-matched controls (n=9) using real-time RT-PCR. Experiments were performed in triplicates and the results were analyzed by a two-tailed t-test, indicating no statistically significant difference in CRP40 mRNA expression between controls and stroke patients ($p>0.05$).

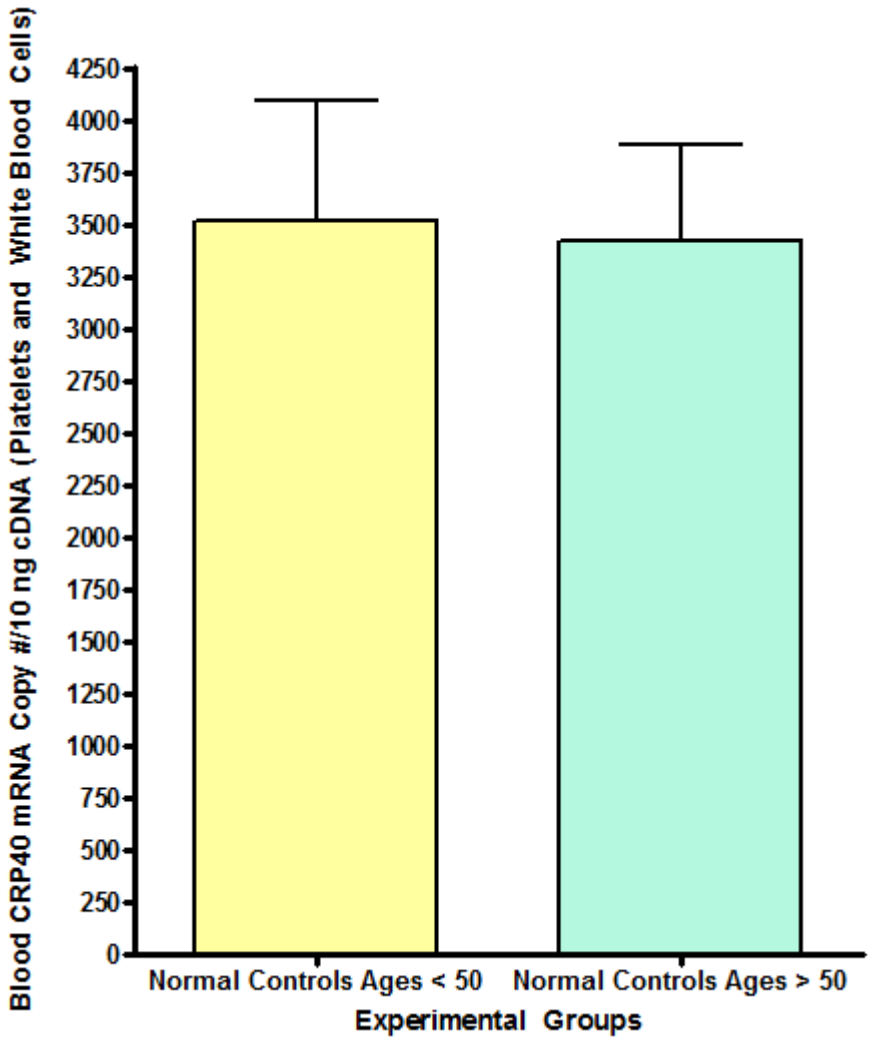

Figure 5.5 CRP40 mRNA Expression is Not Altered by the Ageing Process.

FIGURE LEGEND

Figure 5.5: CRP40 mRNA expression was examined in the platelets and white blood cells of normal controls (n=17) for subjects under 50 years of age and also for subjects over 50 years of age (n=17) using real-time RT-PCR. Experiments were performed in triplicates and the results were analyzed by a two-tailed t-test, indicating no statistically significant difference in CRP40 mRNA expression between the two age groups ($p>0.05$).

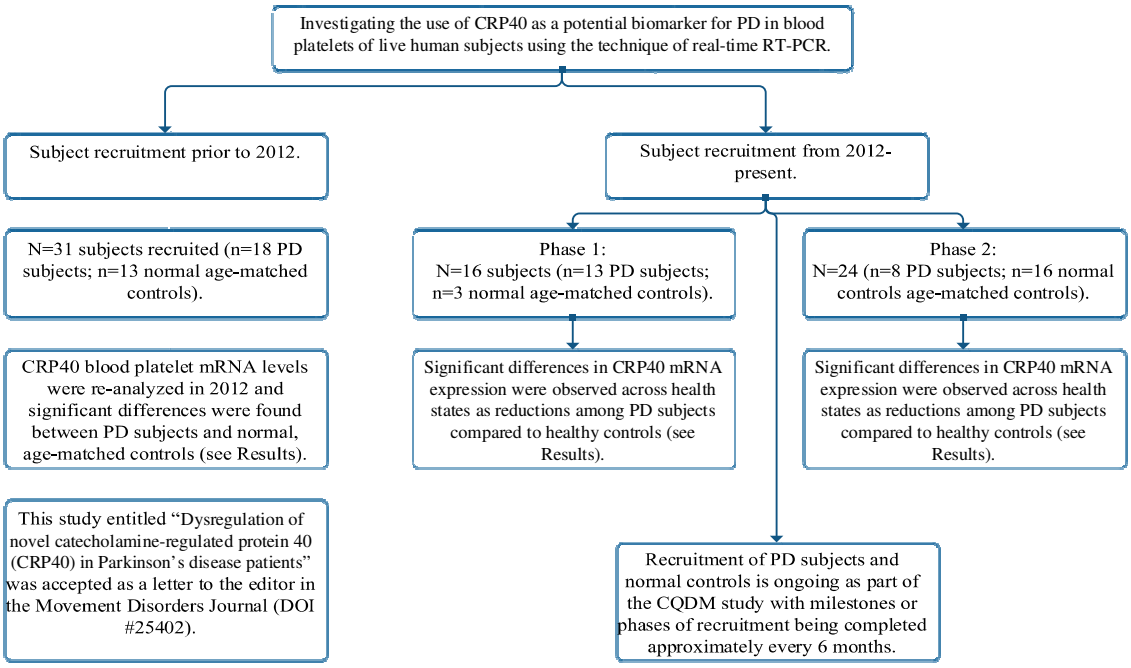

Figure 5.6 Investigating CRP40 as a Potential Biomarker for Parkinson's Disease: Plan of Experiments and Short Results Summary.

5.2 Materials and Methods

5.2.1 Preparation of platelets from blood samples of PD patients

20-30 mL of blood was received in BD vacutainer tubes (prepared with acetate citrate dextrose solution) from PD patients (e.g., either drug naïve or chronically treated) who were recruited by the Toronto Western Hospital. Platelets were collected from 20-30 mL of blood using the Acid Citrate Dextrose anticoagulant cocktail. The blood was centrifuged at 980 g for 2 minutes in an Eppendorf Centrifuge 5810R at 21°C without brake. Two thirds of the top layer (platelet-rich plasma region) were removed and transferred to a 15 mL polypropylene Falcon tube. The collected platelet-rich plasma was centrifuged at 1200 g for 7 minutes and the supernatant was removed. The pellet was washed twice in 7 mL of Phosphate Buffer Saline-EDTA-Bovine Serum Albumin (PEB) wash solution and centrifuged again at 1200 g for 7 minutes. The existing pellet was resuspended in 1 mL of PEB wash solution. The final platelet pellet was then centrifuged at 1200 g for 7 minutes in an Eppendorf tube and the supernatant was removed and the pellet was stored at -80 °C until further analysis. Platelet RNA preparation was performed using TRIzol according to the manufacturer's protocol. The RNA pellet was dissolved in 20μL RNase-free water and RNA platelet purity was determined by measuring absorption at 260 nm and 280 nm using a spectrophotometer.

5.2.2 Preparation of white blood cells from blood samples of PD patients

20 to 30 mL of blood was collected from subjects and white blood cells were prepared as per the following methods: 10 mL of whole blood was collected in 1.42 mL

of acetate citrate dextrose (ACD) BD vacutainers, mixed with 10 mL of PBS and layered over 15 mL of Ficoll Paque (GE Healthcare Life Sciences, Baie D'Urfe, Quebec, Canada). The gradient was spun at 400 g for 30 minutes (zero brake) and the buffy coat was collected and washed twice with 30 mL of PBS by spinning at 110 g for 10 minutes (zero brake). The pellet was then re-suspended in 1 mL PBS in an Eppendorf tube spun at 110 g for 10 minutes in an Eppendorf Centrifuge 5810R. The supernatant was removed and the pellet was stored at -80°C until further analysis. White blood cell RNA preparation was performed with TRIzol according to the manufacturer's protocol. The RNA pellet was dissolved in 20μL RNase-free water and RNA platelet purity was determined by absorption at 260 nm and 280 nm using a spectrophotometer.

5.2.3 RNA isolation from PD platelets and white blood cells using TRIzol method

RNA isolation from platelets and white blood cells was performed in a fume hood treated with RNase Zap (Invitrogen Life Technologies, Burlington, ON, Canada) to remove RNase contamination. Approximately 50-100 mg PD white blood cells or platelets were used in the RNA isolation. 1 mL of Tri-pure reagent was added to each sample and the mixtures were homogenized on ice. The mixtures were passed 15 times through a 20G needle using a 1 mL syringe. The samples were transferred into 1.5 mL micro-centrifuge tubes and incubated at room temperature for 5 minutes. 200 μL of chloroform was then added to the tubes, which were shaken vigorously for 15 seconds and incubated at room temperature for 20 minutes. The samples were centrifuged in an Eppendorf 5415-R centrifuge at 12, 000 g for 15 min at 4ºC. Following centrifugation, the

colorless phase was removed and transferred to a new 1.5 mL micro-centrifuge tube and 500 μL isopropanol was added to the colorless phase solution, inverted several times and allowed to precipitate for 10 minutes at room temperature. Samples were then centrifuged for 10 minutes at 12 000 g and the supernatant was discarded. The pellet was re-suspended in 75% ethanol and centrifuged at maximum speed for 5 minutes, discarding the supernatant at the end. The pellets were left to air dry for approximately 5 minutes, and re-suspended in 30 μL diethylpyrocarbonate (DEPC)-treated RNase-free H_20. The RNA solutions were incubated for 10 minutes at 55ºC and then 2 μL of RNA was diluted in 98 μL DEPC H_20 and analyzed with a Beckman spectrophotometer DU-640 to determine RNA concentration and purity.

5.2.4 DNase Treatment of Isolated RNA samples

Isolated platelet and white blood cell RNA from PD patients was treated with TURBO DNA–free kit (Ambion, Austin, Texas, USA) as per manufacturer's instructions in order to remove contaminating DNA. First, the amounts of required reagents from the kit were calculated for 5 μg of RNA such that 0.1 volume of 10X TURBO DNase Buffer and 1 μL TURBO DNase were added to the RNA and mixed gently. The volume of the reaction was made up to 50 μL with DEPC H_2O. The reagents were added to a 1.5 mL micro-centrifuge tube and mixed by pipetting up and down. The RNA solutions were incubated at 37°C for 30 minutes after which 5 μL of the DNase inactivation reagent was added to the micro-centrifuge tube and incubated for 2 minutes at room temperature. Solutions were centrifuged for 1.5 min at room temperature and transferred to a new tube.

RNA amounts were determined by measuring absorption at 260/280nm using a Beckman DU-640 spectrophotometer.

5.2.5 cDNA Preparation from DNase-treated RNA

cDNA solution was prepared using the following reagents: 0.5 μL of Oligo (dT); 0.5 μL of random hexamer; 1 μg of RNA; 1 μL of 10 nM dNTP mix; and H_2O- 9 μL. Reagents were added to a 1.5 mL micro-centrifuge tube and heated at 65°C for 5 minutes and allowed to cool on ice. Samples were centrifuged briefly and 4 μL of 5X First strand buffer, 2 μL 0.1 M DTT, and 1 μL RNase OUT reagents were added. Samples were mixed and incubated at 42°C for 2 minutes. Next, 1 μL of superscript III was added at room temperature and samples were mixed and incubated at 42°C for 50 minutes. The reaction was inactivated by incubating the sample at 70°C for 15 minutes after which RNase H was added in order to degrade any existing RNA, at 37°C for 20 minutes.

5.2.6 Real-Time Reverse-Transcriptase Polymerase Chain Reaction

Real-time RT-PCR was used to determine absolute copy numbers of CRP40 mRNA in all samples of platelets. This protocol was also complementary for CRP40 analysis in white blood cells. Mortalin is highly homologous to CRP40; therefore, primers used in this study amplified both CRP40 and mortalin. Real-time RT-PCR was performed in triplicate for each sample using MX3000P Real-Time RT-PCR (Stratagene, Mississauga, ON, Canada). In preliminary experiments using CRP40 specific primers to quantify mRNA levels in the platelets and white blood cells, no primer-dimers were

detected and transcripts showed optimal real-time RT-PCR efficiencies. An absolute standard curve was generated using six different concentrations of cDNA: 1 pg; 100 fg; 10 fg; 1 fg; 100 ag; and10 ag-10 ag. MX3000P real-time RT-PCR conditions were optimized to ensure the amplifications were in the exponential phase and the efficiencies remained constant in the course of the real-time RT-PCR. Components of the reaction mixture were 10 ng of cDNA, 300 nM each of CRP40 primers (forward primer 5' TTG GCC GGC GAT GTC ACG GAT GTG 3'; reverse primer 5' ACA CAC TTT AAT TTC CAC TTG CGT 3'), 0.3 μL Rox (reference dye), 10 μL SYBR Green 2xMix (Applied Biosystems, Streetsville, ON, Canada) and nuclease-free water to a final volume of 20 uL. Representative real-time RT-PCR products each showed 100% homology with the CRP40 gene regions. Data were normalized against a human housekeeping gene, cyclophilin.

5.2.7 Data Analysis

Student's unpaired t-test was used to compare levels of CRP40/mortalin mRNA between patients with PD and healthy controls. Multiple regression analysis was used to examine the relationship between health status and CRP40/mortalin mRNA, controlling for the potential confounding effects of subject age and sex. Statistical tests were two-sided with α=0.05. Data were analyzed using Graph Pad Prism 6.0.

5.3 Results

5.3.1 Results from subjects recruited prior to 2012: CRP40 mRNA expression in blood platelets is reduced in subjects with PD compared to controls

CRP40 as well as mortalin mRNA concentrations were measured in 31 subjects (n=18 PD and n=13 age-matched controls) (Figure 5.6). Subjects were recruited from McMaster University Health Sciences/St. Joseph's Healthcare (Hamilton, ON). All subjects gave written informed consent to provide a blood sample prior to participation in this study. PD was diagnosed in subjects and confirmed by physical examination. A second opinion was also attained from a movement disorders specialist. Controls were analyzed by the same method and included based on lack of PD, and age-matching. The study was single-blinded with respect to analysis of the subjects' blood samples. The subject descriptive statistics are presented in Table 5.1. The mean age of subjects was 61.1 (±19.5) years and 71.4% were male (Table 1).

Mean CRP40/mortalin mRNA were significantly lower in PD subjects compared to controls [824.8 (783.7) vs. 2005.6 (1149.9), t=3.41, p=0.0019] (Table 5.2). Given potential imbalances in the age and sex distribution between patients with PD and controls, an adjusted analysis controlling for subject age and sex was conducted using multiple regression. The association between PD and CRP40 levels remained after controlling for the potential confounding effects of subject age and sex (Table 5.1). This study was submitted as a letter to the editor and accepted and published in the Movement Disorders Journal (Lubarda et al., 2013).

5.3.2 Results for subjects recruited post 2012: CRP40/Mortalin mRNA expression in blood platelets is specifically reduced in subjects with PD compared to controls in both Phase I and Phase II of subject recruitment (Figure 5.6)

Following the commencement of the CQDM project, 16 subjects (n=3 normal and n=13 PD subjects) were recruited from the Toronto Western Hospital Movement Disorders Clinic in the first six months of the study (Phase I). All of the subjects gave informed consent prior to participation in the study. The subjects were over 50 years of age. The subjects' blood was processed as outlined in the methods section of Chapter 5, and CRP40 mRNA was measured using real-time RT-PCR. The results of the study are shown in Figure 5.7. One of the control samples' values was very low and this may have occurred due to platelet processing errors. Therefore, this sample was removed as an outlier, resulting in a total of 2 normal subjects for analysis. In phase I of subject recruitment, there were significant differences in CRP40 mRNA expression between health states [mean of normal controls was 2820; mean of PD samples was 580.5, t=3.2, p=0.0061] (Figure 5.7). The association between PD and CRP40 levels remained after controlling for the potential confounding effects of subject age and sex. The findings from phase I provide support for the hypothesis that CRP40 is genetically dysregulated in PD. This impairment can be observed in blood samples from live PD patients. This study is ongoing and we plan to recruit more PD subjects, drug naïve PD subjects, and more healthy age-matched controls.

Due to the low number of healthy, age-matched controls in Phase I, we set out to recruit more normal, age-matched controls for inclusion into this study as part of Phase II

(Figure 5.6), which occurred at a time point of 6-12 months from the commencement of the CQDM study. 16 normal control subjects were recruited in total at McMaster University. These subjects did not have a clinical diagnosis of PD and careful accounts of their medication status were accounted for in order to eliminate potential confounding factors in the study. The subjects' ages ranged from 46-82, and 10 subjects were female while 6 were male. All of the normal subjects gave informed consent before participation in this study. In conjunction with normal subject recruitment, we were able to obtain 8 more PD subjects' samples from Toronto Western Hospital Movement Disorders Clinic.

The blood from the normal controls and PD subjects was processed as per previously described methods and CRP40/mortalin mRNA was quantified using the technique of real-time RT-PCR. In phase II of subject recruitment, there were significant differences in CRP40 mRNA expression between health states [mean of normal controls was 3074; mean of PD samples was 379.9, t=2, p=0.0222] (Figure 5.8).

N=31	Mean ±S.D./n (%)
Health Status	
Control	13 (41.9%)
Parkinson's disease	18 (58%)
Age	61.1 (±19.5)
Sex[1]	
Male	20 (71.4%)
Female	8 (28.6%)
[1]Frequencies may not sum to N=31 due to missing data.	

Table 5.1 Subject Descriptive Statistics for Parkinson's Study Prior to 2012.

	β-coefficient	Standard Error	t	P-value
Parkinson's disease	-1605.1	607.2	-2.64	0.0145
Subject Age	9.1	16.0	0.57	0.5750
Subject Sex[1]	-475.5	511.7	-0.93	0.3624
[1]Reference category: males.				

Table 5.2 Association Between Decreased CRP40 Levels and Parkinson's Disease Showed a Significantly Lower Mean CRP40/Mortalin mRNA Level in PD Subjects Compared to Controls Even After Controlling for Subject Age and Sex.

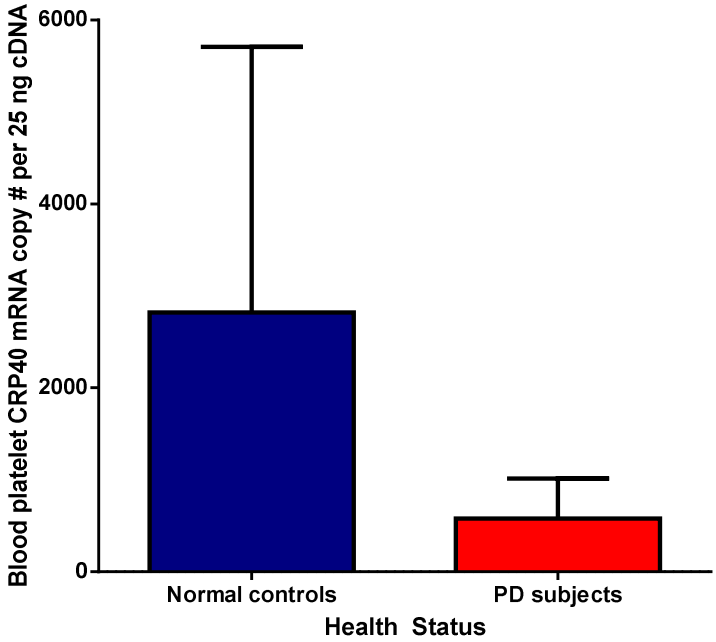

Figure 5.7 CRP40 mRNA Expression is Significantly Lower in PD Subjects Compared to Normal, Age-Matched Controls in Phase I of the CQDM Study.

FIGURE LEGEND

Figure 5.7: CRP40 mRNA expression was examined in the platelets of PD subjects (n=13) versus normal age-matched controls (n=2) using real-time RT-PCR. Experiments were performed in triplicates and the results were analyzed by a two-tailed, unpaired t-test. The results indicated a statistically significant difference in CRP40 mRNA copy number in PD subjects compared to normal controls (p=0.0061); specifically, significant reductions in CRP40 expression were observed in PD subjects compared to controls.

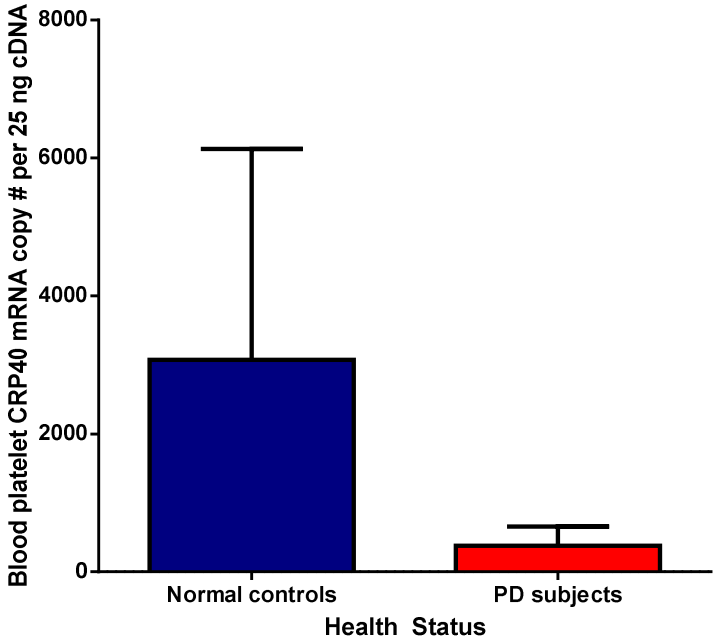

Figure 5.8 CRP40 mRNA Expression is Significantly Lower in PD Subjects Compared to Normal, Age-Matched Controls in Phase II of the CQDM Study.

FIGURE LEGEND

Figure 5.8: CRP40 mRNA expression was examined in the platelets of PD subjects (n=8) versus normal age-matched controls (n=16) using real-time RT-PCR. Experiments were performed in triplicates and the results were analyzed by a two-tailed, unpaired t-test. There was a statistically significant difference in CRP40 mRNA copy number in PD subjects, where PD subjects had significant reductions in CRP40 expression compared to normal controls ($p=0.0222$).

5.4 Discussion

There are currently no validated blood biomarkers for PD that are able to establish a valid diagnosis and predict patient response to treatment. Since the discovery of CRP40 and its expression in the blood and the brain, our laboratory has produced evidence for its dysregulation in animal models of PD (Figure 5.1), and significant reductions of CRP40 in post-mortem PD brain specimens (Figure 5.2) compared to normal, age-matched control brain samples. Furthermore, CRP40 genetic expression was not found to be altered in Alzheimer's disease and stroke patients, and these groups have been identified as potential negative controls (Figure 5.3; Figure 5.4). Thus, we developed methods to assess CRP40 mRNA expression in blood platelets of living PD patients using the technique of real-time RT-PCR. We are now conducting a large scale study to validate the potential use of CRP40 as a diagnostic tool in PD (Figure 5.6). The goal of this initiative is to develop and eventually commercialize a diagnostic test that is highly reliable, affordable, reproducible, and may facilitate the early diagnosis of PD as well as monitor its progression and efficacy of treatments.

Thus far, our results have demonstrated a significant reduction in CRP40 mRNA concentrations in PD subjects compared to normal, age-matched healthy controls (Table 5.2; Figure 5.7; Figure 5.8). Our group is the first to report significant reductions of CRP40/mortalin mRNA expression in the blood of live PD patients. These findings are in agreement with previous studies that have shown significant reductions in the molecular chaperone mortalin concentrations in human post-mortem PD brain specimens, with progressive decreases in the later stages of the disorder (Jin et al., 2006; Shi et al., 2008).

Further, our findings fall in line with several studies that have implicated heat-shock proteins in neurodegenerative diseases. Recent theories have found an association between defects in protein folding and pathogenesis for several diseases, including PD, Alzheimer's, familial amyotrophic lateral sclerosis, Huntington's disease and related polyglutamine expansion diseases (Hartl et al., 2011). The evidence for this comes from observations of abnormal accumulation of insoluble neuronal or extracellular aggregates of proteins in the CNS (Hartl et al., 2011). Regulation of protein quality or proteostasis is performed by an integrated network of molecular chaperone proteins that have been shown to perform diverse functions in the cell including refolding of misfolded proteins, assisting with *de novo* protein folding, protein trafficking and degradation (Hartl et al., 2011). Many heat-shock proteins are also classified as molecular chaperones. Several classes of Hsp, including the Hsp70s, Hsp90s, and the chaperonins (Hsp60s), function in *de novo* protein folding and refolding. These classes of proteins have the ability to refold proteins by recognizing exposed hydrophobic amino-acid side chains and assisting folding through ATP- and cofactor- mediated mechanisms (Hartl et al., 2011). Due to the multifunctional nature of molecular chaperone proteins and important roles in protein folding and cellular homeostasis, these proteins are currently being investigated as potential targets in a variety of neurodegenerative disorders, including PD.

Along with involvement of molecular chaperone proteins in PD, the last decade of research has produced conclusive evidence for the dysregulation of key genes that play a role in the pathology of this disorder. Interestingly, it is hypothesized that mutations in these genes may lead to the dysfunction of the ubiquitin-proteasome system and result in

abnormal protein folding and aggregation – a process regulated by molecular chaperone proteins (McNaught et al., 2004). There have been a variety of genetic mutations identified in different clinical phenotypes of PD. In particular, one of the first discoveries for pathogenic mutations involved the gene *SNCA* that encodes α-synuclein, a protein that is abundantly found in Lewy bodies and has been shown to regulate synaptic vesicle size, DA storage, and may have potential roles in learning and synaptic plasticity (Farrer, 2006; Le and Appel, 2004). Mutations in α-synuclein have been shown to contribute to impairment of proteasomal protein degradation, alteration of protein synthesis, abnormal mitochondrial function, and neuronal cell death (Tanaka et al., 2001). It is intuitive that proper molecular chaperone function is necessary to mediate the effects of mutated α-synuclein. Indeed, α-synuclein, at nanomolar concentrations, has been shown to increase Hsp70 protein expression in PC12 cells that helped defend the cells against toxicity and α-synuclein aggregation (Kluchen et al., 2004). Interestingly, mortalin, the protein related to CRP40 has been shown to be associated with α-synuclein, as well as DJ-1, which is another protein that has been linked to PD pathology (Jin et al., 2007). DJ-1 is an oncogene that has been linked to familial PD through recessively inherited mutations as well as missense mutations (Farrer, 2006). DJ-1 mutations have been associated with oxidative stress and impaired mitochondrial function that contribute to neuronal cell death (Farrer, 2006). Further, DJ-1 and its mutants associate with mitochondrial Hsp70, or mortalin, and it has been suggested that mortalin may mediate DJ-1 sequestration into mitochondria following oxidative insult (Li et al., 2005). Other mutations in genes associated with PD have been linked to the Hsp70 family of proteins. For instance,

mutations in *parkin*, an E3 ligase in the ubiquitin-proteasome system have been shown to impair targeting of protein substrates for proteasomal degradation, leading to neurotoxicity (Kim et al., 2003). A substrate of Parkin, the bcl-2-associated athanogene 5 (BAG5) has been shown to suppress the chaperone activity of Hsp70 in an *in vivo* model of PD and lead to enhanced dopaminergic neuron death (Kalia et al., 2004). The intricate involvement of Hsp70 family of proteins, and specifically mortalin, in neurotoxicity, suggests that the related protein, CRP40, may also play an important role in maintaining neuronal homeostasis. The alterations of CRP40 expression in live PD patients reported here provide clues for its possible role in PD pathology. Future studies, such as proteomics analyses, should be conducted to investigate whether PD-associated proteins interact with CRP40; these studies would shed light on the function of this novel molecular chaperone and its mechanism of action in PD. Further, such studies would help to illuminate the important roles of molecular chaperones in the bigger process of neurodegeneration.

The findings of the current study implicate the novel CRP40 in PD and neurodegenerative processes through reductions of its expression in live human PD patients. Preliminary data from our laboratory examined CRP40 mRNA steady-state expression in both drug naïve and drug treated PD patients. We observed that CRP40 mRNA steady-state expression is most depleted drug naïve patients, suggesting that anti-Parkinson's drug treatment can affect protein concentrations. This finding needs to be explored further utilizing larger sample sizes. This is the basis for the current study funded by CQDM. Our plan is to recruit newly diagnosed, drug naïve PD subjects and

compare CRP40 mRNA expression in platelets with chronically-treated subjects. In order to circumvent the potential confounding effects of chronicity, these newly diagnosed, drug naïve patients will be followed longitudinally every three months, from the point of diagnosis and throughout their treatment period, to determine CRP40 expression and how it is altered throughout the progression of the disease.

The increasing prevalence of PD necessitates the development of more sensitive and accurate biomarkers. As previously described, current diagnostic methods are based on clinical criteria, and detect the disease in relatively late stages. Advances in technology have allowed for the development of several imaging techniques to evaluate potential structural, biochemical and perfusion pattern alterations in PD (Cummings et al., 2011). The first ever diagnostic imaging tool for PD was approved in 2011 by the United States Food and Drug Administration. This technology is based on the use of the DA transporter ligand ioflupane and single-photon emission computed tomography (SPECT, DaTscan) to assess PD and differentiate this disease from essential tremor (Cummings et al., 2011). However, this technology is not useful in distinguishing PD from multisystem atrophy or corticobasal degeneration, and has not been tested for prodromal detection or use as a disease-progression marker. Currently, ultrasound measurements of the substantia nigra, as well as the use of magnetic resonance imaging (MRI) are gaining interest for their potential applications in PD diagnosis (Cummings et al., 2011). A recent diffusion tensor imaging study has reported that PD patients display changes in the microscopic integrity of white matter and basal ganglia, which was based on alterations in fractional anisotropy and mean diffusivity (Zhan et al. 2012). Further, a reduction in fractional anisotropy in

the substantia nigra has been linked with a greater severity of motor symptoms (Zhan et al., 2012). In addition to MRI, magnetic resonance spectroscopy (MRS) has been utilized as a potential method to investigate pathophysiological processes in PD. A recent proton MRS study of neurochemical indices of substantia nigra, pons, and the putamen brain regions found significantly increased GABA concentrations in the pons (64% elevation) and putamen (32% elevation) of PD patients in comparison to controls (Emir et al., 2012). The findings of elevated GABA in the putamen in this study were consistent with previous post-mortem studies and *in vivo* animal models of PD (Emir et al., 2012). However, the more significant alteration of GABA in the pons compared to the putamen represented a novel finding in early to moderate PD cases that were examined. Since it has been previously suggested that there is an earlier involvement of the lower brainstem in PD, the study by Emir and colleagues (2012) may serve as a good starting point for obtaining an imaging biomarker that can also track disease progression. However in the overall scheme of things, the use of imaging technologies for PD detection is not yet widely available and still in early stages of development and validation, representing a costly and somewhat invasive avenue for PD sufferers. Thus, biochemical tissue biomarkers represent a more realistic option for diagnosis, detection of disease progression, and possibly early recognition of PD at this point in time.

Recently, there has been a focus on investigation of cerebrospinal fluid and plasma biomarkers for PD and other neurodegenerative disorders. This has been aided by technological advances in the areas of proteonomics and microRNA analysis. α-synuclein has become a focus for biomarker research (Mollenhauer et al., 2011). Recent studies

have found significantly lower levels of α-synuclein in the cerebrospinal fluid of PD patients, multiple system atrophy patients, and dementia with Lewy bodies patients, in comparison to patients with Alzheimer's disease and other neurological disorders (Mollenhauer et al., 2011). Similar findings for α-synuclein were reported in the saliva of Parkinson's patients; however this same study found increased DJ-1 levels compared to controls (Devic et al., 2011). In contrast, low levels of DJ-1 have been reported in the cerebrospinal fluid of sporadic PD cases (Hong et al., 2010). Researchers are now investigating a wide range of gene mutations, such as in *parkin* and *PINK1*, to determine how alterations in proteins may be related to PD, and how they may be exploited as potential biomarkers. In addition, a recent study reported decreased expression of the DA D2 and D3 receptors in blood lymphocytes of PD patients, indicating that species related to the DA pathway may be worth investigating in the search for optimal biomarkers (Gui et al., 2011). Researchers have also examined various metabolic pathways related to the disease, and found PD-specific fingerprints, such as an increased xanthine/homovallinic acid ratio in PD patients, that was further modified by disease-severity (LeWitt et al., 2011). The hypothesis of increased inflammation in PD has received support from recent studies that have identified the human leukocyte antigen as a new *PARK18* locus, and reported increased levels of high-sensitivity C-reactive protein in PD patients, which are a marker of systemic inflammation in PD (Hamza et al. 2010; Song et al., 2011). Further, a recent blood study of drug naïve PD patients, chronically treated PD patients, and healthy controls identified six differentially expressed microRNAs. In this study, alterations in miR-1, miR-22, and miR-29 expression distinguished between drug naïve and healthy

patients, and differences in miR-16-2, miR-26a2, and miR30a were found between chronically-treated PD patients versus drug naïve patients (Margis and Rieder, 2011).

Indeed, a variety of biomarkers, including molecular, biochemical, genetic, and imaging markers have been explored for PD thus far. However, many of these biomarkers have been attributed to genetic causes of PD and may not be sufficient since the majority of cases of this disease have been found to be environmentally-related. As well, many of the biomarkers described here have not been tested in prodromal stages of PD, which will be an important future undertaking. Further, while imaging methodologies are promising, they come with high costs and are not yet widely available. Therefore, there is a critical need for a simple, cost-effective, rapid, and non-invasive diagnostic test. The CRP40 blood diagnostic test would aim to have the following advantages:

- Use of a **single gene** to diagnose PD (genetic and environmental causes), in contrast to a multitude of separate genes.
- Less complex, and therefore more cost-effective test.
- Simple data management since it is a single biomarker, as opposed to multiple biomarkers.
- Would be able to monitor disease progression, in contrast to other tests which are an “all or none” diagnosis.
- Allows for monitoring of the therapeutic efficacy of drugs.
- More sensitive than competing techniques, offering 88-97% accuracy.

- Would not require extensively trained personnel as it would be easily administered and carried out.
- Highly specific compared to others since commonality genes for several disorders are ruled out.
- Preliminary analysis of CRP40 has sampled a variety of subjects and proved to be accurate in a heterogeneous sample pool.
- Uses real-time RT-PCR technology to increase accuracy. This can be complemented with the enzyme-linked immunosorbent assay (ELISA) platform technology in the future.

In conclusion, the evidence gathered for the function of CRP40 points to its potential role as a molecular chaperone that may assist cells with protein folding, regulating oxidative stress, and maintaining mitochondrial function – all of which are impaired in PD. Further, the findings of this study directly implicate CRP40 in PD through its reductions in the blood of PD patients. This is a compelling finding that suggests the possible roles of CRP40 in the disease process and its potential use as a biomarker for valid diagnosis, monitoring of disease progression, examination of efficacy of treatments, and possibly for prodromal detection of PD. The ongoing analysis of CRP40 concentrations in live PD patients, in both chronic and newly diagnosed populations, will shed light on the mechanism of action of this novel protein, and delineate its roles in regulation of the DA system, mitochondrial homeostasis and

oxidative stress. Further, this study may lead to the commercialization of a CRP40-based diagnostic test that would revolutionize the diagnosis and treatment of PD.

Chapter 6: General Conclusions and Future Directions

6.1 Parkinson's Disease Research and Future Prospects for Catecholamine-Regulated Protein 40 as a Therapeutic and Biomarker

Neurodegenerative diseases such as PD represent one of the leading global causes of disability. Developed countries are experiencing an increase in the prevalence and incidence of PD due to their rapidly aging populations and changes in demographic structure. The combination of these factors, including an increased burden on global healthcare systems, is changing the landscape of neurodegenerative disease research today. The focus for reducing the burden of PD on the individual as well as the society should involve the identification of validated biomarkers for early diagnosis, and the development of neuroprotective, and sustainable therapies. The two objectives are closely related – the discovery of novel therapeutics is limited by the availability of biomarkers that can track disease progression and monitor drug efficacy. The present research investigated the mechanisms of action of a recently discovered multifunctional molecular chaperone, CRP40. The findings support future translational research of CRP40 and its relevance to PD therapeutics and diagnostics. The flow chart below (Figure 6.1) illustrates the implications and future prospects for research into CRP40 that is geared towards validating clinical diagnosis, prevention, early detection, and development of sustainable neuroprotective approaches for treatment for PD that has the potential to improve the lives of millions of people.

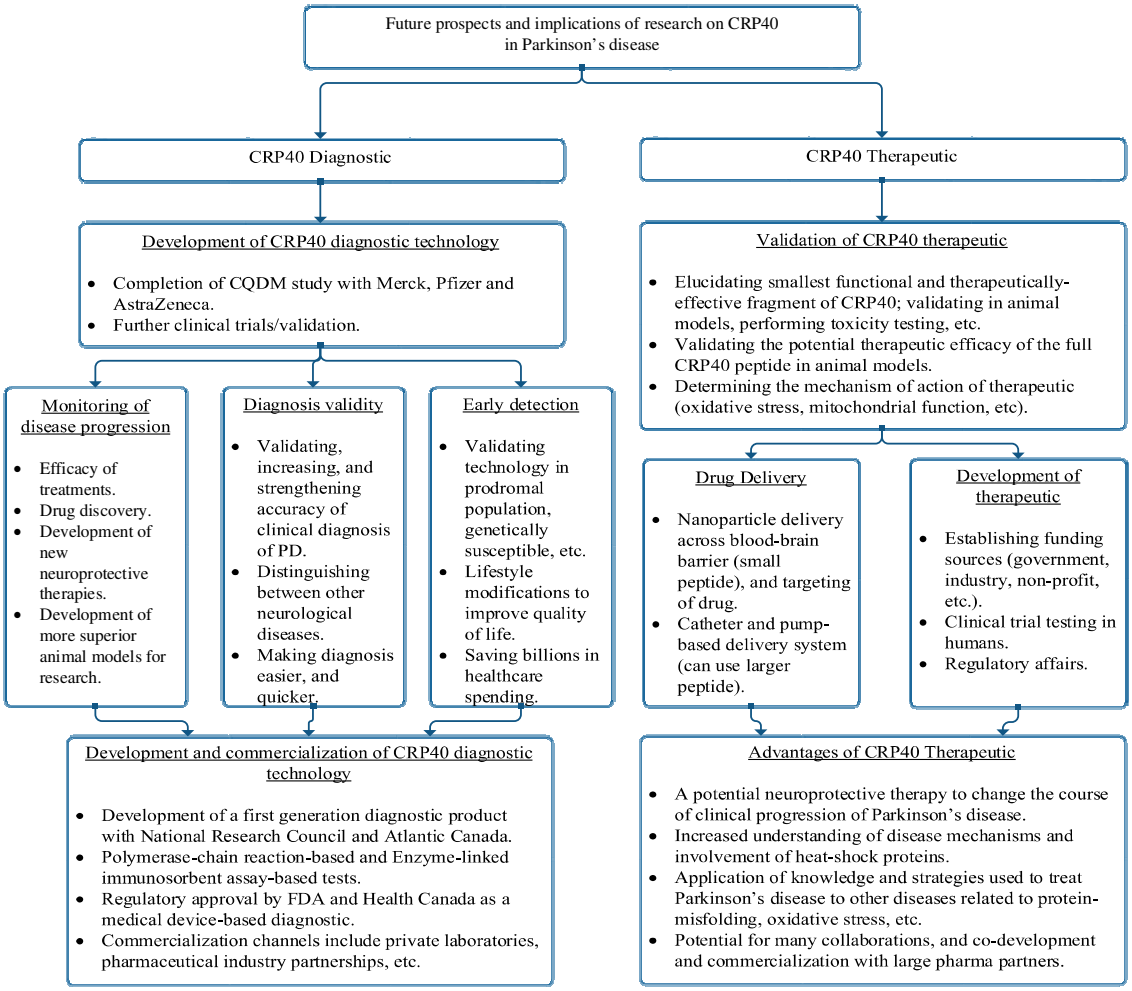

Figure 6.1 Implications and future research and proposed development for CRP40 as a diagnostic and therapeutic agent in Parkinson's disease.

References

Aarsland D, Beyer MK, and Kurz MW. (2008). Dementia in Parkinson's disease. Curr Opin Neurol. 21:676-682.

Abbott NJ. (2002). Astrocyte–endothelial interactions and blood–brain barrier permeability. J Anat. 200:629-638.

Auluck PK, Chan HYE, Trojanowski JQ, Lee VM, and Bonini NM. (2002). Chaperone suppression of alpha-synuclein toxicity in a Drosophila model for Parkinson's disease. Science 295:865-868.

Banks, WA. (1999). Physiology and pathology of the blood-brain barrier: implications for microbial pathogenesis, drug delivery and neurodegenerative disorders. J Neurovirol. 5: 538-555.

Beauchamp MH, Dagher A, Panisset M, and Doyon J. (2008). Neural substrates of cognitive skill learning in Parkinson's disease. Brain Cogn. 68:134-143.

Beaulieu JM, and Gainetdinov RR. (2011). The Physiology, Signaling, and Pharmacology of Dopamine Receptors. Pharmacol Rev. 63:1182-1121.

Berman SB, and Hastings TG. (1999). Dopamine oxidation alters mitochondrial respiration and induces permeability transition in brain mitochondria: implications for Parkinson's disease. J Neurochem. 73:1127-1137.

Bisaglia M, Soriano ME, Arduini I, Mammi S, and Bubacco L. (2010). Molecular characterization of dopamine-derived quinones reactivity toward NADH and glutathione: implications for mitochondrial dysfunction in Parkinson disease. Biochim Biophys Acta. 1802: 699-706.

Broadley SA, and Hartl FU. (2009). The role of molecular chaperones in human misfolding diseases. FEBS Lett. 583(16):2647-2653.

Burbulla LF, Schelling C, Kato H, Rapaport D, Woitalla D, Schiesling C, Schulte C, Sharma M, Illig T, Bauer P, Jung S, Nordheim A, Schöls L, Riess O, and Krüger R. (2010). Dissecting the role of the mitochondrial chaperone mortalin in Parkinson's disease: functional impact of disease-related variants on mitochondrial homeostasis. Hum Mol Genet. 19:4437-4452.

Cave, and Baker H. (2009). Dopamine systems in the forebrain. Adv Exp Med Biol. 651:15-35.

Ceroni A, Passerini A, Vullo A, and Frasconi P. (2006). DISULFIND: a disulfide bonding state and cysteine connectivity prediction server. Nucl Acid Res. 34 (Web Server issue): W177-W181.

Cartwright, H. (2011). Medtronic and Eli Lilly in Drug-Device Pact for Parkinson's Disease. Pharma Deals Rev. 4:44.

Chang HC, Tang YC, Hayer-Hartl M, and Hartl FU. (2007). SnapShot: molecular chaperones, Part I. Cell. 128-212.

Chen H, and Chan DC. (2009). Mitochondrial dynamics–fusion, fission, movement, and mitophagy—in neurodegenerative diseases. Hum Mol Genet. 18:R169-R176.

Chinta SJ, and Anderson JK. (2005). Dopaminergic neurons. Int J Biochem Cell Biol. 37:942-946.

Choi J, Forster MJ, McDonald SR, Weintraub ST, Carroll CA, and Gracy RW. (2004). Proteomic identification of specific oxidized proteins in ApoE-knockout mice: relevance to Alzheimer's disease. Free Radic Biol Med. 36:1155-1162.

Cummings JL, Henchcliffe C, Schaier S, Simuni T, Waxman A, and Kemp P. (2011). The role of dopaminergic imaging in patients with symptoms of dopaminergic system neurodegeneration. Brain. 134:3146–3166.

Dauer W, and Przedborski S. (2003). Parkinson's disease: mechanisms and models. Neuron 39: 889-909.

Daugaard M, Rohde M, and Jaattela M. (2007). The heat shock protein 70 family: Highly homologous proteins with overlapping and distinct functions. FEBS Lett. 581(19):3702-3710.

Decressac M, Ulusoy A, Mattsson B, Georgievska B, Romero-Ramos M, Kirik D, and Björklund A. (2011). GDNF fails to exert neuroprotection in a rat α-synuclein model of Parkinson's disease. Brain. 134(Pt 8):2302-2311.

De Mei C, Ramos M, Iitaka C, and Borrelli E. (2009). Getting specialized: presynaptic and postsynaptic dopamine D2 receptors. Curr Opin Pharmacol. 9:53-58.

Denora N, Trapani A, and Laquintana V. (2009). Recent advances in medicinal chemistry and pharmaceutical technology–strategies for drug delivery to the brain. Curr Top Med Chem. 9:182-196.

Deocaris CC, Kaul SC, and Wadhwa R. (2008). From proliferative to neurological role of an hsp70 stress chaperone, mortalin. Biogerontol. 9(6):391-403.

Devic I, Hwang H, Edgar JS, Izutsu K, Presland R, Pan C, Goodlett DR, Wang Y, Armaly J, Tumas V, Zabetian CP, Leverenz JB, Shi M, and Zhang J. (2011). Salivary alpha-synuclein and DJ-1: potential biomarkers for Parkinson's disease. Brain. 134 (Pt 7):e178.

Dorsey ER, Constantinescu R, Thompson JP, Biglan KM, Holloway RG, Kieburtz K, Marshall FJ, Ravina BM, Schifitto G, Siderowf A, and Tanner CM. (2007). Projected number of people with Parkinson disease in the most populous nations, 2005 through 2030. Neurol. 68:384-386.

Edwards YJ, and Cottage A. (2003). Bioinformatics methods to predict protein structure and function. A practical approach. Mol Biotechnol. 23(2):139-166.

Ehringer H, and Hornykiewicz O. (1960). Distribution of noradrenaline and dopamine (3-hydroxytyramine) in the human brain and their behavior in diseases of the extrapyramidal system. Klin Wochenschr. 38:1236-1239.

Ellis, J. (1987). Proteins as molecular chaperones. Nature. 328:378-379.

Emir UE, Tuite PJ, and Oz G. (2012). Elevated pontine and putamenal GABA levels in mild-moderate Parkinson disease detected by 7 tesla proton MRS. PLoS One. 7:e30918.

Farrer M, Kachergus J, Forno L, Lincoln S, Wang DS, Hulihan M, Maraganore D, Gwinn-Hardy K, Wszolek Z, Dickson D, and Langston JW. (2004). Comparison of kindreds with parkinsonism and alpha-synuclein genomic multiplications. Ann Neurol. 55:174-179.

Farrer MJ. (2006). Genetics of Parkinson disease: paradigm shifts and future prospects. Nat Rev Genet. 7:306-318.

Fornai F, Lenzi P, Gesi M, Ferrucci M, Lazzeri G, and Busceti CL. (2003). Fine structure and biochemical mechanisms underlying nigrostriatal inclusions and cell death after proteasome inhibition. J Neurosci. 23:8955-8966.

Gabriele J, Rajaram M, Zhang B, Sharma S, and Mishra RK. (2002). Modulation of a 40-kDa catecholamine-regulated protein following D-amphetamine treatment in discrete brain regions. Eur J Pharmacol. 453:13-19.

Gabriele J, Thomas N, N-Marandi S, and Mishra RK. (2007). Differential modulation of a 40 kDa catecholamine regulated protein in the core and shell subcompartments of the nucleus accumbens following chronic quinpirole and haloperidol administration in the rat. Syn. 61:835-842.

Gabriele J, Pontoriero GF, Thomas N, Thomson CA, Skoblenick K, Pristupa ZB, and Mishra RK. (2009). Cloning, characterization, and functional studies of a human 40-kDa catecholamine-regulated protein: implications in central nervous system disorders. Cell Stress Chaperones. 14(6):555-567.

Gabriele JP, Chong VZ, Pontoriero GF, and Mishra RK. (2005). Decreased expression of a 40-kDa catecholamine-regulated protein in the ventral striatum of schizophrenic brain specimens from the Stanley Foundation Neuropathology Consortium. Schizophr Res. 74:111-119.

Groleau SE, Lubarda J, Thomas N, Ferro MA, Pristupa ZB, Mishra RK, and Gabriele JP. (2013). Human blood analysis reveals differences in gene expression of catecholamine-regulated protein 40 (CRP40) in schizophrenia. Schizophr Res. 143(1):203-206.

Gingrich JA, and Caron MG. (1993). Recent advances in the molecular biology of dopamine receptors. Annu Rev Neurosci. 16:299-321.

Goldman-Rakic PS, Castner SA, Svensson TH, Siever LJ, and Williams GV. (2004).Targeting the dopamine D1 receptor in schizophrenia: insights for cognitive dysfunction. Psychopharmacol. 174:3-16.

Gorman AM. (2008). Neuronal cell death in neurodegenerative diseases: recurring themes around protein handling. J Cell Mol Med. 12:2263-2280.

Goto A, Doering L, Nair VD, and Mishra RK. (2001). Immunohistochemical localization of a 40-kDa catecholamine regulated protein in the nigrostriatal pathway. Brain Res. 900:314-319.

Gui YX, Wan Y, Xiao Q, Wang Y, Wang G, and Chen SD. (2011). Verification of expressions of Kir2 as potential peripheral biomarkers in lymphocytes from patients with Parkinson's disease. Neurosci Lett. 505:104-108.

Gu M, Cooper JM, Taanman JW, and Schapira AH. (1998). DNA Mitochondrial transmission of the mitochondrial defect in Parkinson's disease. Ann Neurol. 44:177-186.

Hamza TH, Zabetian CP, Tenesa A, Laederach A, Montimurro J, Yearout D, Kay DM, Doheny KF, Paschall J, Pugh E, Kusel VI, Collura R, Roberts J, Griffith A,Samii A, Scott WK, Nutt J, Factor SA, and Payami H. (2010). Common genetic variation in the HLA region is associated with late-onset sporadic Parkinson's disease. Nat Genet. 42:781-785.

Hartl FU, Bracher A, and Hayer-Hartl M. (2011). Molecular chaperones in protein folding and proteostasis. Nature. 475(7356):324-332.

Hartl FU, and Hayer-Hartl M. (2009). Converging concepts of protein folding in vitro and in vivo. Nature Struct Mol Biol. 16:574-581.

Hassani OK, Francois C, and Yelnik J. (1997). Evidence for a dopaminergic innervation of the subthalamic nucleus in the rat. Brain Res. 749:88-94.

Hayes MW, Fung VS, Kimber TE, and O'Sullivan JD. (2010). Current concepts in the management of Parkinson disease. Med J Aust. 192(3):144-149.

Herbst M, and Wanker EE. (2007). Small molecule inducers of heat-shock response reduce polyQ-mediated huntingtin aggregation. A possible therapeutic strategy. Neurodegener Dis. 4(2-3):254-260.

Hernan MA, Hernandez-Diaz S, and Robins JM. (2004). A structural approach to selection bias. Epidemiol. 15(5):615-625.

Hong Z, Shi M, Chung KA, Quinn JF, Peskind ER, Galasko D, Jankovic J, Zabetian CP, Leverenz JB, Baird G, Montine TJ, Hancock AM, Hwang H, Pan C, Bradner J, Kang UJ, Jensen PH, and Zhang J. (2010). DJ-1 and alpha-synuclein in human cerebrospinal fluid as biomarkers of Parkinson's disease. Brain. 133:713-726.

Iosefson O, and Azem A. (2010). Reconstitution of the mitochondrial Hsp70 (mortalin)-p53 interaction using purified proteins—Identification of additional interacting regions. FEBS Lett. 584:1080-1084.

Jenner P, and Olanow CW. (2006). The pathogenesis of cell death in Parkinson's disease Neurol. 66:S24-S36.

Jin J, Hulette C, Wang Y, Zhang T, Pan C, and Wadhwa R. (2006). Proteomic identification of a Stress Protein, Mortalin/mthsp70/GRP75: relevance to Parkinson disease. Mol Cell Proteomics. 5:1193-1204.

Jin J, Li GJ, Davis J, Zhu D, Wang Y, Pan C, and Zhang J. (2007). Identification of novel proteins associated with both alpha-synuclein and DJ-1. Mol Cell Proteomics. 6(5):845-859.

Joseph JD, Wang YM, Miles PR, Budygin EA, Picetti R, Gainetdinov RR, Caron MG, and Wightman RM. (2002). Dopamine autoreceptor regulation of release and uptake in mouse brain slices in the absence of D(3) receptors. Neurosci. 112:39-49.

Kalia SK, Lee S, Smith PD, Liu L, Crocker SJ, Thorarinsdottir TE, Glover JR, Fon EA, Parkin DS, and Lozano AM. (2004). BAG5 inhibits parkin and enhances dopaminergic neuron degeneration. Neuron. 44:931-945.

Katzenschlager R, Head J, Schrag A, Ben-Shlomo Y, Evans A, and Lees AJ. (2008). Fourteen-year final report of the randomized PDRG-UK trial comparing three initial treatments in PD. Neurol. 71:474-480.

Kaul SC, Deocaris CC, and Wadhwa R. (2007). Three faces of mortalin: a housekeeper, guardian and killer. Exp Gerontol. 42(4):263-274.

Kiang JG, and Tsokos GC. (1998). Heat shock protein 70 kDa: molecular biology, biochemistry, and physiology. Pharmacol Ther. 80(2):183-201.

Kim SJ, Sung JY, Um JW, Hattori N, Mizuno Y, Tanaka K, Paik SR, Kim J, and Chung KC. (2003). Parkin cleaves intracellular alpha-synuclein inclusions via the activation of calpain. J Biol Chem. 278(43):41890-41899.

Kimura K, Tanaka N, Nakamura N, Takano S, and Ohkuma S. (2007). Knockdown of mitochondrial heat shock protein 70 promotes progeria-like phenotypes in Caenorhabditis elegans. J Biol Chem. 282:5910-5918.

Kluchen J, Shin Y, Masliah E, Hyman BT, and McLean PJ. (2004). Hsp70 reduces alpha-synuclein aggregation and toxicity. J Biol Chem. 279(24):25497-25502.

Lang AE, and Obeso JA. (2004). Challenges in Parkinson's disease: restoration of the nigrostriatal dopamine system is not enough. Lancet Neurol. 3:309-316.

Lannuzel A, Michel PP, Hoglinger GU, Champy P, Jousset A, Medja F, Lombes A, Darios F, Gleye C, Laurens A, Hocquemiller R, Hirsch EC, and Ruberg M. (2003). The mitochondrial complex I inhibitor annonacin is toxic to mesencephalic dopaminergic neurons by impairment of energy metabolism. J Neurosci. 121:287-296.

LaVoie MJ, Ostaszewski BL, Weihofen A, Schlossmacher MG, and Selkoe DJ. (2005). Dopamine covalently modifies and functionally inactivates parkin. Nat Med. 11:1214-1221.

Le W, and Appel SH. (2004). Mutant genes responsible for Parkinson's disease. Curr Opin Pharmacol. 4:79-84.

LeWitt P, Schultz L, Auinger P, and Lu M. (2011). CSF xanthine, homovanillic acid, and their ratio as biomarkers of Parkinson's disease. Brain Res. 1408:88-97.

Liang CL, Wang TT, Luby-Phelps K, and German DC. (2007). Mitochondria mass is low in mouse substantia nigra dopamine neurons: implications for Parkinson's disease. Exp Neurol. 203:370-380.

Li HM, Niki T, Taira T, Iguchi-Ariga SM, and Ariga H. (2005). Association of DJ-1 with chaperones and enhanced association and colocalization with mitochondrial Hsp70 by oxidative stress. Free Radic Res. 39:1091-1099.

Ling YH, Liebes L, Zou Y, and Perez-Soler R. (2003). Reactive oxygen species generation and mitochondrial dysfunction in the apoptotic response to Bortezomib, a novel proteasome inhibitor, in human H460 non-small cell lung cancer cells. J Biol Chem. 278: 33714-33723.

Liu Y, Liu W, Song XD, and Zuo J. (2005). Effect of GRP75/mthsp70/PBP74/mortalin overexpression on intracellular ATP level, mitochondrial membrane potential and ROS accumulation following glucose deprivation in PC 12 cells. Mol Cell Biochem. 268:45-51.

Lubarda J, Groleau SE, Thomas N, Ferro MA, Mishra RK, and Gabriele JP. (2013). Dysregulation of novel catecholamine-regulated protein 40 (CRP40) in Parkinson's disease patients. Mov Disord. doi: 10.1002/mds.25402. [Epub ahead of print]

Lutz AK, Exner N, Fett ME, Schlehe JS, Kloos K, Lämmermann K, Brunner B, Kurz-Drexler A, Vogel F, Reichert AS, Bouman L, Vogt-Weisenhorn D, Wurst W, Tatzelt J, Haass C, and Winklhofer KF. (2009). Loss of parkin or PINK1 function increases Drp1-dependent mitochondrial fragmentation. J Biol Chem. 284:22938-22951.

Mala JG, and Rose C. (2010). Interactions of heat shock protein 47 with collagen and the stress response: an unconventional chaperone model? Life Sci. 87(19-22):579-586.

Malavolta L, and Cabral FR. (2011). Peptides: important tools for the treatment of central nervous system disorders. Neuropept. (5):309-316.

Mandemakers W, Morais VA, and De Strooper B. (2007) A cell biological perspective on mitochondrial dysfunction in Parkinson disease and other neurodegenerative diseases. J Cell Sci. 120:1707- 1716.

Margis R, and Rieder CR. (2011). Identification of blood microRNAs associated to Parkinson's disease. J Biotechnol. 152:96–101.

Mayer MP, Rudiger S, and Bukau B. (2000). Molecular basis for interactions of the DnaK chaperone with substrates. Biol Chem. 381:877-885.

McNaught KS, Perl DP, Brownell AL, and Olanow CW. (2004). Systemic exposure to proteasome inhibitors causes a progressive model of Parkinson's disease. Ann Neurol. 56(1):149-162.

Meara J, Bhowmick BA, and Hobson P. (1999). Accuracy of diagnosis in patients with presumed Parkinson's disease. Age and Ageing. 28:99-102.

Missale C, Nash SR, Robinson SW, Jaber M, and Caron MG. (1998). Dopamine receptors: from structure to function. Physiol Rev. 78:189-225.

Miyazaki I, and Asanuma M. (2009). Approaches to prevent dopamine quinone-induced neurotoxicity. Neurochem Res. 34(4):698-706.

Mizuno Y, Matuda S, Yoshino H, Mori H, Hattori N, and Ikebe S. (1994). An immunohistochemical study on alpha-ketoglutarate dehydrogenase complex in Parkinson's disease. Ann Neurol. 35:204-210.

Modi PI, Kashyap A, Nair VD, Ross GM, Fu M, Savelli JE, Marcotte ER, Barlas C, and Mishra RK. (1996). Modulation of brain catecholamine absorbing proteins by dopaminergic agents. Eur J Pharmacol. 299:213-220.

Mollenhauer B, Locascio JJ, Schulz-Schaeffer W, Sixel-Döring F, Trenkwalder C, and Schlossmacher MG. (2011). Alpha-Synuclein and tau concentrations in cerebrospinal fluid of patients presenting with parkinsonism: a cohort study. Lancet Neurol. 10:230–240.

Muchowski PJ, and Wacker JL. (2005). Modulation of neurodegeneration by molecular chaperones. Nat Rev Neurosci. 6:11-22.

Nagata. (1996). Hsp47: A collagen-specific molecular chaperone. Trends Biochem Sci. 21:22-26.

Nagata. (1998). Expression and function of heat shock protein 47: A collagen-specific molecular chaperone in the endoplasmic reticulum. Matrix Biol. 16:379-386.

Nair VD, and Mishra RK. (2001). Molecular cloning, localization and characterization of a 40-kDa catecholamine-regulated protein. J Neurochem. 76:1142-1152.

Obeso JA, Rodriguez-Oroz MC, Goetz CG, Marin C, Kordower JH, Rodriguez M, Hirsch EC, Farrer M, Schapira AH, and Halliday G. (2010). Missing pieces in the Parkinson's disease puzzle. Nat Med.16:653-661.

Ohtsuki S, and Terasaki T. (2007). Contribution of carrier-mediated transport systems to the blood–brain barrier as a supporting and protecting interface for the brain; importance for CNS drug discovery and development. Pharm Res. 24:1745-1758.

Okun MS. (2012). Deep-brain stimulation for Parkinson's disease. N Engl J Med. 367(16):1529-1538.

Osorio C, Sullivan PM, He DN, Mace BE, Ervin JF, and Strittmatter WJ. (2007). Mortalin is regulated by APOE in hippocampus of AD patients and by human APOE in TR mice. Neurobiol Aging. 28:1853-1862.

O'Sullivan SS, Williams DR, Gallagher DA, Massey LA, Silveira-Moriyama L, and Lees AJ. (2008). Nonmotor symptoms as presenting complaints in Parkinson's disease: a clinicopathological study. Mov Disord. 23:101-106.

Pan TH, Li XQ, Xie WJ, Jankovic J, and Le WD. (2005). Valproic acid-mediated Hsp70 induction and anti-apoptotic neuroprotection in SH-SY5Y cells. FEBS Lett. 579(30):6716-6720.

Perese DA, Ulman J, Viola J, Ewing SE, and Bankiewicz KS. (1989). A 6-hydroxydopamine induced selective Parkinsonian rat model. Brain Res. 494: 285-293.

Qu M, Zhou Z, Xu S, Chen C, Yu Z, and Wang D. (2011). Mortalin overexpression attenuates beta-amyloid-induced neurotoxicity in SH-SY5Y cells. Brain Res. 12(1368):336-345.

Ramsay RR, Salach JI, and Singer TP. (1986). Uptake of the neurotoxin 1-methyl-4-phenylpyridine (MPP+) by mitochondria and its relation to the inhibition of the mitochondrial oxidation of NAD+-linked substrates by MPP+. Biochem Biophys Res Commun. 134:743-748.

Rankin ML, Hazelwood LA, Free RB, Namkung Y, Rex EB, Roof RA, and Sibley DR. (2010). Molecular pharmacology of the dopamine receptors, in Dopamine Handbook (Iversen LL, Dunnett SB, Iversen SD, Bjorklund A ed). 63-87, Oxford University Press, New York.

Rao CM, Raman B, Ramakrishna T, Rajaraman K, Ghosh D, Datta S, Trivedi VD, and Sukhaswami MB. (1998). Structural perturbation of α-crystallin and its chaperone-like activity. Int J Biol Macromol. 22:271-281.

Ravagnan L, Gurbuxani S, Susin SA, Maisse C, Daugas E, Zamzami N, Mak T, Jaattela M, Penninger JM, Garrido C, and Kroemer G. (2001). Heat-shock protein 70 antagonizes apoptosis-inducing factor. Nat Cell Biol. 3:839-843.

Rondou P, Haegeman G, and Van Craenenbroeck K. (2010). The dopamine D4 receptor: biochemical and signalling properties. Cell Mol Life Sci. 67:1971-1986.

Ross GM, McCarry BE, and Mishra RK. (1995). Covalent affinity labeling of brain catecholamine-absorbing proteins using a high-specific-activity substituted tetrahydronaphthalene. J Neurochem. 65:2783-2789.

Ross GM, McCarry BE, Thakur S, and Mishra RK. (1993). Identification of novel catecholamine absorbing proteins in the central nervous system. J Mol Neurosci. 4:141-148.

Roth BL, Sheffler DJ, and Kroeze WK. (2004). Magic shotguns versus magic bullets: selectively non-selective drugs for mood disorders and schizophrenia. Nat Rev Drug Discov. 3:353-359.

Schapira AH. (1994). Evidence for mitochondrial dysfunction in Parkinson's disease–a critical appraisal. Mov Disord. 9:125-138.

Schapira AH. (2011). Mitochondrial pathology in Parkinson's disease. Mt Sinai J Med. 78:872-881.

Schapira, AH. (2009). Neurobiology and treatment of Parkinson's disease. Trends Pharmacol Sci. 30:41-47.

Schapira AH, Cooper JM, Dexter D, Clark JB, Jenner P, and Marsden CD. (1990). Mitochondrial complex I deficiency in Parkinson's disease. J Neurochem. 54:823-827.

Schapira AH, and Jenner P. (2011). Etiology and pathogenesis of Parkinson's disease. Mov Disord. 26:1049-1055.

Schrag A, Dodel R, Spottke A, Bornschein B, Siebert U, and Quinn NP. (2007). Rate of clinical progression in Parkinson's disease. A prospective study. Mov Disord. 22:938-945.

Selikhova M, Williams DR, Kempster PA, Holton JL, Revesz T, and Lees AJ. (2009). A clinico-pathological study of subtypes in Parkinson's disease. Brain. 132:2947-2957.

Sharan N, Chong VZ, Nair VD, Mishra RK, Hayes RJ, and Gardner EL. (2003). Cocaine treatment increases expression of a 40 kDa catecholamine-regulated protein in discrete brain regions. Syn. 47:33-44.

Sharan N, Nair VD, and Mishra RK. (2001). Modulation of a 40-kDa catecholamine regulated protein by dopamine receptor antagonists. Eur J Pharmacol. 413:73-79.

Shen HY, He JC, Wang Y, Huang QY, and Chen JF. (2005). Geldanamycin induces heat shock protein 70 and protects against MPTP-induced dopaminergic neurotoxicity in mice. J Biol Chem. 280(48):39962-39969.

Shi M, Jin J, Wang Y, Beyer RP, Kitsou E, and Albin RL. (2008). Mortalin: a protein associated with progression of parkinson disease? J Neuropathol Exp Neurol. 67:117-124.

Shulman JM, De Jager PL, and Feany MB. (2011). Parkinson's disease: genetics and pathogenesis. Annu Rev Pathol. 6:193-222.

Siderowf A, and Lang AE. (2012) Premotor Parkinson's disease: concepts and definitions. Mov Disord. 27(5):608-616.

Simola MM, and Carta AR. (2007). The 6-hydroxydopamine model of Parkinson's disease. Neurotox Res. 11:151-167.

Song IU, Chung SW, Kim JS, and Lee KS. (2011). Association between high-sensitivity C-reactive protein and risk of early idiopathic Parkinson's disease. Neurol Sci. 32:31-34.

Sõti C, Nagy E, Giricz Z, Vígh L, Csermely P, and Ferdinandy P. (2005). Heat shock proteins as emerging therapeutic targets. Br J Pharmacol. 146(6):769-780.

Spano PF, Govoni S, and Trabucchi M. (1978). Studies on the pharmacological properties of dopamine receptors in various areas of the central nervous system. Adv Biochem Psychopharmacol. 19:155-165.

Sun Y, Ouyang YB, Xu L, Chow AM, Anderson R, Hecker JG, and Giffard RG. (2006). The carboxyl-terminal domain of inducible Hsp70 protects from ischemic injury in vivo and in vitro. J Cereb Blood Flow Metab. 26:937-950.

Tanaka Y, Engelender S, Igarashi S, Rao RK, Wanner T, Tanzi RE, Sawa A, L Dawson V, Dawson TM, and Ross CA. (2001). Inducible expression of mutant alpha-synuclein decreases proteasome activity and increases sensitivity to mitochondria-dependent apoptosis. Hum Mol Genet. 10(9):919-926.

Thomson CA, and Ananthanarayanan VS. (2001). A method for expression and purification of soluble, active Hsp47, a collagen-specific molecular chaperone. Protein Exp and Purif. 23:8-13.

Tse DC, McCreery RL, and Adams RN. (1976). Potential oxidative pathways of brain catecholamines. J Med Chem. 19:37-40.

Twig G, Elorza A, Molina AJ, Mohamed H, Wikstrom JD, Walzer G, Stiles L, Haigh SE, Katz S, Las G, Alroy J, Wu M, Py BF, Yuan J, Deeney JT, Corkey BE, and Shirihai OS. (2008). Fission and selective fusion govern mitochondrial segregation and elimination by autophagy. EMBO J. 27:433-446.

Ungerstedt U, and Arbuthnott G. (1970). Quantitative recording of rotational behavior in rats after 6-hydroxydopamine lesions of the nigrostriatal dopamine system. Brain Res. 24:485-493.

Vallone D, Picetti R, and Borrelli E. (2000). Structure and function of dopamine receptors. Neurosci Beh Rev. 24:125-132.

Van Laar VS, Dukes AA, Cascio M, and Hastings TG. (2008). Proteomic analysis of rat brain mitochondria following exposure to dopamine quinone: implications for Parkinson disease. Neurobiol Dis. 29:477-489.

Verheij MM, and Cools AR. (2008). Twenty years of dopamine research: individual differences in the response of accumbal dopamine to environmental and pharmacological challenges. Eur J Pharmacol. 13;585(2-3):228-244.

Volles MJ, Lee SJ, Rochet JC, Shtilerman MD, Ding TT, and Kessler JC. (2001). Vesicle permeabilization by protofibrillar alpha-synuclein: implications for the pathogenesis and treatment of Parkinson's disease. Biochem. 40:7812-7819.

Volobоueva LA, Duan M, Ouyang Y, Emery JF, Stoy C, and Giffard RG. (2008). Overexpression of mitochondrial Hsp70/Hsp75 protects astrocytes against ischemic injury *in vitro*. J Cereb Blood Flow & Metab. 28:1009-1016.

Wadhwa R, Takano S, Kaur K, Deocaris CC, Pereira-Smith OM, Reddel RR, and Kaul SC. (2006). Upregulation of mortalin/mthsp70/Grp75 contributes to human carcinogenesis. Int J Cancer. 118:2973-2980.

Weaver FM, Follett K, Stern M, Hur K, Harris C, Marks WJ Jr, Rothlind J, Sagher O, Reda D, Moy CS, Pahwa R, Burchiel K, Hogarth P, Lai EC, Duda JE, Holloway K, Samii A, Horn S, Bronstein J, Stoner G, Heemskerk J, Huang GD; and CSP 468 Study Group. (2009). Bilateral deep brain stimulation vs best medical therapy for patients with advanced Parkinson disease: a randomized controlled trial. JAMA. 301(1):63-73.

Weiss ML, Medicetty S, Bledsoe AR, Rachakatla RS, Choi M, Merchav S, Luo Y, Rao MS, Velagaleti G, and Troyer D. (2006). Human umbilical cord matrix stem cells: preliminary characterization and effect of transplantation in a rodent model of Parkinson's disease. Stem Cells. 24(3):781-792.

Wolburg H, and Lippoldt A. (2002). Tight junctions of the blood-brain barrier: development, composition and regulation. Vascul Pharmacol. 38:323-337.

Xu L, Voloboueva LA, Ouyang Y, Emery JF, and Giffard RG. (2009). Overexpression of mitochondrial Hsp70/Hsp75 in rat brain protects mitochondria, reduces oxidative stress, and protects from focal ischemia. J Cereb Blood Flow Metab. 29(2):365-374.

Yang H, Zhou X, Liu X, Yang L, Chen Q, Zhao D, Zuo J, and Liu W. (2011). Mitochondrial dysfunction induced by knockdown of mortalin is rescued by Parkin. Biochem Biophys Res Commun. 410(1):114-120.

Yao Z, and Wood NW. (2009). Cell death pathways in Parkinson's disease: role of mitochondria. Antiox & Redox Sig. 11(9):2135-2149.

Zhan W, Kang GA, Glass GA, Zhang Y, Shirley C, Millin R, Possin KL, Nezamzadeh M, Weiner MW, Marks WJ Jr, and Schuff N. (2012). Regional alterations of brain microstructure in Parkinson's disease using diffusion tensor imaging. Mov Disord. 27:90-97.

Zhu X, Zhao X, Burkholder WF, Gragerov A, Ogata CM, Gottesman ME, and Hendrickson WA. (1996). Structural analysis of substrate binding by the molecular chaperone DnaK. Science 272: 1606-1614.

Zimprich A, Biskup S, Leitner P, Lichtner P, Farrer M, Lincoln S, Kachergus J, Hulihan M, Uitti RJ, Calne DB, Stoessl AJ, Pfeiffer RF, Patenge N, Carbajal IC, Vieregge P, Asmus F, Müller-Myhsok B, Dickson DW, Meitinger T, Strom TM, Wszolek ZK, and Gasser T. (2004). Mutations in LRRK2 cause autosomal-dominant parkinsonism with pleomorphic pathology. Neuron. 44:601-607.